



HAL
open science

Contribution à l'analyse et à la compréhension des signaux des réseaux électriques par des techniques issues du traitement du signal et de l'apprentissage machine

Thien-Minh Nguyen

► To cite this version:

Thien-Minh Nguyen. Contribution à l'analyse et à la compréhension des signaux des réseaux électriques par des techniques issues du traitement du signal et de l'apprentissage machine. Autre [cs.OH]. Université de Haute Alsace - Mulhouse, 2017. Français. NNT : 2017MULH9234 . tel-02080529

HAL Id: tel-02080529

<https://theses.hal.science/tel-02080529>

Submitted on 26 Mar 2019

HAL is a multi-disciplinary open access archive for the deposit and dissemination of scientific research documents, whether they are published or not. The documents may come from teaching and research institutions in France or abroad, or from public or private research centers.

L'archive ouverte pluridisciplinaire **HAL**, est destinée au dépôt et à la diffusion de documents scientifiques de niveau recherche, publiés ou non, émanant des établissements d'enseignement et de recherche français ou étrangers, des laboratoires publics ou privés.

Thèse

Présentée pour obtenir le grade de
Docteur de l'Université de Haute Alsace

Discipline : Traitement du Signal

par

Thien-Minh NGUYEN

Contribution to the analysis and understanding of electrical-grid signals with signal processing and machine learning techniques

**Contribution à l'analyse et à la compréhension des signaux des réseaux électriques
par des techniques issues du traitement du signal et de l'apprentissage machine**

Soutenue publiquement le 20 septembre 2017 devant le jury :

Pr. Dirk BENYOUCEF	Hochschule Furtwangen University (Germany)	Président
Dr. Salah LAGHROUCHE	Université de technologie Belfort-Montbéliard	Rapporteur
Dr. Antonio PINTI	Université de Valenciennes et du Hainaut-Cambrésis	Rapporteur
Dr. Ngac-Ky NGUYEN	Arts et Métiers ParisTech – CER de Lille	Examinateur
Pr. Lhassane IDOUMGHAR	Université de Haute Alsace	Examinateur
Pr. Patrice WIRA	Université de Haute Alsace	Directeur de thèse

Laboratoire Modélisation, Intelligence, Processus et Systèmes (MIPS, EA 2332)
École Doctorale Mathématiques, Sciences de l'Information et de l'Ingénieur (MSII, ED 269)

Acknowledgements

First of all, I would like to say thanks and express my most sincere gratitude to my thesis supervisor Pr. Patrice WIRA, for all his help for my study and for my family during the time I do my PhD thesis at Université de Haute-Alsace.

I would like to thank and express my appreciation to other members of the thesis defense jury, Pr. Dirk BENYOUCEF (the jury president) at Hochschule Furtwangen University (Germany), Pr. Lhassane IDOUMGHAR at Université de Haute Alsace, Dr. Salah LAGHROUCHE at Université de Technologie Belfort-Montbéliard, Dr. Antonio PINTI at Université de Valenciennes et du Hainaut-Cambrésis and Dr. Ngac-Ky NGUYEN at Arts et Métiers ParisTech – CER de Lille.

I also would like to acknowledge and express my appreciation to Pr. Olivier HAEBERLÉ, Pr. Jean MERCKLÉ, Pr. Jean-Philippe URBAN, Dr. Jean-Luc BUESSLER, Dr. Djaffar OULD ABDESLAM at MIPS Laboratory of Université de Haute-Alsace, for all their help and encouragement give me while studying and learning French.

I take this opportunity to express my appreciation and to say thanks to all my friends in France for their emotional supports.

Finally, some special thanks are for my family, my wife and my three lovely children, always beside me in France.

Thien-Minh NGUYEN

Mulhouse, 2017

Contribution à l'analyse et à la compréhension des signaux des réseaux électriques par des techniques issues du traitement du signal et de l'apprentissage machine

Résumé

Ce travail de thèse propose des approches d'identification et de reconnaissance des harmoniques de courant qui sont basées sur des stratégies d'apprentissage automatique. Les approches proposées s'appliquent directement dans les dispositifs d'amélioration de la qualité de l'énergie électrique.

Des structures neuronales complètes, dotées de capacités d'apprentissage automatique, ont été développées pour identifier les composantes harmoniques d'un signal sinusoïdal au sens large et plus spécifiquement d'un courant alternatif perturbé par des charges non linéaires. L'identification des harmoniques a été réalisée avec des réseaux de neurones de type Multi-Layer Perceptron (MLP). Plusieurs schémas d'identification ont été développés, ils sont basés sur un réseau MLP composé de neurones linéaire ou sur plusieurs réseaux MLP avec des apprentissages spécifiques. Les harmoniques d'un signal perturbé sont identifiées avec leur amplitude et leur phase, elles peuvent servir à générer des courants de compensation pour améliorer la forme du courant électrique.

D'autres approches neuronales a été développées pour reconnaître les charges. Elles consistent en des réseaux MLP ou SVM (Support Vector Machine) et fonctionnent en tant que classificateurs. Leur apprentissage permet à partir des harmoniques de courant de reconnaître le type de charge non linéaire qui génère des perturbations dans le réseau électrique.

Toutes les approches d'identification et de reconnaissance des harmoniques ont été validées par des tests de simulation à l'aide des données expérimentales. Des comparaisons avec d'autres méthodes ont démontré des performances supérieures et une meilleure robustesse.

Mots-clés:

Perceptron Multicouche ; Apprentissage Machine; Réseaux de Neurones Artificiels ; Classification ; Identification des Courants Harmoniques ; Charges Non Linéaires ; Qualité de l'Energie ; Appareil Electrique.

Contribution to the analysis and understanding of electrical-grid signals with signal processing and machine learning techniques

Abstract

This thesis proposes identifying approaches and recognition of current harmonics that are based on machine learning strategies. The approaches are applied directly in the quality improvement devices of electric energy and in energy management solutions.

Complete neural structures, equipped with automatic learning capabilities have been developed to identify the harmonic components of a sinusoidal signal at large and more specifically an AC disturbed by non-linear loads. The harmonic identification is performed with multilayer perceptron neural networks (MLP). Several identification schemes have been developed. They are based on a MLP neural network composed of linear or multiple MLP networks with specific learning. Harmonics of a disturbed signal are identified with their amplitude and phases. They can be used to generate compensation currents fed back into the network to improve the waveform of the electric current.

Neural approaches were developed to distinguish and to recognize the types of harmonics and is nonlinear load types that are at the origin. They consist of MLP or SVM (Support Vector Machine) acting as classifier that learns the harmonic profile of several types of predetermined signals and representative of non-linear loads. They entry are the parameters of current harmonics of the current wave. Learning can recognize the type of nonlinear load that generates disturbances in the power network.

All harmonics identification and recognition approaches have been validated by simulation tests or using experimental data. The comparisons with other methods have demonstrated superior characteristics in terms of performance and robustness.

Keywords:

Multilayer Perceptron; Machine Learning; Artificial Neural Networks; Classification; Current Harmonic Identification; Nonlinear Loads; Power Quality; Electrical Appliance.

Table of Contents

Chapter 1 : Introduction	1
1.1 Artificial Neural Networks	2
1.2 Identification of Power System Harmonics.....	5
1.3 Nonlinear Load Classification.....	7
1.4 Research Contributions	9
1.5 Thesis Structure	12
Chapter 2 : Harmonic Identification	13
2.1 Introduction	13
2.2 Non-Neural Techniques.....	13
2.2.1 Discrete Fourier Transform.....	13
2.2.2 Kalman Filtering	14
2.2.3 Wavelet Transform	15
2.2.4 Hilbert-Huang Transform.....	15
2.2.5 Chirp Z-Transform	15
2.2.6 Prony's Method.....	15
2.2.7 MUSIC.....	16
2.2.8 ESPRIT	16
2.2.9 PLL	16
2.2.10 GA.....	16
2.2.11 Particle Swarm Optimization.....	17
2.3 Neural Techniques.....	17
2.3.1 ADALINE.....	17
2.3.2 Multilayer Perceptron	26
2.3.3 Recurrent Neural Network.....	31

2.3.4	Radial Basis Function Neural Network	33
2.4	Hybrid Techniques	33
2.5	Summary	35
Chapter 3	: Load Signature Discrimination	36
3.1	Introduction	36
3.2	Signature Analysis Based Techniques.....	36
3.2.1	Steady–State Signature Analysis Based Approaches	36
3.2.2	Transient–State Signature Analysis Based Approaches	36
3.2.3	Non–traditional Appliance Features Based Approaches	38
3.3	Machine Learning Based Techniques	39
3.3.1	Supervised Learning Based Approaches	39
3.3.2	Unsupervised Learning Based Approaches	41
3.4	Summary	41
Chapter 4	: Harmonic Estimation Using Artificial Neural Networks.....	42
4.1	Introduction	42
4.2	Background	45
4.2.1	Fourier Analysis	45
4.2.2	The Multilayer Perceptron.....	46
4.3	Proposed Method 1 : A Linear MLP for Harmonic Estimation	47
4.3.1	Proposed Linear MLP	47
4.3.2	Results of Harmonic Identification in Electrical Power System	54
4.3.3	Results in Estimating Harmonics of Biomedical Signals	59
4.3.4	The linear MLP with one hidden neuron compared to an ADALINE.....	64
4.4	Proposed Method 2 : A Multiple MLP for Harmonic Estimation.....	67
4.4.1	Proposed Multiple MLP.....	68
4.4.2	Experiments and Results.....	70
4.5	Summary	74
Chapter 5	: Electric Appliances Classification Using Artificial Neural Networks.....	76
5.1	Introduction	76
5.2	Proposed Methods for Nonlinear load classification.....	77
5.2.1	Proposed Model 1 : A Binary–Output MLP	77
5.2.2	Proposed Model 2 : A Multiple Binary–Output MLP	78
5.2.3	Proposed Model 3 : A Multiple Support Vector Machine.....	79
5.3	Experimental Setup	80

5.4 Experimental Results.....	91
5.4.1 Experimental Result 1: Test with harmonic signatures extracted by the linear MLP harmonic estimator.....	91
5.4.2 Experimental Result 2: Test with harmonic signatures extracted by the multiple MLP harmonic estimator.....	95
5.4.3 Experimental Result 3: Test with noised signals.....	98
5.4.4 Discussion and comparison of classification accuracy.....	101
5.5 Summary.....	102
Chapter 6 : Conclusions.....	103
6.1 Proposed Methods for Harmonic Estimation.....	103
6.2 Proposed Methods for Electric Appliances Classification.....	104
6.3 Limitations and Future Work.....	105
Abbreviations.....	107
List of Figures.....	108
List of Tables.....	110
List of References.....	111

Chapter 1 : Introduction

Since a couple of decades, the number of electrical nonlinear devices has increased continually in domestic and industrial installations. The unwanted harmonics generated by nonlinear loads or devices yield many problems in power systems (Arrillaga and Watson, 2003). These harmonics interact with system impedances and badly affect sensitive loads. Additional equipment like active power filters must be inserted in the power lines for improving the electrical waveforms. They need some robust and efficient harmonic identification techniques in order to precisely compensate for harmonic distortions (Akagi, 1996; Akagi, 2005) by re-injecting them phase opposite. Hence, harmonic identification approaches are more important than ever for power quality issues. Figure 1.1 shows a detailed block diagram of an enhanced shunt active power filter (APF).

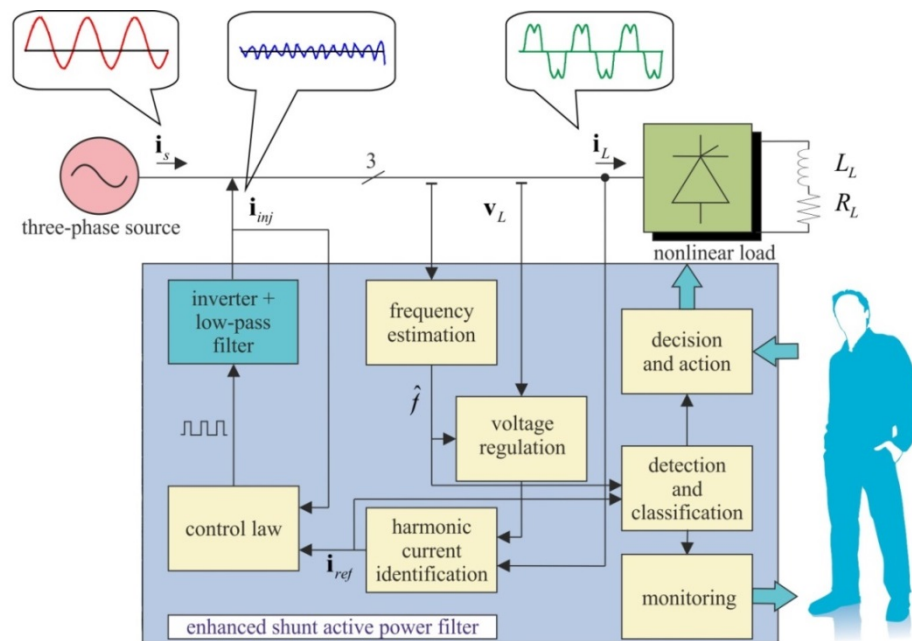


Figure 1.1 Detailed block diagram of an enhanced shunt APF.

In a power system, a harmonic term is defined as a sinusoidal component with a frequency that is an integer multiple of the fundamental signal. The fundamental signal is either the main current or main voltage of a power line. Various harmonic distortion identification schemes have been developed to improve the quality of the power line signals. Among them, the Discrete Fourier Transform (DFT), the Fast Fourier Transform (FFT), Time–Frequency Distributions (TFDs), Transform Domain Adaptive Filters (TDAFs), Wavelet Transforms (WTs), and Instantaneous Power Theory (IPT) are well–known techniques that have been applied in active compensation strategies (Akagi, 2005).

1.1 Artificial Neural Networks

From 1990s to present, artificial neural networks for signal processing is one of the most interesting topics in scientific researches and engineering applications. Artificial neural network (ANN) schemes have been successfully implemented in active power filtering applications (Bose, 2007). Several successful neural network approaches have been applied for higher-order harmonic currents identification and for other tasks involved in power quality management: Voltage sags and swells detection, reactive power compensation, fundamental frequency estimation, and phase tracking for grid synchronization (Wira *et al.*, 2010; Nguyen *et al.*, 2011).

ANNs with their ability to learn from sample data have shown that they are excellent solutions for performing advanced digital signal processing tasks (Hagan *et al.*, 1995; Haykin, 1999). Therefore, several ANN approaches have been developed for harmonic identification. They are based on different neural structures, and have to identify the amplitude and the phase of each higher-order harmonic of the current measured on a power line. Once estimated, they can be used to generate compensation currents. This is achieved by a voltage-source inverter under the supervision of a control law. The controller produces a reference signal that takes into account the necessary harmonic components but phase-opposite. The inverter converts the reference signal into a high-intensity current that will be injected into the power line. This principle is represented in Figure 1.2. The skills related to each block are also mentioned.

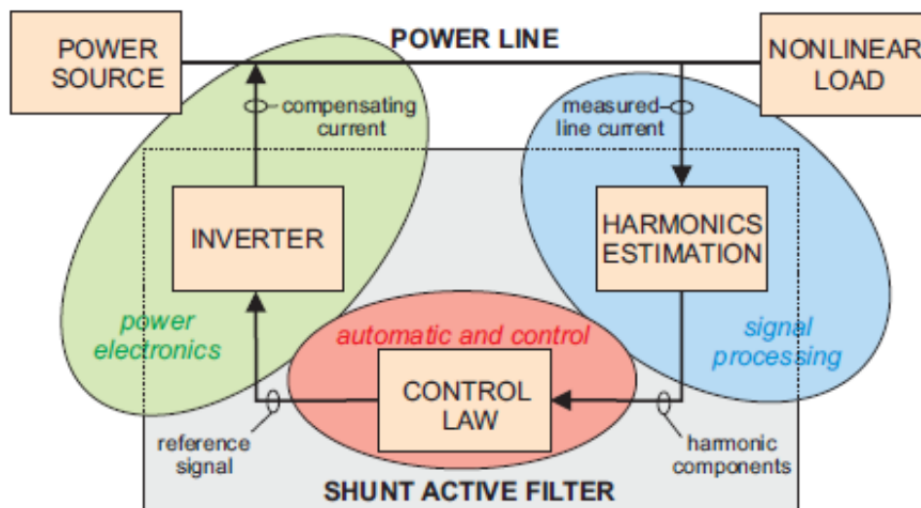


Figure 1.2 A shunt APF.

An artificial neural network is a statistical learning model inspired by biological neural network. In 1943, McCulloch and Pitt proposed the first mathematical neuron model of an artificial neural network as in [Figure 1.3](#) (McCulloch and Pitts, 1943).

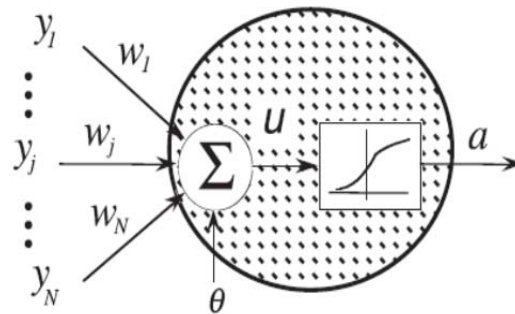


Figure 1.3 The first neuron model of McCulloch and Pitts in 1943.

A few years later, in 1957, Frank Rosenblatt, who was also motivated by the paper of W. McCulloch and W. Pitts, investigated the computation of the image recognition machine called "Mark 1 perceptron". His work led to the first generation of neural networks, known as the perceptron in (Rosenblatt, 1958) as in [Figure 1.4](#).

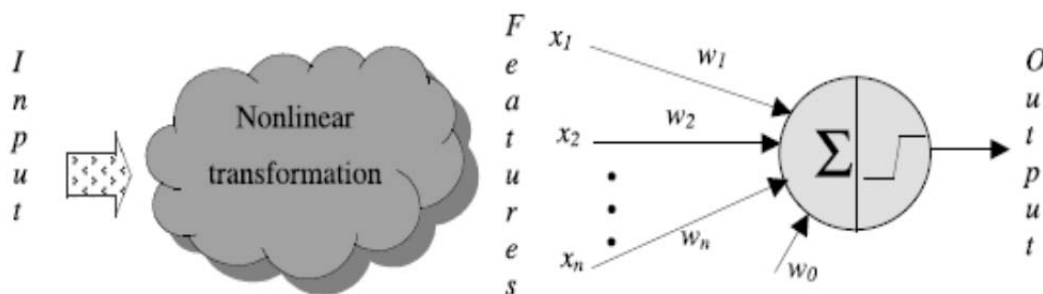


Figure 1.4 A perceptron neural network model of Rosenblatt in 1958.

An Adaptive linear element (ADALINE) in [Figure 1.5](#) is an early single-layer artificial neural network and the name of the physical device that implemented this network. It was developed by Professor Bernard Widrow and Ted Hoff at Stanford University in 1960. It is based on the McCulloch–Pitts neuron. It consists of a weight, a bias and a summation function. ADALINE uses the mean square error (MSE) to update its weights in the training process.

A multilayer perceptron (MLP) network in [Figure 1.6](#) is composed of neurons organized in layers, with those on one layer connected to those on the next layer (except for the last layer also called the output layer). The MLP architecture is thus structured into an input layer, one or more hidden layer of neurons (called hidden neurons), and one output layer of neurons (output neurons).

Neurons belonging to adjacent layers are usually fully connected. The feedforward network is a MLP that allows only for a one directional signal flow, from the input to the output layer.

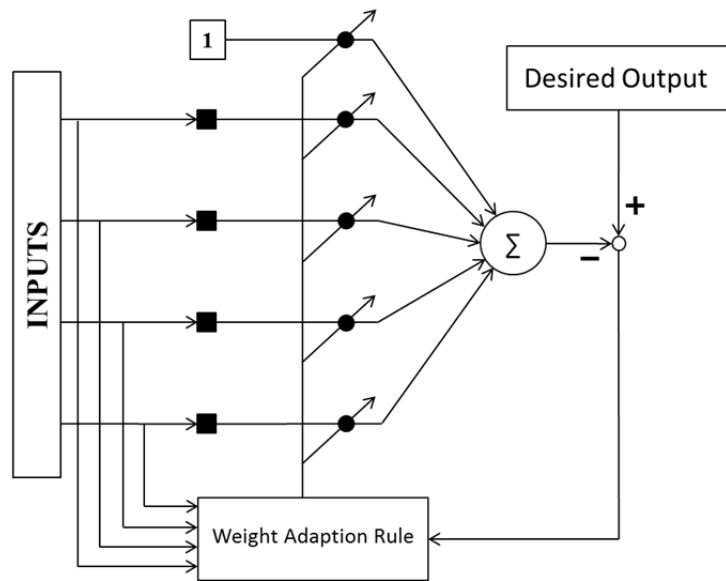


Figure 1.5 Typical architecture of an ADALINE network.

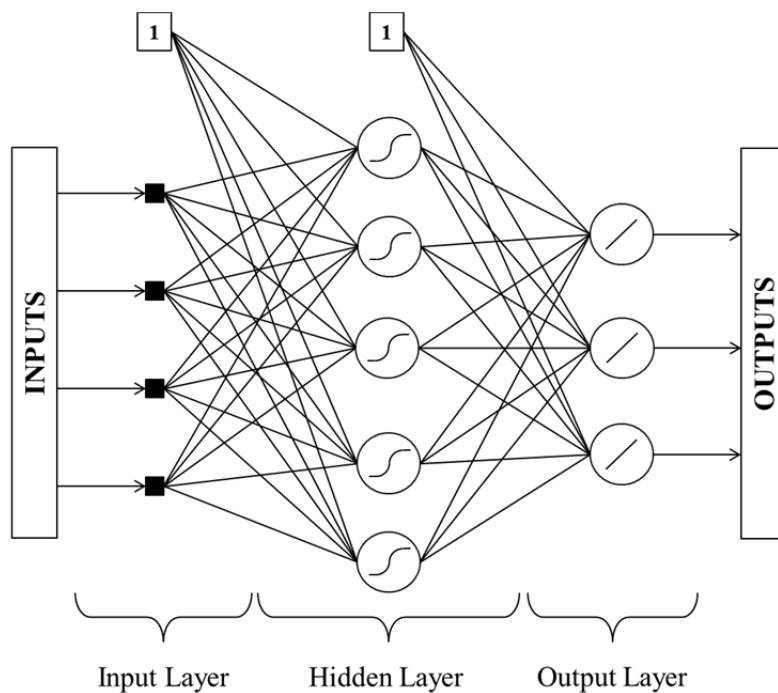


Figure 1.6 Typical architecture of a multilayer perceptron network.

In addition, we also have Radial Basic Function (RBF) neural network, Support Vector Machine (SVM), Self-Organizing Map (SOM) and many other learning machines with supervised and unsupervised learning techniques that were introduced in (Hagan *et al.*, 1995; Haykin, 1999).

1.2 Identification of Power System Harmonics

Harmonic content is a fundamental concept in power system analysis, operation, and control; hence its fast and precise estimation is prime importance. Consequences and problems induced by higher-order harmonic terms in power systems have been well established (Arrillaga and Watson, 2003). Digital devices with high computational capabilities will expand the design of new and precise harmonics identification techniques as in Figure 1.7.

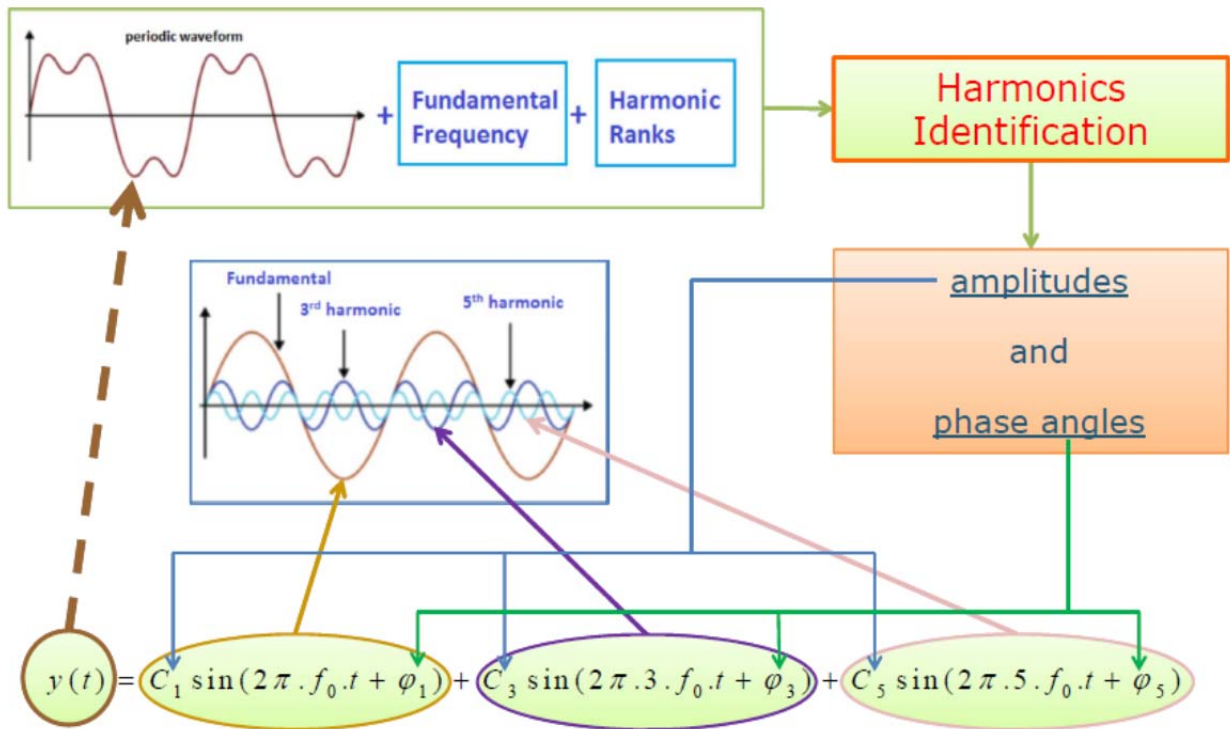


Figure 1.7 Identification of power system harmonics.

Fourier-based approaches are among the most fundamental techniques in frequency analysis processing. However, they imply sliding window implementations and convolution operations which make their computational requirements a heavy burden in most applications. Furthermore, Fourier-based approaches only provide a response after a complete period of the measured signal and cannot calculate the dynamic characteristics of measured signals over time because of the consumption that analyzed signals are stationary (Chang *et al.*, 2009). Since the harmonic content

varies constantly in power system, fast and real-time estimation techniques are necessary for efficient actions.

The last decades have seen many studies about harmonic distortion identification techniques to improve power quality. In this thesis, a harmonic term is defined as a component of a periodic wave having a frequency that is an integer multiple of the fundamental power line frequency. In the following, we focus on online and iterative algorithms to estimate harmonic terms in real-time applications.

Any periodic, distorted waveform can be expressed as a sum of pure sinusoids. The sum of sinusoids is referred to as a Fourier series. The Fourier analysis permits a periodic distortion waveform to be decomposed into an infinite series containing a DC component, a fundamental component (50/60 Hz for power systems) and its integer multiples called the harmonic components. The harmonic number n usually specifies a harmonic component, which is the ratio of its frequency to the fundamental frequency.

An ideal power signal, i.e. a voltage or a current, is a sinusoidal signal of period T (scalar)

$$y(k) = a \sin(\omega k + \phi) \quad (1.1)$$

where a is the amplitude, $\omega = 2\pi / T$ represents the actual angular frequency, and ϕ is the initial phase angle. This signal is measured and digitalized with sampling frequency of f_s , the time interval between two successive samples is thus $T_s = 1 / f_s$.

A non-ideal power signal contains harmonic terms and noise can be generally be approximated by

$$y'(k) = a'_0 + a'_1 \sin(\omega k + \phi_1) + \sum_{n=2}^N a'_n \sin(n\omega k + \phi_n) + \eta(k) \quad (1.2)$$

where a'_0 is the DC component and $\eta(k)$ represents a noise. Each harmonic component is defined by its amplitude a'_n and its phase angle ϕ_n . Practically, the sum of the harmonic components $a'_n \sin(n\omega k + \phi_n)$ is limited (to $n = N$).

According to Fourier, every periodic signal can be estimated by a function f :

$$f(k) = a_0 + \sum_{n=1}^{\infty} a_n \cos(n\omega k) + \sum_{n=1}^{\infty} b_n \sin(n\omega k) \quad (1.3)$$

where a_0 is the DC part and n is called the n -th harmonic. The sum of the terms $a_n \cos(n\omega k)$ is called the even part and the sum of the terms $b_n \sin(n\omega k)$ is called the odd part of the signal. Rearranging the even and odd part gives (1.4) which is a well-known result:

$$f(k) = c_0 + \sum_{n=1}^{\infty} c_n \cos(n\omega k - \theta_n), \quad (1.4)$$

with c_n the harmonic amplitudes and θ_n the phase angles:

$$c_0 = a_0, \quad c_n = \sqrt{a_n^2 + b_n^2}, \quad \theta_n = \tan^{-1}\left(\frac{b_n}{a_n}\right). \quad (1.5)$$

In this thesis, we propose two new approaches based on multilayer perceptrons to identify the parameters a_0, a_n, b_n of (1.3) with a limited of $n = N$ terms in (Nguyen and Wira, 2013a; Nguyen and Wira, 2013b; Nguyen and Wira, 2015).

1.3 Nonlinear Load Classification

We know that the nonlinear loads or devices in a power system generate unwanted harmonics that cause many problems in power systems. Harmonic sources identification in a power system has been an important challenging task for many years. Non-intrusive appliance load monitoring (NILM) using the input current waveform was introduced in (Hart, 1992) and in (Sultanem, 1991). In these studies, they used appliance signatures to monitor residential loads. The current waveform amplitudes and load cycles were used to identify devices. This has been represented by [Figure 1.8](#) and a diagram of various nonlinear load classification techniques is showed in [Figure 1.9](#).

In this thesis, nonlinear load classification is separated in two main steps. The first step consists in extracting and identifying important features obtained from the signals and the second step is the classification which is based on the estimated features. The second step, i.e., the classifier of nonlinear loads, takes the features as the input and has several binary outputs. Obviously, the feature must significantly represent and characterize distorted waveforms. After analysis, this system is able to provide outputs showing which nonlinear load is ON or OFF.

The complete strategy for the identification and classification of nonlinear loads in a power system is shown on [Figure 1.10](#). We propose some new learning approaches for each of the two steps.

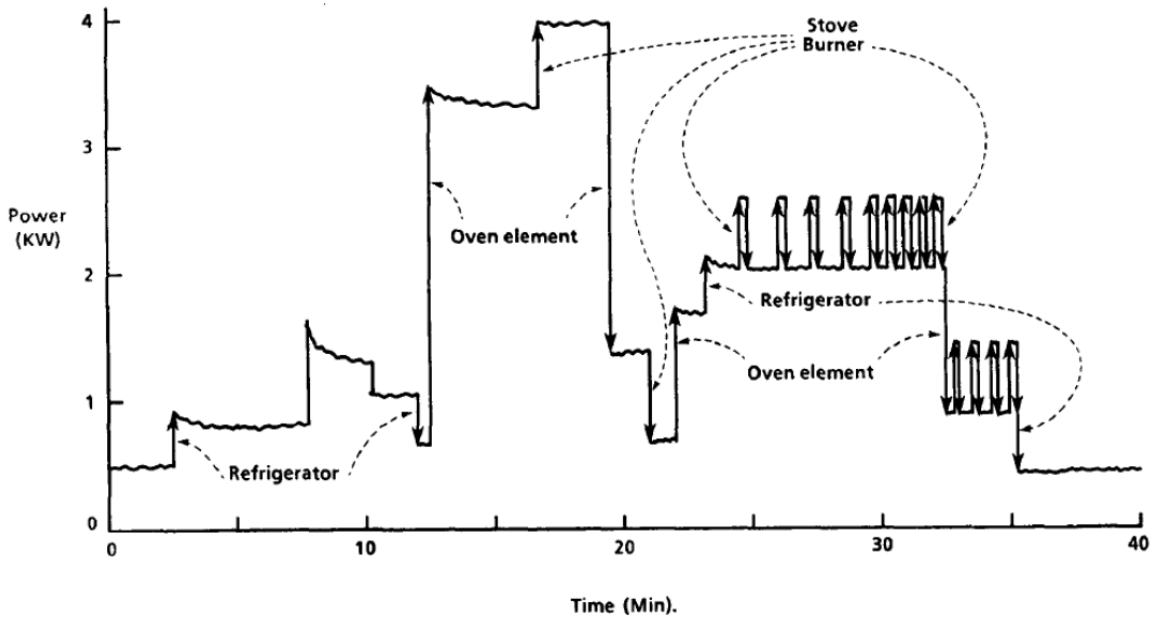


Figure 1.8 Appliance signatures on total load waveform in (Hart, 1992).

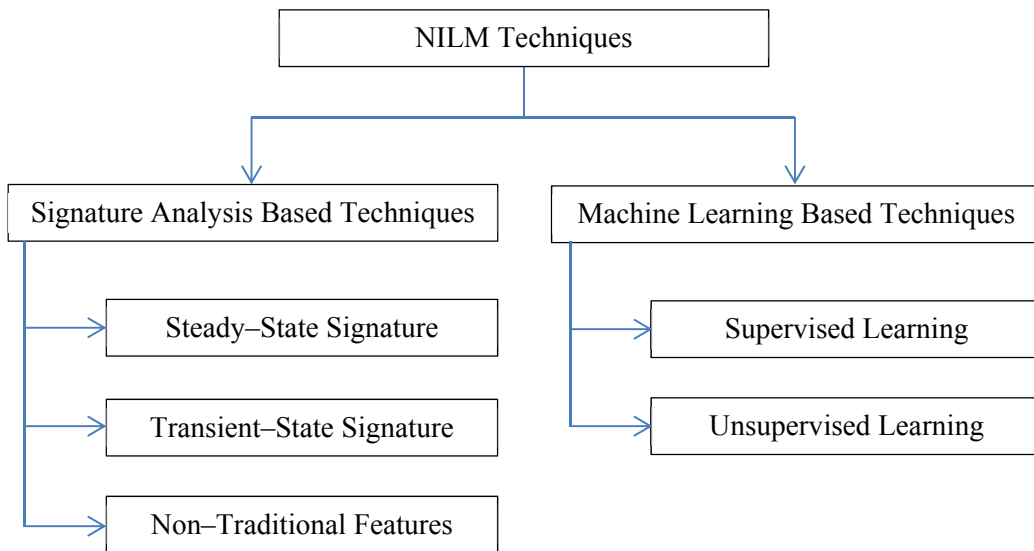


Figure 1.9 Classification of NILM techniques.

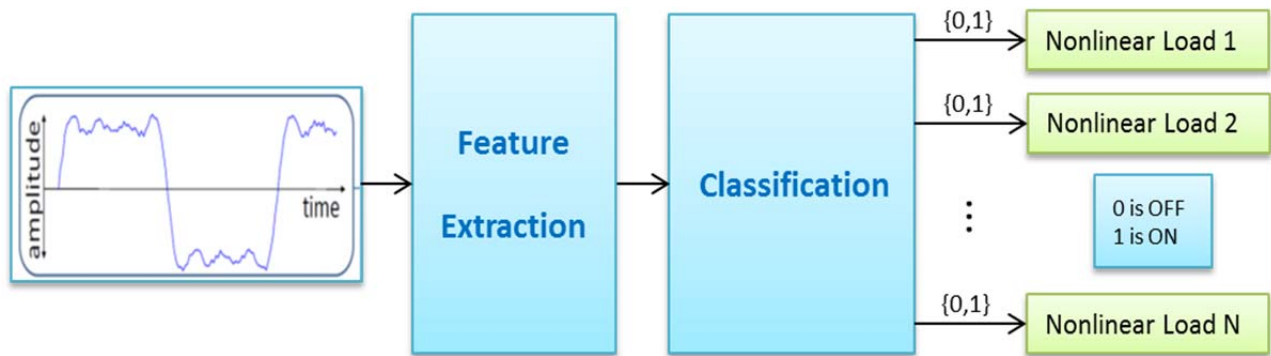


Figure 1.10 System diagram of nonlinear load classification.

1.4 Research Contributions

In this research, we have proposed several new approaches that based on multilayer perceptron networks for solving the two problems: The estimation of power system harmonics and the classification of non-linear loads from the distorted waveform in power systems. Our contributions are illustrated by the diagram of [Figure 1.11](#).

To solve the first problem, harmonics estimation, we proposed two methods. The first method is called the linear multilayer perceptron and the second method bases on a structure with several multilayer perceptron networks.

In the first new approach (Nguyen and Wira, 2013a; Nguyen and Wira, 2013b), a simple linear MLP has been developed for estimating the harmonics of distorted signals. The linear MLP is able estimate any periodic signal by expressing its output as a sum of harmonic components according to Fourier series. The network takes some specific harmonic elements with unit amplitudes as inputs and uses neurons that have linear activation functions. The measured signal serves as a reference and is compared to the network output. The amplitudes of the fundamental and high-order harmonics are deduced from the combination of the weights of the neurons. The linear MLP identifies the amplitudes of the fundamental component and high-order harmonic components with good precision even under noisy conditions.

In second new approach (Nguyen and Wira, 2015), we propose another new neural network approach based on the structure of MLPs for identifying current harmonics in power systems. The

learning approach is based on several MLP, adopts the Fourier decomposition of a signal and a training set generated from harmonic waveforms is used to calculate the weights. After training, each MLP is able to identify two coefficients for each harmonic term of the input signal. The effectiveness of the new approach is evaluated by experiments. Results show that the proposed MLPs of the new approach enable to identify effectively the amplitudes of harmonic terms from the signals under noisy condition. Results are compared to other and recent MLP approaches. The new approach can be applied in harmonic compensation strategies by being implement in an active power filter to ensure the power quality in electrical power systems.

To solve the second problem, non-linear load classification, we proposed 3 approaches based on machine learning techniques, 2 MLP technique based approaches and 1 SVM technique based approach. These systems receive the inputs that come from the output of the first step, i.e., harmonic components, and provide binary outputs (with values 0 or 1) that mean that non-linear devices are switched “OFF” or “ON” and working in the power system.

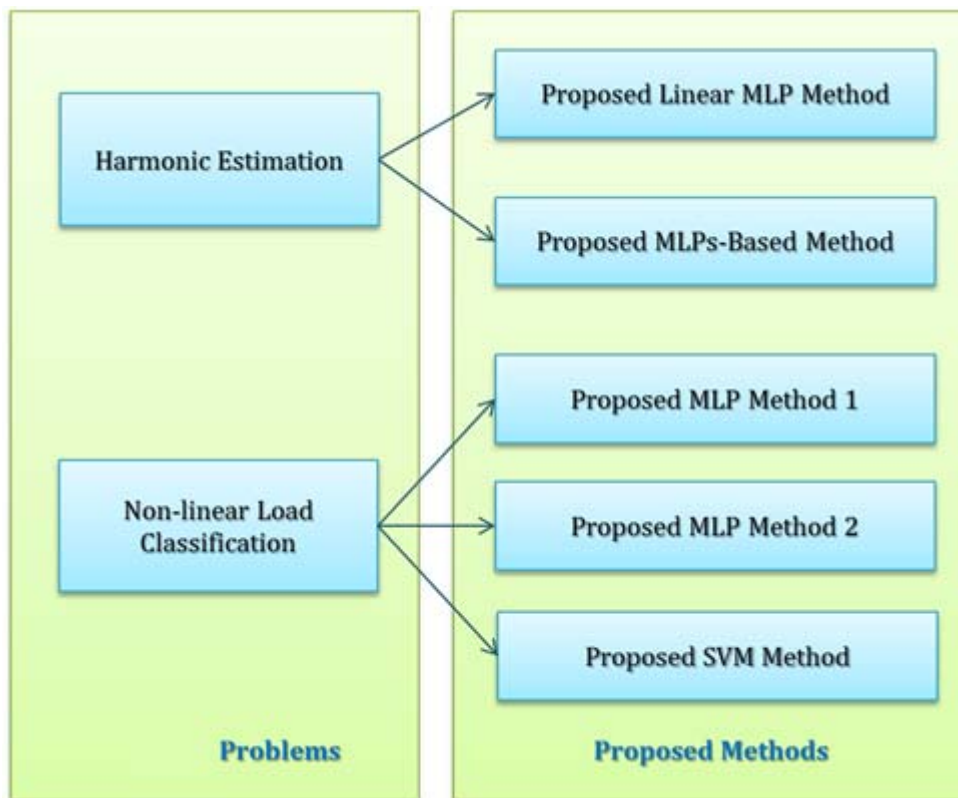


Figure 1.11 Thesis research contributions.

As a contribution for scientific research, the following is the list of our scientific publication from 2013 to 2015. They are four conference papers, one poster and one journal article as follows.

Four conference papers:

- (Wira and Nguyen, 2013) P. Wira and T. M. Nguyen, “Adaptive learning for on–line harmonic identification: An overview with study cases,” *International Joint Conference on Neural Networks (IJCNN 2013)*, Dallas, Texas, August 4–9, 2013
- (Nguyen and Wira, 2013a) T. M. Nguyen and P. Wira, “A new approach based on a linear Multi–Layer Perceptron for identifying on–line harmonics,” *39th Annual Conference of the IEEE Industrial Electronics Society (IECON 2013)*, Vienna, Austria, November 10–13, 2013
- (Nguyen and Wira, 2013b) T. M. Nguyen and P. Wira, “A linear Multi–Layer Perceptron for identifying harmonic contents of biomedical signals,” *9th International Conference on Artificial Intelligence Applications and Innovation (AIAI 2013)*, Paphos, Cyprus, September 30 – October 2, 2013
- (Nguyen and Wira, 2015a) T. M. Nguyen and P. Wira, “Power grid higher–order harmonics estimation with multilayer perceptrons,” *11th International Conference of Computational Methods in Sciences and Engineering (ICCMSE 2015)*, Athens, Greece, March 20–23, 2015

One scientific poster and presentation:

- (Nguyen and Wira, 2014) T.M. Nguyen and P. Wira, “Artificial neural network approaches for identifying power system harmonics”, *Poster dans la Journée Doctorale Sciences de l’École Doctorale 269 « Mathématiques, Sciences de l’Information et de l’Ingénieur (MSII) »*, Université de Haute–Alsace, 9 juillet 2014

One journal article:

- (Wira and Nguyen, 2017) P. Wira and T.M. Nguyen, “Current harmonic estimation in power transmission lines using Multi–Layer Perceptron learning strategies,” *Journal of Electrical Engineering*, vol. 5, pp. 219-230, July-Aug. 2017 (DOI: 10.17265/2328-2223/2017.05.001).

1.5 Thesis Structure

There are two main scientific problems that need to be solved in this thesis. The first problem is the power system harmonic estimation/identification in a power system. The second problem is the load signature discrimination in a power system. The following chapters of this thesis are organized as follows.

Chapter 2 presents a literature review of existing techniques on the power system harmonic identification problem. The non-neural techniques, the neural techniques, and the hybrid techniques are presented.

Chapter 3 presents a literature review of existing techniques on the nonintrusive appliance load monitoring (NILM) that relate to the nonlinear load classification problem.

Chapter 4 presents two new proposed artificial neural network based approaches that have been developed for harmonic estimation/identification of the distorted signals. The first proposed approach method is based on a new proposed linear MLP. In this model, all of transfer functions of all neurons are linear in order that it can represent a Fourier series for a distorted waveform. The second new approach is a structure that is based on several typical MLPs. Each MLP network in this structure is able to learn off-line and estimate the coefficients of each harmonic component in the distorted waveform. The computer experiments and experimental results of these proposed approach methods for solving the power system harmonic identification problem are also presented in this chapter.

Chapter 5 presents three our proposed methods for the nonlinear load classification problem. The first proposed approach method is based on a binary output multilayer perceptron. The second proposed method is based on a structure of single-binary-output multilayer perceptrons. And the third proposed approach method is based on a structure of multiple support vector machines. The computer experiments and experimental results of these proposed approach methods for solving the nonlinear load classification problem are also presented in this chapter.

Finally, Chapter 6 summarizes and provides a discussion about the new methods proposed in this thesis. This chapter also gives some recommendations for some future works.

Chapter 2 : Harmonic Identification

2.1 Introduction

For power system harmonic estimation, many existing techniques have been developed in the field of digital signal processing. In this chapter, we present several existing techniques of power system harmonics identification. We categorize them into three groups of techniques: the non-neural techniques, the neural techniques, and the hybrid techniques. Section 2.2 reviews the existing non-neural approaches for harmonic identification in power systems. In Section 2.3, we present the neural approaches for this problem. The recent hybrid techniques are also introduced in Section 2.4.

2.2 Non-Neural Techniques

In this section, we introduce to several non-neural techniques for harmonic estimation as follows: discrete Fourier transforms, Kalman filtering, wavelet transform, Hilbert-Huang transform, chirp z-transform, Prony's method, multiple signal classification, estimation of signal parameters via rotational invariance technique (ESPRIT), phase-locked loop, genetic algorithm and particle swarm optimization.

2.2.1 Discrete Fourier Transform

Over last many decades, discrete Fourier transform (DFT) and fast Fourier transform (FFT) have been most chosen by the practitioners and researchers. DFT is the most basic method in spectral analysis for analyzing harmonics of stationary discrete signals in wide applications. In direct computation, the DFT algorithm requires N^2 operations.

To reduce the number of operations of DFT, Cooley and Tukey proposed an algorithm for machine calculation of complex Fourier series, today called the FFT, in their publication in 1965 (Cooley and Tukey, 1965). In 1978, Winograd proposed an improvement of DFT in his publication titled "On Computing the Discrete Fourier Transform" (Winograd, 1978). Today, FFT is the most common algorithm applied for solving the harmonic analysis problem in many useful power system applications. FFT is the simplest method for identifying power system harmonics.

However, applications of FFT still have the inherent limitations such as spectral leakage, aliasing, and the picket-fence effect (Girgis *et al.*, 1991). Moreover, FFT needs many cycles of the

voltage or current waveform data. To improve these limitations, many extensions and improvements of DFT and FFT have been proposed in (Harris, 1978; Portnoff, 1980; Testa *et al.*, 2004; Barros and Diego, 2006; Ren and Wang, 2010).

2.2.2 Kalman Filtering

In 1960, R. E. Kalman proposed a new approach to linear filtering and prediction problems in his publication (Kalman, 1960). Kalman filtering or Kalman Filter (KF) is an algorithm and a model, with a set of state equations and measurement equations, that uses noisy and inaccurate data measured over time and provide an efficient estimation of past, present or future values by minimizing the mean of the squared error. In order to estimate different states or parameters, a number of power system applications have used KF. This technique uses a simple and robust algorithm for estimating the magnitude of the known harmonics in the signal along with stochastic noise.

A harmonic analysis based on KF technique was reported in (Sharma and Mahalanabis, 1973). An extended KF based technique was proposed in (Andria *et al.*, 1992) for on-line identification of the instantaneous values of fundamental and harmonic contents. In 1996, a KF was used for identification and tracking of harmonic sources in a power system (Ma and Girgis, 1996). Their study shows that the Kalman filter can be employed as a solution for harmonic source identification: the optimal location of a limited number of harmonic meters and the optimal dynamic estimation of harmonic injections and their locations. In 1998, S. Liu proposed an adaptive KF for dynamic estimation of harmonic signals of a measured vehicle line current and the simulation illustrates the effectiveness of the proposed method especially for railway vehicle applications (Liu, 1998).

In 2003, an application of the KF was proposed to harmonic signal analysis in power system (Kennedy *et al.*, 2003). There were three test signals that were used to test the KF analysis. Each signal included 5th, 7th, 11th, and 13th harmonics with the Gaussian white noise with a standard deviation of 0.01, representing a SNR of 40dB. To improve convergence of non-linear models, an adaptive algorithm was used. This algorithm was demonstrated that by adopting a methodical approach to choosing the error covariance of Q and R the Kalman filter can be successfully tuned to provide accurate analysis of harmonic content and fundamental frequency even during extreme power system disturbance. (Köse *et al.*, 2010) employed a combination of extended KF and linear KF for spectral decomposition of distorted supply to estimate harmonics and interharmonics.

2.2.3 Wavelet Transform

Nowadays, the Wavelet Transform (WT) (Grossman and Morlet, 1984; Mallat, 1989) is one of the most popular candidates of the time–frequency transformations. WT utilizes wavelets to represent any signal for detailed analysis with multiple time–frequency resolution. In 2002, T. Keaochantranond and C. Boonseng used WT for estimation harmonics and interharmonics in (Keaochantranond and Boonseng, 2002). In 2008, Y. Chen proposed an approach based on wavelet multi–resolution analysis for harmonic detection in electric power system (Chen, 2008).

2.2.4 Hilbert–Huang Transform

The Hilbert–Huang Transform (HHT) (Huang *et al.*, 1998; Huang and Attoh–Okine, 2005) is a method to decompose a signal into so–called intrinsic mode functions along with a trend, and identify instantaneous frequency data. It works well on non–stationary and nonlinear data. In 2009, HHT based techniques for harmonic estimation was proposed in (Yu and Yang, 2009; Chen *et al.*, 2009; Zhang *et al.*, 2009).

2.2.5 Chirp Z–Transform

The Chirp Z–Transform (CZT) (Rabiner *et al.*, 1969) is a generalization of the DFT. While the DFT samples the Z plane at uniformly–spaced points along the unit circle, the chirp Z–transform samples along spiral arcs in the Z–plane, corresponding to straight lines in the S plane. The DFT, real DFT, and zoom DFT can be calculated as special cases of the CZT. T. T. Wang published a segmented CZT based technique that has the advantages of its ability to handle a very large amount of input data and to limit its computation to a portion of the frequency spectrum of interest thus providing greatly increased dynamic range and frequency resolution in (Wang, 1990). In 1996, the segmented CZT was also used by (Daponte *et al.*, 1996) with multiple deep dip windows for electrical power system harmonic analysis. In (Tarasiuk, 2011), the CZT and the DFT were employed to propose for power quality estimator analyzer.

2.2.6 Prony’s Method

Prony's method was developed by Gaspard Riche de Prony in 1795. Similar to the Fourier transform, Prony's method extracts valuable information from a uniformly sampled signal and builds a series of damped complex exponentials or sinusoids. This allows for the estimation of frequency, amplitude, phase and damping components of a signal. F. F. Costa and A.J.M. Cardoso

proposed a technique based on improved Prony's method for identification of harmonics and interharmonics in (Costa and Cardoso, 2006). C.-I. Chen and G.W. Chang proposed an efficient Prony's method for time-varying power system harmonic estimation in (Chen and Chang, 2009).

2.2.7 MUSIC

Multiple signal classification (MUSIC) is an algorithm used for frequency estimation. MUSIC estimates the frequency content of a signal or autocorrelation matrix using an eigenspace method. In 2006, a harmonic extraction algorithm based on MUSIC was presented in (Wang and Lu, 2006). However, MUSIC is not still popular in power harmonics estimation because of its high computational cost.

2.2.8 ESPRIT

Estimation of signal parameters via rotational invariant techniques (ESPRIT) (Paulraj *et al.*, 1986) is a technique to determine parameters of a mixture of sinusoids in a background noise. ESPRIT was successfully applied for harmonics estimation in papers (Lobos *et al.*, 2000; Bracale and Carpinelli, 2009; Tao *et al.*, 2010).

2.2.9 PLL

A Phase Locked Loop (PLL) is simply an oscillator that generates an output signal whose phase is related to the phase of an input signal. Phase-locked loops are commonly used in radio, telecommunications, computers and other wide electronic applications. An enhanced PLL is employed for measurement of harmonics and inter-harmonics of time-varying frequencies in (Karimi-Ghartemani and Iravani, 2003). PLL was applied for real-time estimation of fundamental frequency and harmonics for shunt active power filters in aircraft electrical systems in papers (Lavopa *et al.*, 2009; Cupertino *et al.*, 2011).

2.2.10 GA

Genetic Algorithm (GA) is a search heuristic that mimics the process of natural selection. This heuristic (also sometimes called a meta-heuristic) is routinely used to generate useful solutions to optimization and search problems. In 2007, Seifossadat's research group proposed a technique using adaptive perceptrons based on a GA for harmonic estimation in power system (Seifossadat *et al.*, 2007).

2.2.11 Particle Swarm Optimization

Particle Swarm Optimization (PSO) is a computational method that optimizes a problem by iteratively trying to improve a candidate solution with regard to a given measure of quality. PSO optimizes a problem by having a population of candidate solutions, here dubbed particles, and moving these particles around in the search-space according to simple mathematical formulae over the particle's position and velocity. Each particle's movement is influenced by its local best known position but, is also guided toward the best known positions in the search-space, which are updated as better positions are found by other particles. This is expected to move the swarm toward the best solutions. In 2008, Z. Lu et al. presented a new algorithm for harmonic estimation (Lu *et al.*, 2008). They used the PSO with passive congressing to estimate the phase of the harmonics. And a least-square method is employed to estimate the amplitudes. This method is also used to estimate interharmonics and the harmonics with frequency deviation with good results.

2.3 Neural Techniques

In this section, we introduce to the neural techniques for harmonic estimation. They are methods that based on artificial neural networks. Since 1990s, artificial neural networks (ANNs) have been applied for estimating harmonics in power systems. ADALINEs, Multi Layer Perceptrons (MLPs), Recurrent Neural Networks (RNNs), Radial Basis Function Neural Network (RBFNNs) are the most used ANNs for estimating harmonics in power systems.

2.3.1 ADALINE

The architecture of the ADALINE is based on very simple unit which performs a processing. This unit consists of weights, a bias and a summation function, they are shown on [Figure 2.1](#). The processing comprise the calculation of the output for given inputs and the learning phase, i.e., the weights adjustment. The ADALINE is able to fit any linear relationships by providing a scalar output as a weighted sum of the inputs and by adapting its weights. When a multidimensional output space must be considered, i.e., when several outputs are required, several ADALINE having the same inputs are used and this is sometime referred to as a multiple ADALINE.

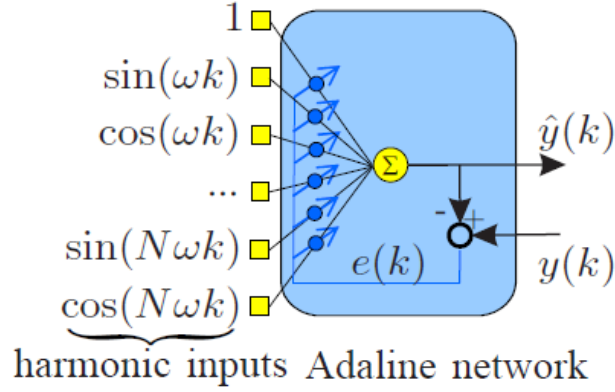


Figure 2.1 ADALINE architecture with harmonic terms as inputs.

Let \mathbf{x} and \mathbf{w} be two vectors, respectively for the inputs and weights. For mathematical convenience, let the first element of \mathbf{x} be equal to 1, so that the first element of \mathbf{w} becomes the bias weights. At instant k , the output $\hat{y}(k)$ is a weighted sum given by the following dot product:

$$\hat{y}(k) = \mathbf{w}^T(k)\mathbf{x}(k). \quad (2.1)$$

The ADALINE network is a supervised learning network that needs to associate a reference value for each input vector. This reference is a desired value corresponding to an input and expressed in the ADALINE's output space. When an input $\mathbf{x}(k)$ is presented to the network, the output $\hat{y}(k)$ is calculated and compared to the desired output $y(k)$ that is associated to it. This defines the error

$$e(k) = y(k) - \hat{y}(k) = y(k) - \mathbf{w}^T(k)\mathbf{x}(k). \quad (2.2)$$

The pairs of input/output values $\mathbf{x}(1), y(1), \mathbf{x}(2), y(2), \dots, \mathbf{x}(Q), y(Q)$ represents the learning data set. Each pair can be used on-line to adapt the weights at each iteration in order to minimize the error $e(k)$. The new value of the weight vector is updated from its previous according to the μ -LMS rule or to the α -LMS rule, i.e., respectively

$$\mathbf{w}(k+1) = \mathbf{w}(k) + \mu e(k) \mathbf{x}(k), \quad (2.3)$$

$$\mathbf{w}(k+1) = \mathbf{w}(k) + \alpha \frac{e(k) \mathbf{x}(k)}{\|\mathbf{x}(k)\|^2}, \quad (2.4)$$

where μ and α are learning rates. The α -LMS algorithm is only a normalized version of the μ -LMS algorithm. Normalizing the input \mathbf{x} , before applying it to the network, leads to the same

result using the μ -LMS algorithm. These learning rules come from the LMS algorithm and it called the Widrow-Hoff learning rule (Widrow and Walach, 1996). Approximately, the ADALINE converges to least squared error when $k \rightarrow \infty$ (Wang *et al.*, 2000), (Zeng *et al.*, 2006). The main characteristic of LMS algorithm is that it safes the error and it reduces the average quadratic error. Variants have been recapitulated in (Wira *et al.*, 2008).

In (Widrow and Walach, 1996) and (Wang *et al.*, 2000), $\mathbf{w}(k+1)$ is the new value that will take the weight vector from its previous value $\mathbf{w}(k)$ which represents the memory of the network. In the weight update process, the learning rate gives more or less importance to the innovation term based on the error compared to the memory term $\mathbf{w}(k)$. Therefore, the values of the rates μ and α are chosen between 0 and 1.

In power system, identifying the harmonics allows to separate the disturbing higher-order harmonics introduced by non-linear loads from the fundamental term carrying the electric energy (Arrillaga and Watson, 2003). These operations are necessary for monitoring and ensuring electric power quality. Efficient methodologies for the analysis and measurement of the basic electric magnitudes in are required. Methods with short computation time for real-time calculation must be employed for the generation of compensating currents in order to instantaneously re-inject them, most often with shunt active power filtering schemes (Akagi, 1996).

The following shows how ADALINE-based approaches can be judiciously used for estimating the frequency/harmonic content of power signals. Frequency estimation means estimating the fundamental frequency and tracking its fluctuations and deviations. Harmonics identification means estimating the amplitudes and phases of the harmonic terms contained in the signal.

The use of an ADALINE to learn the Fourier series of the signal given by (1.2) has been introduced in (Dash *et al.*, 1996). This work corresponds to the general approach detailed in Section 1.2 where a decaying DC quantity is added to the signal model. An additional element ($-kT_s$) s therefore introduced in the ADALINE input vector and allows to efficiently track the amplitude and the phase of 6 harmonic terms. A similar approach is proposed in (Dash *et al.*, 1998), where a signal model with a different expression of the decaying quantity is used. This leads to the modification of one element of the input vector. The estimation error is also fed back recurrently in order to enhance the input vector by 3 elements ($e(k)$, $e(k-1)$, and $e(k-2)$). The very simplest approach, based on the Fourier series, is also used in (Vázquez *et al.*, 2001) and in (Tey *et al.*, 2005). In this last work, only two weights elements of fundamental component are

updated, hence it is independent of the harmonic orders present. In (El Shatshat *et al.*, 2002), the same approach and the same signal model is used, one ADALINE is used for harmonic estimation, another is used for predicting the line voltage.

The S-ADALINE proposed in (Sarkar and Sengupta, 2009) is able to synchronize itself with time-varying signals to the frequency deviation for on-line tracking of single phase reactive power. It contains a fundamental angular frequency deviation measurement algorithm that is used to generate sine and cosine terms of the input vector of the ADALINE. These terms are thus in phase with the fundamental term of the measured signal. In (Chang *et al.*, 2009), two ADALINES in a cascaded two-stage approach is used. In the first stage, an ADALINE implements the Prony's method for tracking the fundamental frequency of the measured signal. In the second stage, an ADALINE learns the Fourier series decomposition of the signal with the very simplest approach for estimating the amplitudes of the harmonics.

The previous approaches identify the harmonics in the measured signal reference frame. This means that the measured signal, i.e., the current, is directly expanded into a Fourier series which is learned by an ADALINE. However, the measured signal can be converted into another reference frame before being expanded, learned and approximated by an ADALINE. If the principle remains the same, the conversion of the signal in a different reference frame allows highlighting more or less some parts of the signal. The current is thus converted into a virtual power space by multiplying the measured current by a sine term in (Ould Abdeslam *et al.*, 2007). In another of (Ould Abdeslam *et al.*, 2007), 2 ADALINES serve to estimate the Fourier series of the instantaneous PQ-powers (Akagi, 1996) which requires the measure of the currents and of the voltages for the 3 phases. In (Wira *et al.*, 2008), measured current of the 3 phases is converted into a current expressed in the DQ-space with the Park transform. A complex ADALINE is proposed in (Sadinezhad and Joorabian, 2009). This approach estimates the fundamental frequency of a power system with an input vector composed of sine and cosine terms. To produce the input vectors and deal with the decaying DC term, the Park transformation is used. The two weights associated to the fundamental frequency are used through a hamming filter to calculate the amplitude of the fundamental term.

The ADALINE for frequency estimation and harmonic identification can be used in different way by replacing the Fourier series expression by a recursive linear expression of a signal. Considering a measured signal of the type given by (1.1), three consecutive samples $y(k)$, $y(k-1)$, and $y(k-2)$ meet the relationship

$$y(k) = (2 \cos \omega_0 T_s) y(k-1) - y(k-2) \quad (2.5)$$

The inputs of the ADALINE therefore become $\mathbf{x} = [y(k-1) \quad y(k-2)]^T$ and its outputs is compared to the reference signal $y(k)$ with is the measured signal at instant k . After minimizing the error, the weights converge to $\mathbf{w}^* = [w_1^* \quad w_2^*]^T = [2 \cos \omega_0 T_s \quad -1]^T$. The frequency can thus be obtained from the first element of \mathbf{w}^* . Indeed, $\hat{f} = (2\pi T_s)^{-1} \cos^{-1}(w_1^*)$. As can be seen, it is simple and therefore well suited for the frequency estimation problem. However, it is sensitive to noise because based on ideal expression of the current waveform.

This simple principle is used in (Dash *et al.*, 1997) where the ADALINE inputs are enhanced by additional harmonic terms to take account of a decaying DC component and harmonic distortion present in the power system signal. Fundamental frequency estimation is thus achieved. In (Abdel-Galil *et al.*, 2003), a tapped delay line of the measured current is used to generate the inputs for the ADALINE. Power quality event detection is thus possible with an ADALINE with only 4 inputs.

In (Ai *et al.*, 2007), a tapped delay line of a large size is used to generate the ADALINE inputs for disturbance detection. The identification of the power system frequency is achieved by another ADALINE that combines delayed signal measures and sine and cosine inputs. More recently, (Abdollahi and Matifar, 2011) proposes an approach for frequency estimation but not with an ADALINE. It a least-squares approach that uses 3 consecutive measures of the signal and that calculates once per iteration the solution (i.e., coefficients equivalent to the weights of the ADALINE) by using a pseudo-inverse computing.

In 1987, B. Widrow *et al.* presented the fundamental relations between the least-mean-square (LMS) algorithm and the DFT in their publication. The paper established a connection between the DFT and the adaptive LMS. The result is the “LMS spectrum analyzer,” a new means for the calculation of the DFT. [Figure 2.2](#) shows a block diagram of LMS spectrum analyzer in (Widrow *et al.*, 1987). In 1996, a new approach in [Figure 2.3](#) was proposed for harmonics estimation using Fourier linear combiner realized using an adaptive linear neuron known as ADALINE in (Dash *et al.*, 1996). This approach is unlike from the previous backpropagation approaches and allows better control the stability and speed of convergence by appropriate choice of parameters of the error difference equation.

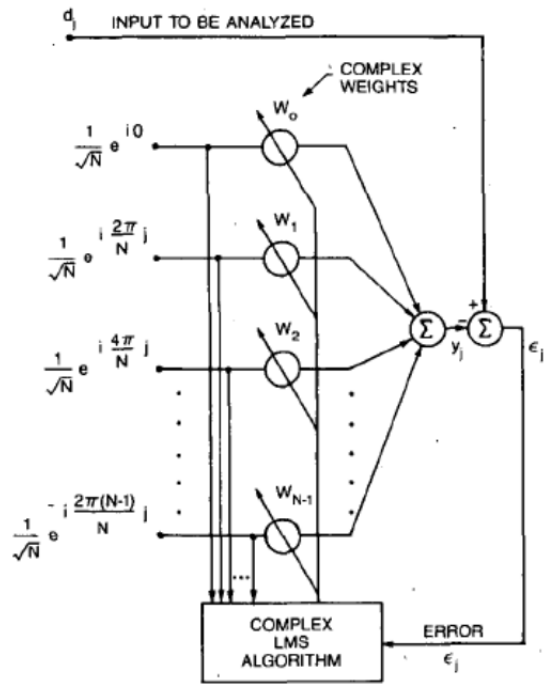


Figure 2.2 Block diagram of the LMS spectrum analyzer in (Widrow *et al.* , 1987).

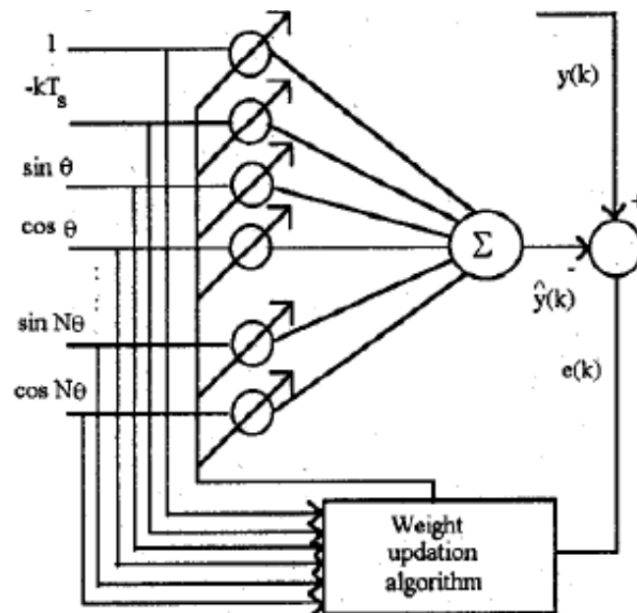


Figure 2.3 Fourier linear combiner for harmonic estimation as an ADALINE.

In 1998, P. K. Dash applied ADALINE for tracking 3-phase voltages and currents (Dash *et al.*, 1998) as in [Figure 2.4](#). In 2009, a two-stage Adaline in [Figure 2.5](#) was proposed for harmonics and interharmonics measurement by (Chang *et al.*, 2009). A. Sakar and S. Sengupta proposed a self-synchronized Adaline network for on-line tracking of single phase reactive power in non-sinusoidal conditions (Sakar and Sengupta, 2009; Sakar *et al.*, 2011) as in [Figure 2.6](#).

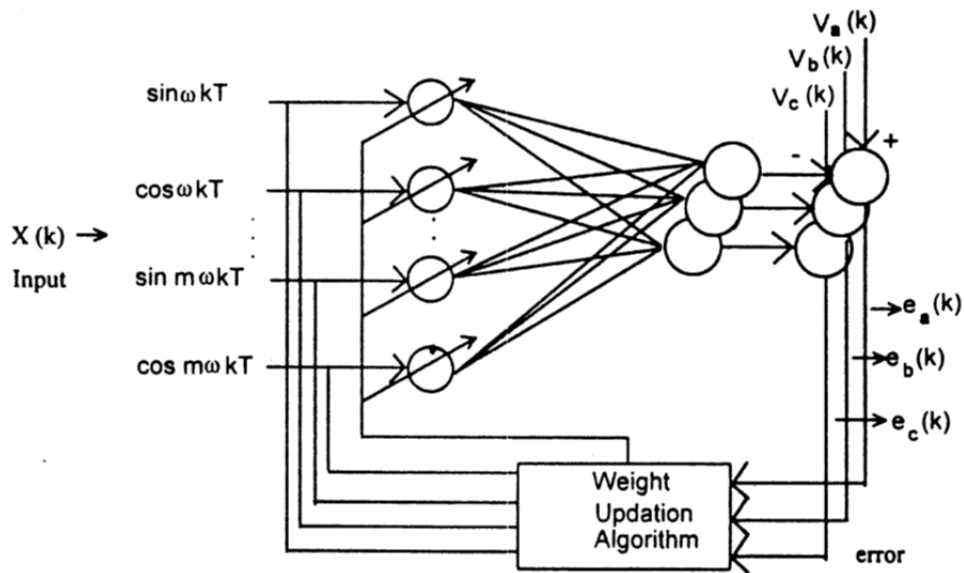


Figure 2.4 An ADALINE for tracking 3-phase voltages and currents in (Dash *et al.*, 1998).

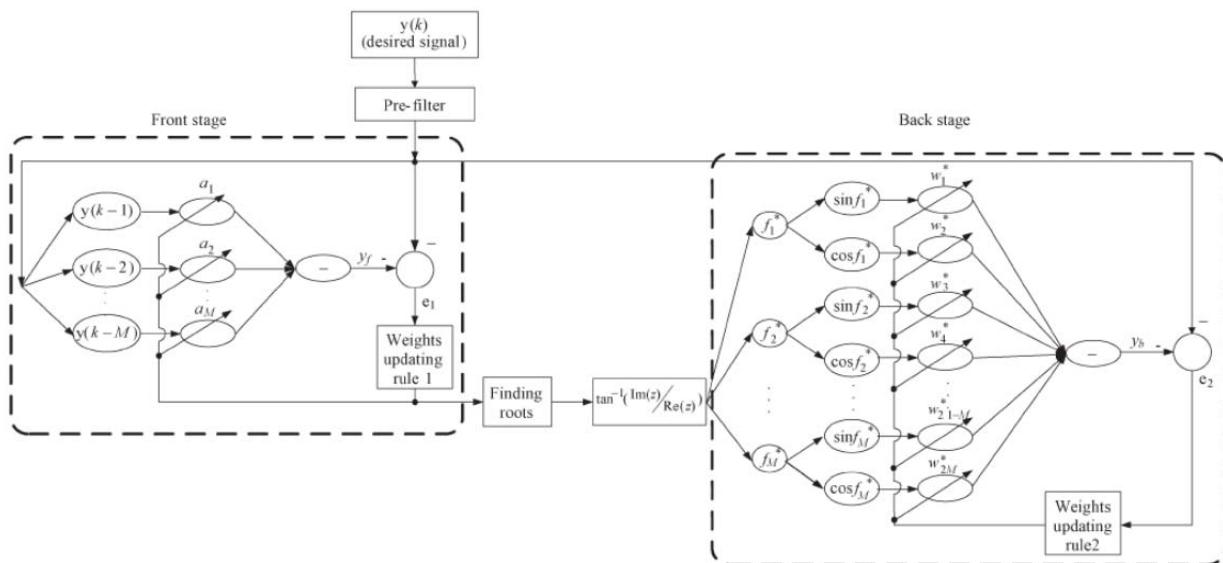


Figure 2.5 A two-stage ADALINE for harmonics and interharmonics measurement.

In 2011, B. Vasumathi and S. Moorthi developed the concept of modified ADALINE algorithm with Time-Variant Widrow – Hoff (TVWH) rule for an optimization problem with selected harmonic elimination in PWM inverter (Vasumathi and Moorthi, 2011). The simulation is for both ADALINE algorithm and modified ADALINE algorithm. The modified ADALINE with TVWH rule is shown in [Figure 2.7](#).

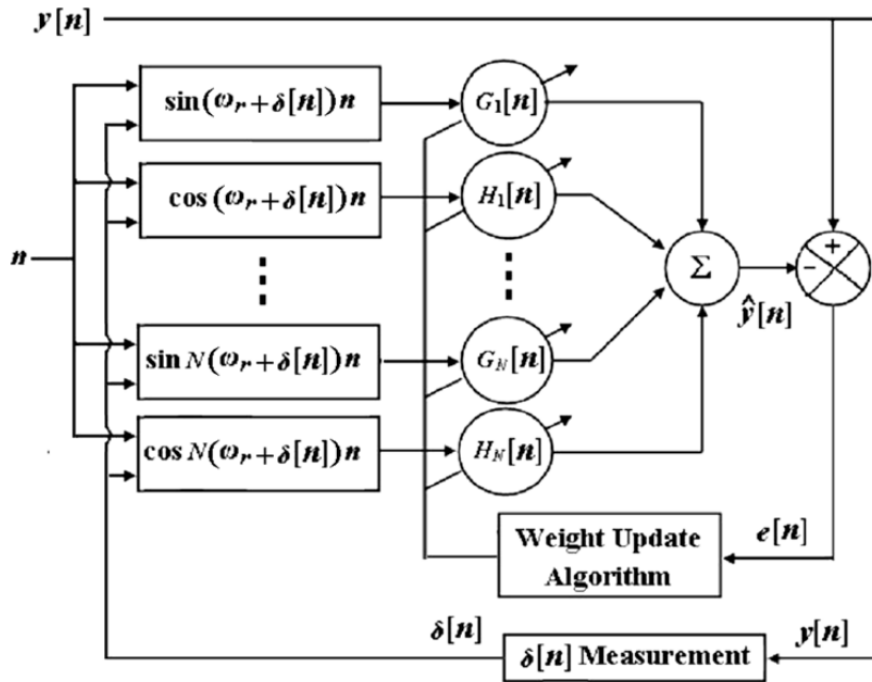


Figure 2.6 The architecture of S-ADALINE (Sakar and Sengupta, 2009).

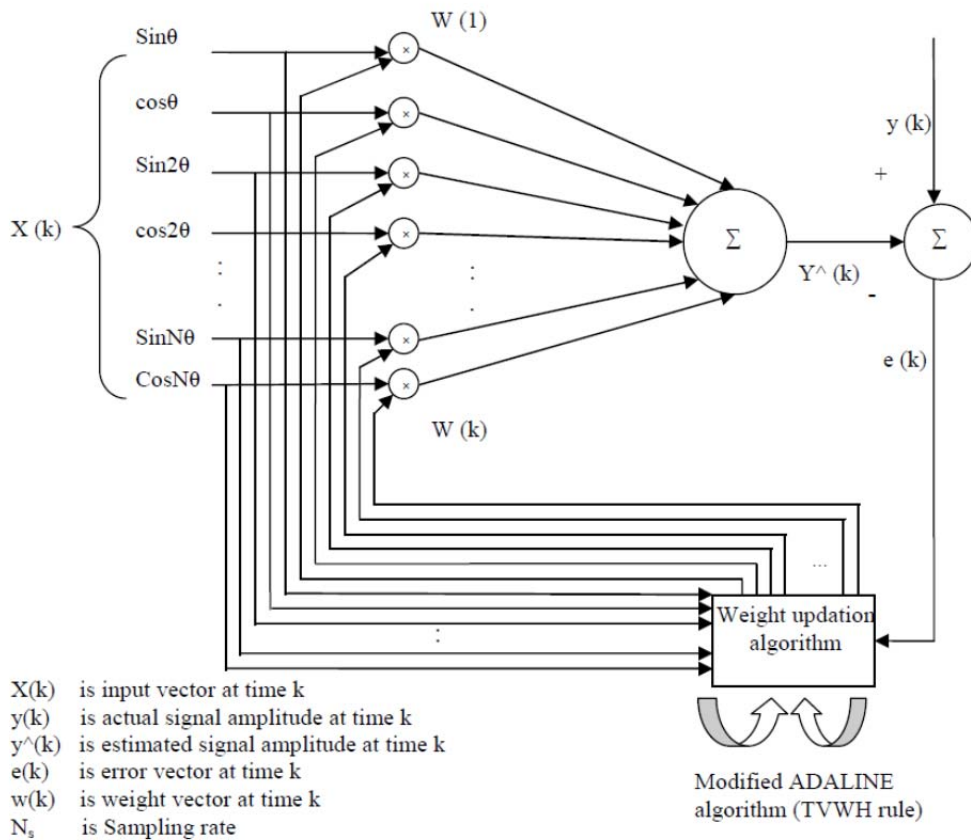


Figure 2.7 Modified ADALINE with TVWH rule.

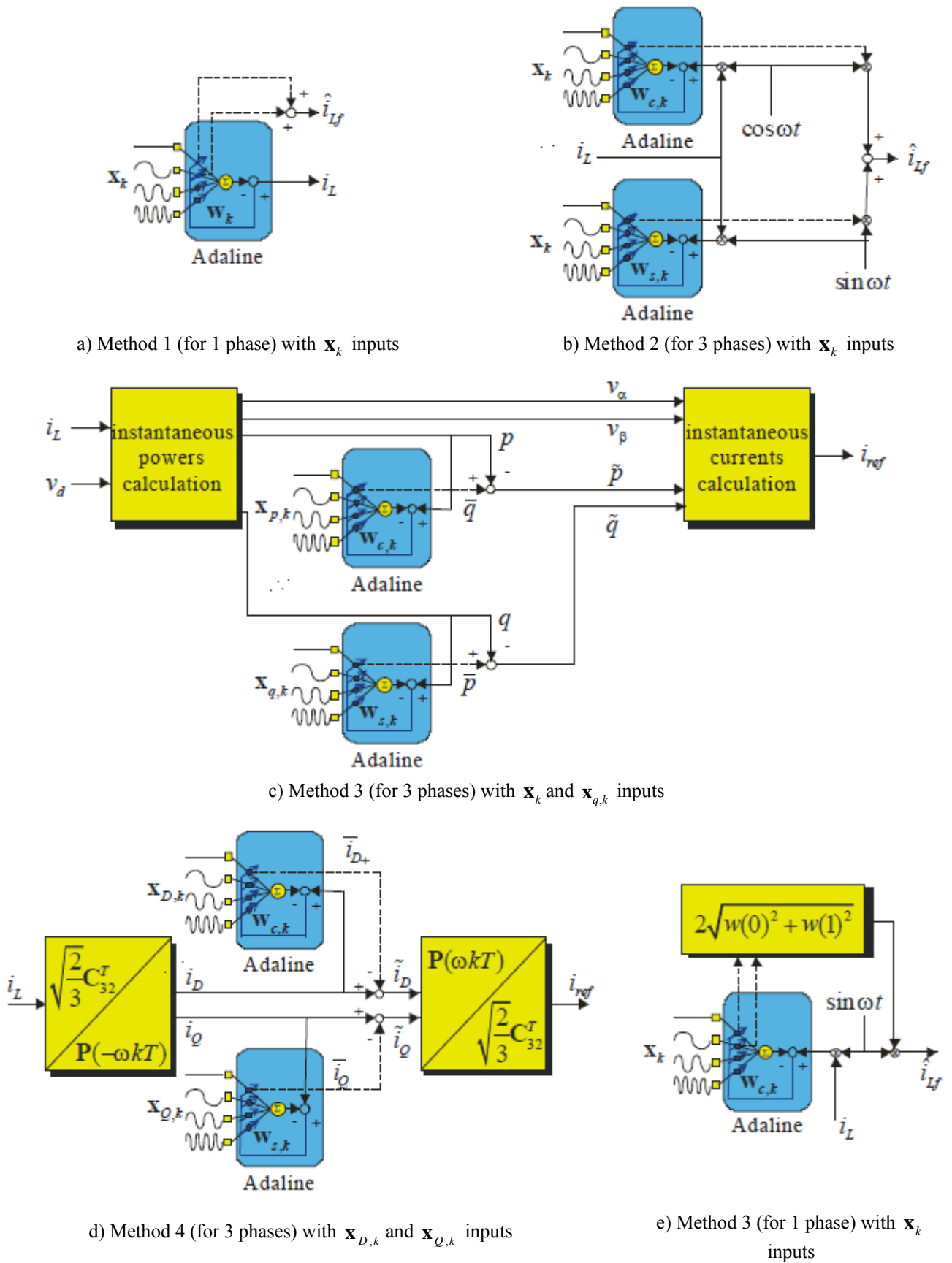


Figure 2.8 Methods based on ADALINE in (Wira *et al.*, 2010).

In (Wira *et al.*, 2010), five ADALINE based methods for harmonic identification are presented to improve the performance of an active power filter (APF) in its on–line control strategy. They are named “method 1: the direct neural method”, “method 2: the three–monophase method”, “method 3: the active and reactive powers method (neural IPT method)”, “method 4: the neural diphas currents method”, and “method 5: neural synchronous method”. Figure 2.8 shows block diagram of the neural schemes based on ADALINEs of methods in (Wira *et al.*, 2010).

2.3.2 Multilayer Perceptron

Multilayer Perceptron (MLP) network is the most artificial neural network model used in the world with its ability that can learning from the training data set and effectiveness for solving problems in nonlinear classification and pattern recognition. There are a number of applications of MLP in industry and commerce. The structure and principle of the MLP is detailed in the following.

MLP network is a kind of a family of feed forward neural network models. In this model, there are artificial neurons with activation function inside. The artificial neurons of a MLP network are structured into the layers (the hidden layers and the output layer). A MLP network has one input layer, one output layer and one or several hidden layers. There is not any artificial neuron in the input layer of the MLP. The input layer is only a layer as the entrance of the data into the model. The data comes into the model via the input layer, passes through the hidden layers and finally exit out of the model by the output layer.

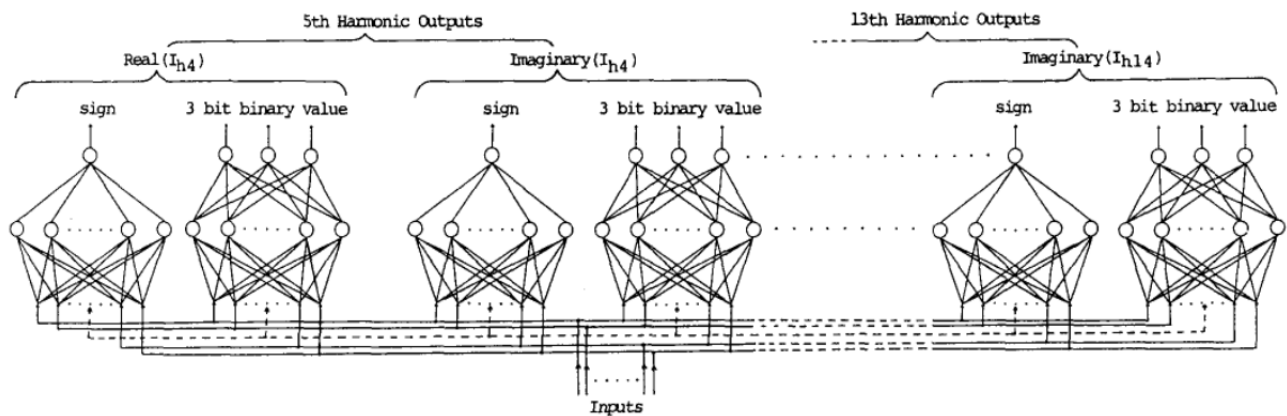


Figure 2.9 The structured NN for harmonic estimator in (Hattana and Richard, 1990).

In 1990, R. K. Hartana and G. G. Richards applied MLP networks in their proposed technique to estimate from 5th harmonic up to 13th harmonic contents in (Hartana and Richard, 1990). In their structured neural network, each harmonic output uses 4 MLPs: 2 MLPs for estimation of the real part and 2 MLPs for estimation of the imaginary part of each harmonic. The outputs of all

MLP are binary values with 0 or 1. Figure 2.9 shows the structure of harmonic estimator in (Hattana and Richard, 1990).

In (Pecharanin *et al.*, 1994 and 1995), they applied two MLPs with 3 layers using backpropagation learning algorithm to design a harmonic detector of 3rd harmonic and 5th harmonic contents in an active filter as showed in Figure 2.10.

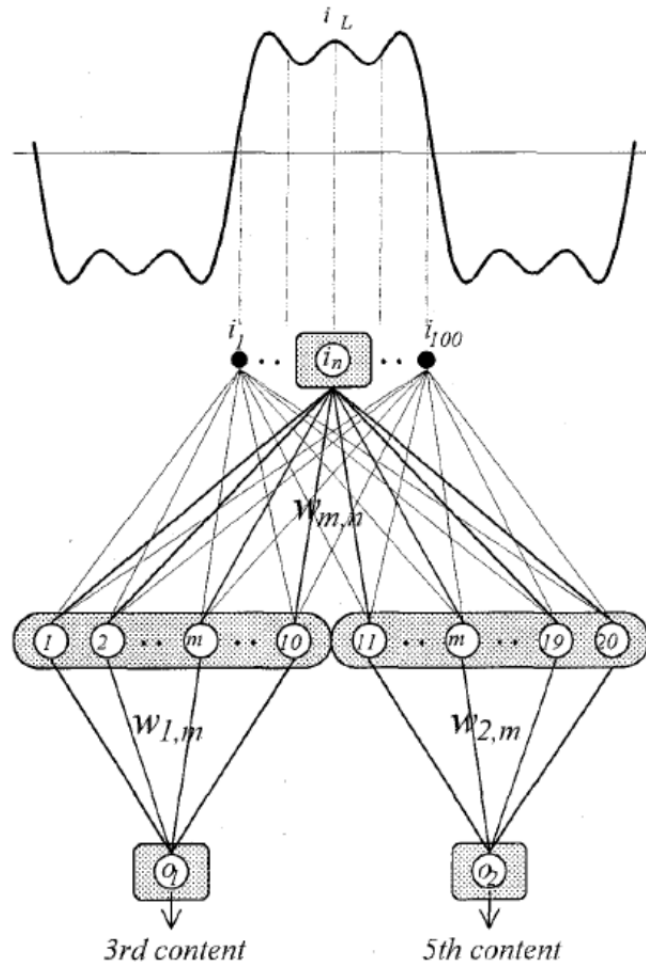


Figure 2.10 A MLP for estimation of 3rd and 5th harmonics (Pecharanin *et al.*, 1995).

In 1998, Md. Rukonuzzaman applied MLPs to an application in power system harmonic detection in (Rukonuzzaman *et al.*, 1998) as in Figure 2.11. The objective of their paper is to detect the components (magnitudes and phases) of harmonics in power distribution system. They used 2 MLPs to do this. The first MLP is used to estimate the A coefficients of 3rd, 5th and 7th harmonics. The second MLP estimate the B coefficients of 3rd, 5th and 7th harmonics. In their simulation to verify the proposed technique, each MLP is designed with 90 inputs, 19 hidden neurons and the number of output neurons depends to the number of harmonics that need to detect.

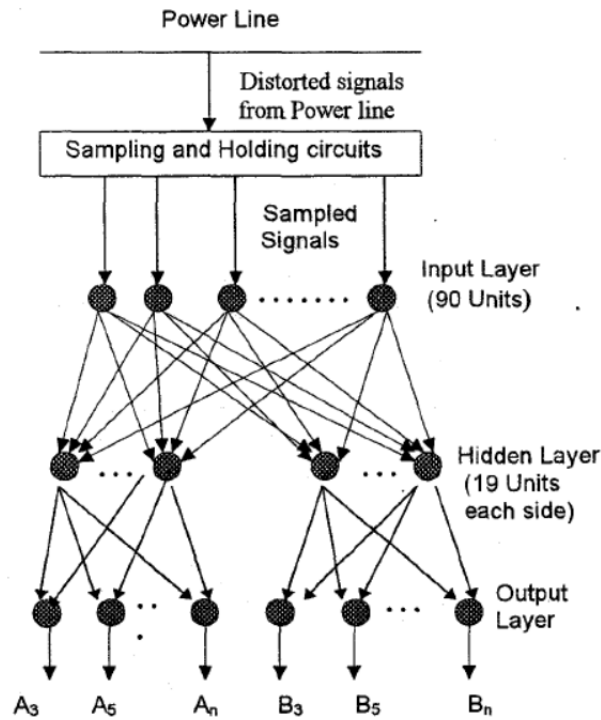


Figure 2.11 Harmonic detection process.

H. C. Lin proposed a MLP with 3 layers to fast detect precise harmonics in noisy environments by using only a half of cycle sampled values of distorted waveforms in his researches (Lin, 2004; Lin, 2007). The detected amplitudes and phases of harmonics are the outputs of the trained MLP. Figure 2.12 shows the MLP configuration for harmonic detection in (Lin, 2007).

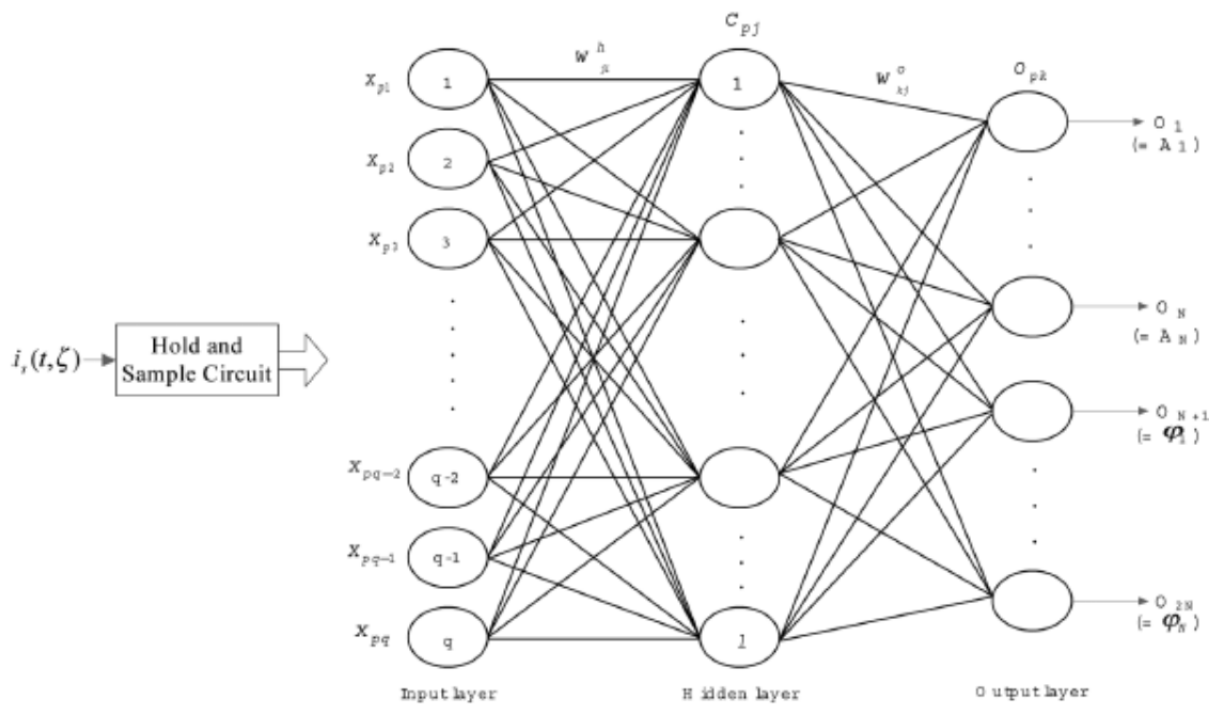


Figure 2.12 The MLP configuration for harmonic detection in (Lin, 2007).

In 2008, M. Tümay and others presented a harmonic extraction algorithm using MLP for dynamic voltage restorers (DVRs) (Tümay *et al.*, 2008). Their method used two different ANN structures such as a fully connection MLP and a partial connection MLP for extracting harmonic from distorted waveforms. The distorted waveforms including 3rd and 5th harmonics are employed as inputs for training the network with backpropagation training algorithm. Their proposed method is shown in Figure 2.13.

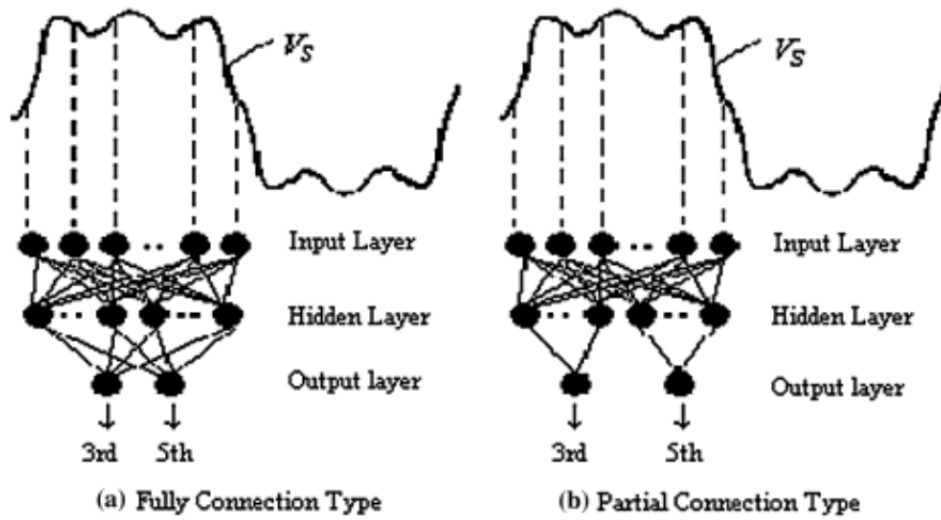


Figure 2.13 MLPs for harmonic extraction in (Tümay *et al.*, 2008).

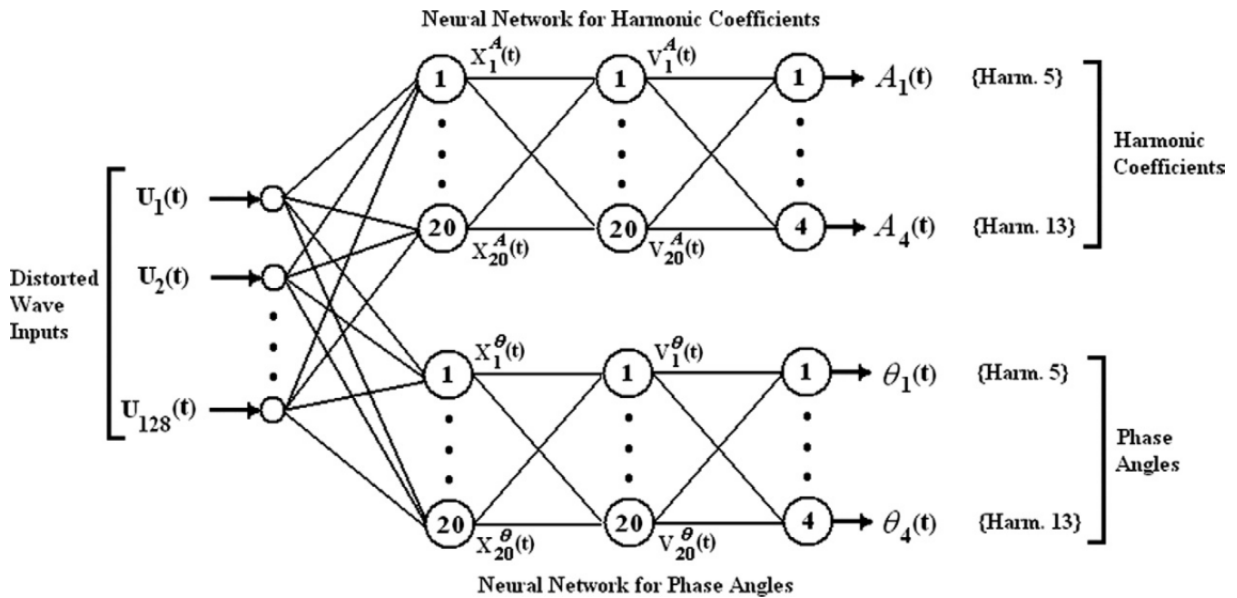


Figure 2.14 A MLP based structure for harmonics coefficient and phase angle detection (Temurtas and Temurtas, 2011).

In 2011, H. Temurtas and F. Temurtas used two MLP for detection of the harmonic coefficient and relative phase shifts. The simulation used the distorted waveform including uniform distributed 5th, 7th, 11th, 13th, 17th, 19th, 23rd, 25th harmonics with up to 20 degrees relative phase shifts. The first trained MLP is used to detect harmonics coefficients. The second trained MLP detects relative phase angles (Temurtas and Temurtas, 2011). The proposed method is shown in Figure 2.14.

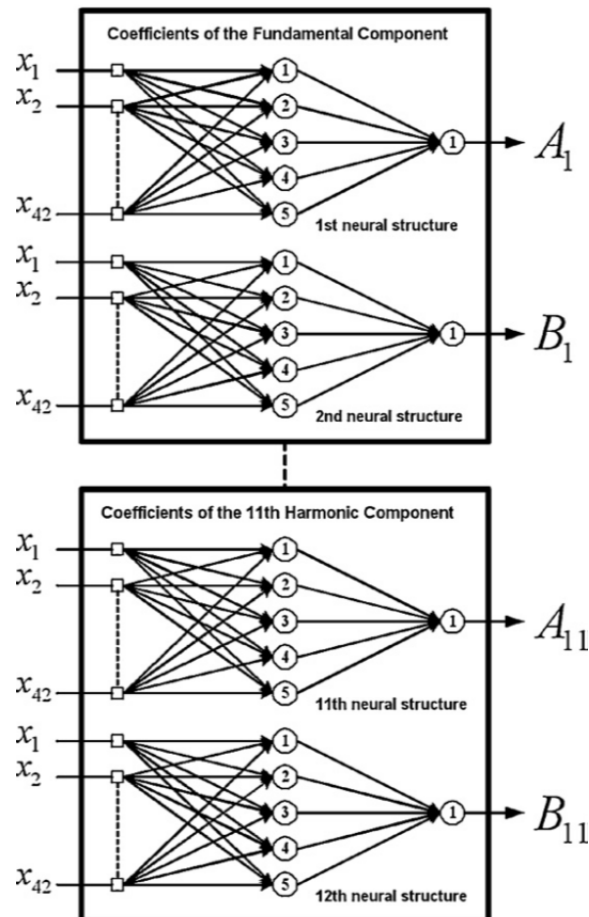


Figure 2.15 MLP based structure for the neural-network-method for estimating A and B coefficients of harmonics (Nascimento *et al.*, 2013).

An efficient approach to distortion monitoring based on MLP applied to estimate harmonic contents of load currents in single-phase systems (Nascimento *et al.*, 2011; Nascimento *et al.*, 2013). In their method, to detect a harmonic, two one-output MLPs are used to detect 2 coefficients of one harmonic, one MLP for A and another for B. There are 5 hidden neurons and only 1 output neuron for each MLP in their simulation. The results from the MLPs based harmonics identification method were compared to the truncated FFT. Figure 2.15 shows MLP based structure for the neural-network-method for estimating A and B coefficients of harmonics in (Nascimento *et al.*, 2013).

2.3.3 Recurrent Neural Network

A recurrent neural network (RNN) is a class of artificial neural network where connections between units form a directed cycle. This creates an internal state of the network which allows it to exhibit dynamic temporal behavior. Unlike feedforward neural networks, RNNs can use their internal memory to process arbitrary sequences of inputs. This makes them applicable to tasks such as un-segmented connected handwriting recognition, where they have achieved the best known results.

In (Mori and Suga, 1992), RNNs are used to handle harmonic dynamics. Four RNN types are introduced to apply for power system harmonic prediction. Four RNNs were tested to predict the fifth harmonic voltage that was measured at the PC-based harmonic measurement system. A comparison was made of four RNN models from standpoint of the accuracy and computational efforts. 4 types of RNN used of harmonic prediction in (Mori and Suga, 1992) are shown in Figure 2.16.

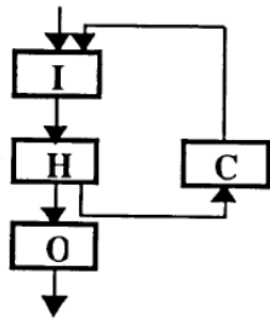


Fig. 2 Recurrent Neural Network Type 1

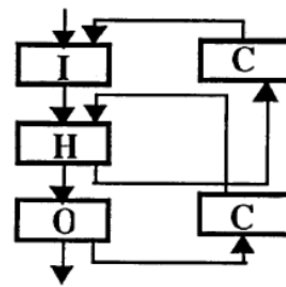


Fig. 4 Recurrent Neural Network Type 3

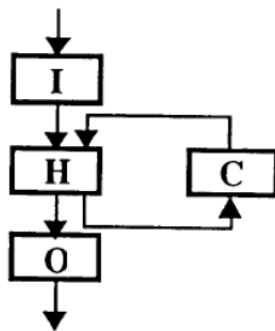


Fig. 3 Recurrent Neural Network Type 2

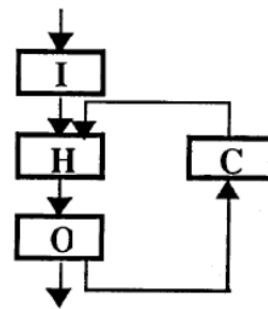


Fig. 5 Recurrent Neural Network Type 4

Note) I: Input Layer H: Hidden Layer C: Context Layer O: Output Layer

Figure 2.16 4 types of RNN used of harmonic prediction in (Mori and Suga, 1992).

In 2004, F. Termutas *et al.* applied the Elman's RNNs for harmonic detection process in active power filter (Temurtas *et al.*, 2004). In this method, the outputs of hidden neurons are used as a part of inputs in input layer of the RNN. The network is able to detect harmonics of orders 5th, 7th, 11th, and 13th in their simulation as shown in Figure 2.17.

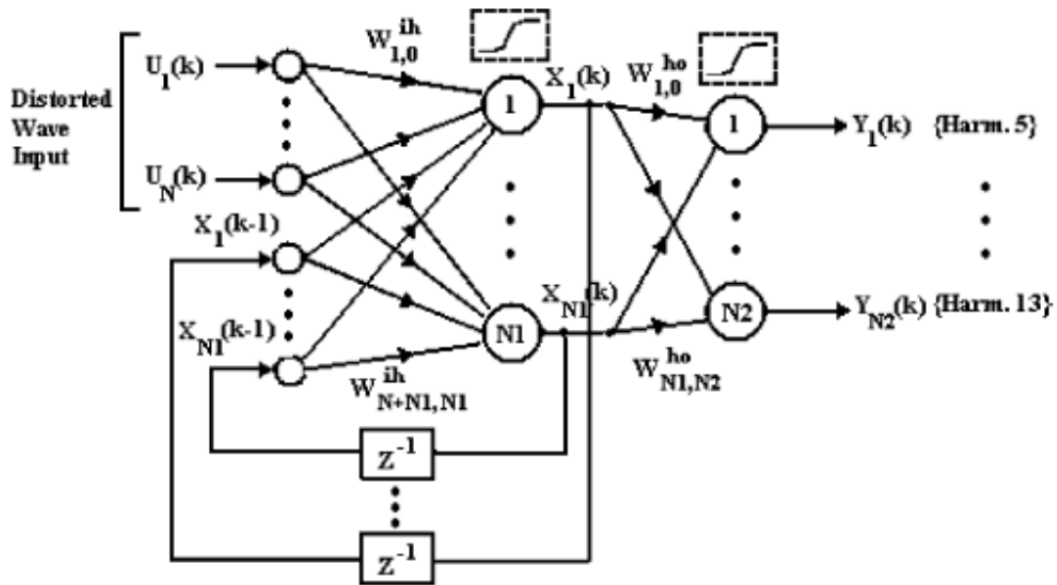


Figure 2.17 Elman's RNN structures for harmonic detection in (Temurtas et al., 2004).

RNNs are trained with the backpropagation through time training algorithm for estimation of non-linear load harmonic current in (Mazumdar and Harley, 2008) as in Figure 2.18. Its advantage is only voltages and currents waveforms have to be measured. This technique is able to apply for single and three phase power networks.

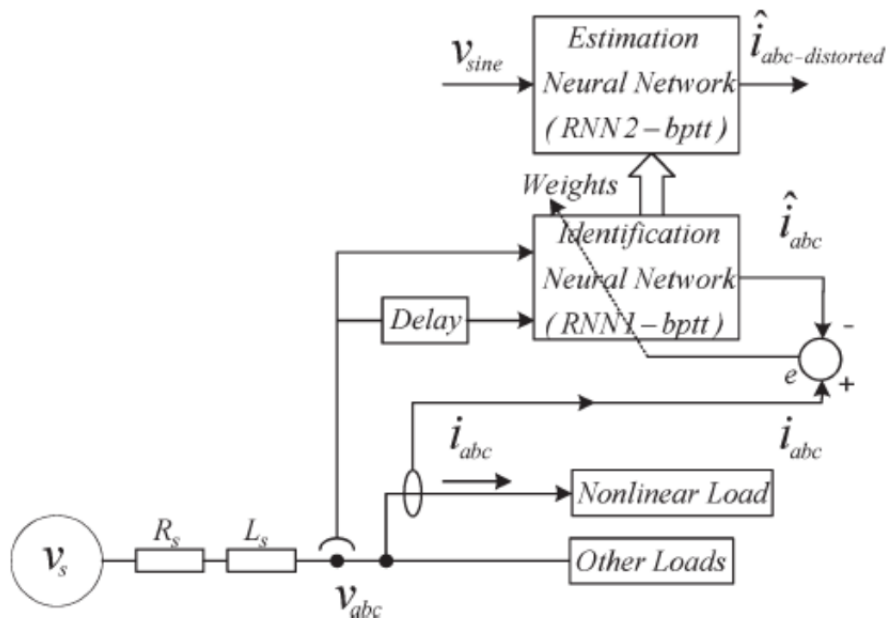


Figure 2.18 Proposed scheme for estimating the true harmonic distortion of a nonlinear load in (Mazumdar and Harley, 2008).

2.3.4 Radial Basis Function Neural Network

A radial basis function neural network (RBFNN) is a feedforward ANN. It uses radial basis functions (RBFs) as activation functions in its hidden neurons. Figure 2.19 illustrates a typical RBFNN.

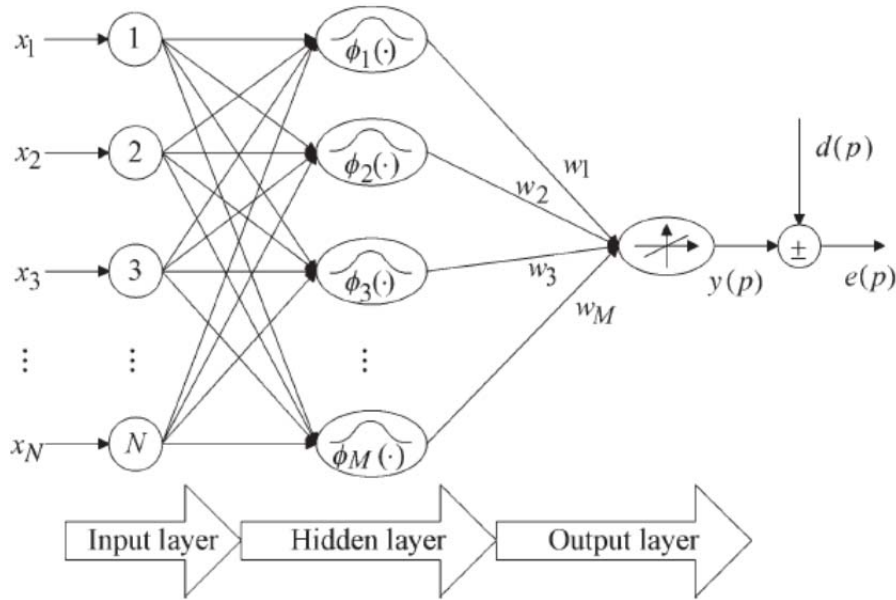


Figure 2.19 A typical RBFNN in (Guangjie and Hailong, 2009).

In 2009, F. Guangjie and Z. Hailong presented their study of the electric power harmonics detecting method based on the immune RBFNN in (Guangjie and Hailong, 2009). In 2010, G. W. Chang et al. proposed a RBFNN-based method to detect the harmonic amplitudes of the measured signal in (Chang *et al.*, 2010). The proposed technique uses only a half of cycle of measured signal to detect all harmonic components. In 2012, E. Almaita and J. A. Asumadu proposed an on-line power system harmonic estimation based on sequential training RBFNN (Almaita and Asumadu, 2012). In this study, a RBFNN is employed for estimating the fundamental, fifth harmonic, and seventh harmonic components.

2.4 Hybrid Techniques

In 2003, an algorithm based on a hybrid least square-GA is proposed for estimating of harmonic in (Bettayeb and Qidwai, 2003). In 2005, a hybrid least square-fuzzy bacterial foraging strategy is presented for harmonic estimation in (Mishra, 2005). In this work, a new algorithm based on the foraging behavior of *E. coli* bacteria in the intestine to estimate harmonics in power system voltage/current waveforms. In the same year, Zhan and Cheng proposed a robust SVM using

interactive reweighted least square method for harmonic and inter-harmonic analysis of electric power system (Zhan and Cheng, 2005). F. T. Wang et al. proposed a hybrid wavelet –Hilbert–Huang spectrum analysis in their publication (Wang *et al.*, 2005).

In 2007, a harmonic analysis based on KF and Prony’s method was proposed in (Costa *et al.*, 2007). In another study, a power system harmonic estimation method is proposed using adaptive perceptron based on a genetic algorithm (Seifossadat *et al.*, 2007). In 2009, B. Subudhi and P.K. Ray proposed 2 hybrid algorithms for power system harmonic estimation, RLS–ADALINE algorithm and KF–ADALINE algorithm in (Subudhi and Ray, 2009). X. M. Ye and X. H. Liu proposed a harmonic detection based on WT and FFT intestine for electric ARC furnaces in (Ye and Liu, 2009). A harmonic estimation in power system was proposed using hybrid H_{∞} –ADALINE algorithm in (Sahoo *et al.*, 2009).

In 2010, P. K. Dash et al. used an Adaptive PSO algorithm to select optimal parameters of unscented KF and measurement error covariance for harmonic analysis of non-stationary signals (Dash *et al.*, 2010). Zadeh *et al.* proposed a new hybrid technique based on combination of KF and least error square techniques in power system in (Zadeh *et al.*, 2010). The modified KF provides precise estimation results. In the same year, B. Subudhi and P. K. Ray proposed a hybrid ADALINE bacterial foraging approach for power system harmonic in (Subudhi and Ray, 2010).

In 2012, S. K. Jain and S. N. Singh presented a new harmonics estimation technique based on adaptively trained ANN assisted by high resolution ESPRIT method (Jain and Singh, 2012). In 2013, a method using sliding window based LMS was presented for estimation of power system harmonics in (Alhaj *et al.*, 2013). Besides that, an artificial bee colony–least square algorithm was proposed for solving harmonic estimation problems in (Biwas et al. 2013). E. Cabal–Yepez et al. proposed harmonic component estimation using discrete Fourier square–wave transform (DFSWT) as a fast processing engine in (Cabal–Yepez *et al.*, 2013).

In 2014, S. K. Singh et al. proposed a fast transverse–RLS algorithm for power system harmonic estimation in (Singh *et al.*, 2014). In 2015, a bilinear RLS algorithm was proposed for estimating power system harmonic parameters (Singh *et al.*, 2015a). P. K. Ray and B. Subudhi proposed neuron–evolutionary approaches to power system harmonics estimation (Ray and Subudhi, 2015). A LMS algorithm based on variable constraint is proposed for power system harmonic parameter estimation in (Singh *et al.*, 2015b).

2.5 Summary

In this chapter, we have presented a state of the art of existing approaches for solving the problem of power system harmonics estimation. For the power system harmonics estimation, we have presented and grouped all of approaches for solving this problem into 3 groups of techniques: non-neural techniques, neural techniques, and hybrid techniques. The non-neural techniques are approaches that don't uses artificial neural networks in their design. The neural techniques are approaches that use at least one or more artificial neural networks in their design. And the last group for power system harmonic estimation approaches contains hybrid techniques that use both non-neural techniques and artificial neural networks. These approaches relate to the development of our proposed approaches for harmonics estimation presented in Chapter 4.

Chapter 3 : Load Signature Discrimination

3.1 Introduction

Non-Intrusive Appliance Load Monitoring (NILM) refers to a set of techniques that automatically estimate the electricity consumed by individual electrical appliances in a building from measurements of the total electrical consumption (Giri and Bergés, 2015). In 1980s and 1990s at the MIT, George Hart developed one of the earliest NILM systems, which based on detailed analysis of the current and the voltage of the total loads in the residential buildings. His approach was described in (Hart, 1992). [Figure 1.9](#) shows the classification of NILM techniques.

3.2 Signature Analysis Based Techniques

3.2.1 Steady-State Signature Analysis Based Approaches

The NILM approaches based on steady-state signature analysis use steady-state features that are derived under the appliance operations. The first steady-state signature analysis based approach was used by Hart (Hart, 1992) to prove the NILM concept. In his work, both of active power P and reactive power Q are recorded over intervals of one second. In NILM, active power P and the reactive power Q are most commonly used steady-state signatures for tracking operations of “turn on” or “turn off” of appliances.

In (Norford and Leeb, 1996; Farinaccio and Zmeureanu, 1999; Marceau and Zmeureanu, 2000), researchers have tried to use active power as a single feature for load disaggregation. They found that the high-power appliances with distinctive power draw characteristics, such as electrical heaters and water pumps, can be easily identified from the aggregated measurement. Moreover, there were several NILM approaches that are summarized in [Table 3.1](#).

3.2.2 Transient-State Signature Analysis Based Approaches

Associated with any turn-on events, transients are momentary fluctuations in powers, voltages or even currents before settling in to a steady-state value. These short-term fluctuations are called transients (Wong *et al.*, 2013). The transient behavior of major appliance is captured to be distinct and its features are less overlapping in comparison with steady-state signatures. However, high sampling rate requirement to capture the transient is the major limitation of this method (Figueiredo *et al.*, 2011). The shape of transient events can be used as a feature for detecting

appliances in (Norford and Leeb, 1996). A summary of transient–state methods is shown in [Table 3.2](#) from (Zoha *et al.*, 2012).

Steady–State Methods	Features	Advantages	Shortcomings
Power Change (Hart, 1992; Marchiori <i>et al.</i> , 2011; Norford and Leeb, 1996; Farinaccio and Zmeureanu, 1999; Marceau and Zmeureanu, 2000)	Steady State Variation of Real and Reactive Power, ΔP , ΔQ	High–Power Residential Loads can easily be identified, Low–sampling rate requirement	Low power appliances overlap in P–Q plane, Poor performance in recognizing Type–II, III and Type–IV loads.
Time and Frequency Domain Characteristics of VI Waveforms (Liang <i>et al.</i> , 2010; Najmeddine <i>et al.</i> , 2008; Kato <i>et al.</i> , 2009; Cole and Albicki, 2000; Suzuki <i>et al.</i> , 2008; Laughman <i>et al.</i> , 2003; Ruzzelli <i>et al.</i> , 2010; Li <i>et al.</i> , 2012)	Higher order Steady–State Harmonics, Irms, Iavg, Ipeak, Vrms, Power factor	Device classes can easily be categorized into resistive, inductive and electronic loads	High sampling rate requirement, Low accuracy for Type–III loads, overlapping features for consumer electronics of Type–I and Type–II category, unable to distinguish between overlapping activation events
V–I Trajectory (Lee <i>et al.</i> , 2004; Lam <i>et al.</i> , 2007)	Shape features of V–I trajectory: asymmetry, looping direction, area, curvature of meanline, self–intersection, slope of middle, segment, area of segments and peak of middle segment	Detail taxonomy of electrical appliances can be formed due to distinctive V–I curves	Sensitive to multi–load operation scenario, computationally intensive, smaller loads have no distinct trajectory patterns
Steady–State Voltage Noise (Patel <i>et al.</i> , 2007; Gupta <i>et al.</i> , 2010)	EMI signatures	Motor–based appliances are easily distinguishable as they generate synchronous voltage noise, Detection of simultaneous activation events, Consumer appliances equipped with SMPS can be recognized with high accuracy	Sensitive to wiring architecture, EMI signature overlap, Not all appliances are equipped with SMPS

Table 3.1 Summary of steady–state methods from (Zoha *et al.*, 2012).

Transient-State Methods	Features	Advantages	Shortcomings
Transient Power (Zeifman and Roth, 2011; Laughman <i>et al.</i> , 2003; Chang <i>et al.</i> , 2008; Chang, 2012; Shaw <i>et al.</i> , 2008)	Repeatable transient power profile, spectral envelopes	Appliances with same power draw characteristics can be easily differentiated, Recognition of Type-I,II,III loads	Continuous monitoring, high sampling rate requirement, not suitable for Type IV loads
Start-Up Current Transients (Norford and Leeb, 1996; Cole and Albicki, 1998; Chang, 2012)	Current spikes, size, duration, shape of switching transients, transient response time	Works well for Type I and Type II loads, distinct transient behavior in multiple load operation scenario	Poor detection of simultaneous activation deactivation of sequences, unable to characterize Type III and IV loads, sensitive to wiring architecture, appliance specific
High Frequency Sampling of Voltage Noise (Patel <i>et al.</i> , 2007; Hazas <i>et al.</i> , 2011)	Noise FFT	Multi-state devices, consumer Electronics with SMPS	Appliance specific, computationally expensive, Data annotation is very hard

Table 3.2 Summary of transient-state methods from (Zoha *et al.*, 2012).

3.2.3 Non-traditional Appliance Features Based Approaches

Apart from traditional appliance features (steady-state and transient-state signatures), other feature extraction methods have been developed to acquire non-traditional appliance features. In 2012, Z. Wang and G. Zheng proposed that the power consumption of residential appliances can be described by the combination of two basic units, triangle and rectangles, neglecting the smaller fluctuations and errors (Wang and Zheng, 2012). Their new approach can reduce the appliance feature overlap problem. The rectangle can be expressed by *starttime*, *peaktime*, *steadytime* and *steadypower* whereas the triangle unit can be described by *starttime*, *peaktime*, *peakvalue* and *endtime*.

In (Liang *et al.*, 2010), researchers proposed to combine several features including P, Q harmonics of the appliances, eigenvalues of the current waveforms, admittance etc. for disaggregating load. This combination of features improves the load identification performance. In (Suzuki *et al.*, 2008), authors have tried to examine the use of raw waveforms for appliance identification. However, the experimental evaluations provided that it offers no advantages whereas in comparison the processed features are better suited for load identification. Other non-traditional features including on and off duration distribution, time of the day, frequency of appliance usage and correlation between different appliance usages were examined to improve the load disaggregation algorithms performance (Kim *et al.*, 2011; Zeifman, 2012).

3.3 Machine Learning Based Techniques

3.3.1 Supervised Learning Based Approaches

In (Baranski and Voss, 2003; Liang *et al.*, 2010; Baranski and Voss, 2004; Suzuki *et al.*, 2008), researchers have proposed different optimization based approaches including genetic algorithm and integer programming in order to tackle the NILM problem as the optimization problem. However, the challenge is how to reduce the computational complexity of these methods and more especially if any unknown load which are not included in the database, are present in the aggregated load data.

Pattern recognition based approaches are the most frequently used in the study of load disaggregation. Hart proposed a simple clustering based approach in which appliances form their unique clusters in $P-Q$ plane (Hart, 1992). In 1994, J. G. Roos *et al.* proposed using neural networks for NILM systems (Roos *et al.*, 1994). In (Farinaccio and Zmeureanu, 1999), researchers proposed a pattern recognition approach to disaggregate the total electricity consumption in a house into the end-uses. In their method, filtering and smoothing mechanisms were employed to deal with power variations and instead of power consumption change in real power values are used as a feature for detecting appliances. However, this method works well only with high power loads and furthermore it requires excessive training.

Support vector machines and boosting techniques were applied to a NILM system for household electric appliances with inverters. Figure 3.1 shows sketch of large margin classifiers metering system in (Onoda *et al.*, 2000; Onoda *et al.*, 2002).

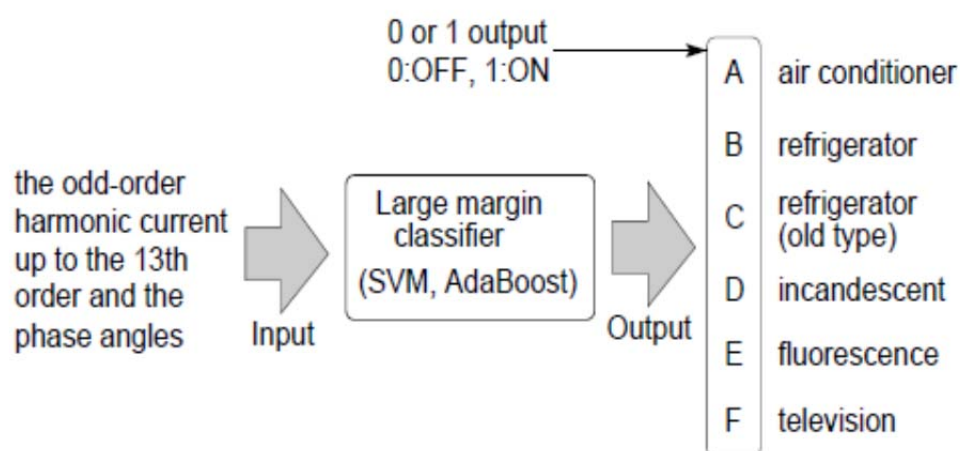


Figure 3.1 Sketch of large margin classifiers metering system in (Onoda *et al.*, 2000).

In 2000, a MLP based NILM system in Figure 3.2 was developed to ascertain the behavior of each electrical appliance in a household by disaggregating the total household load demand. The load consumption of household appliances is identified by the pattern recognition ability of a MLP (Yoshimoto *et al.*, 2000).

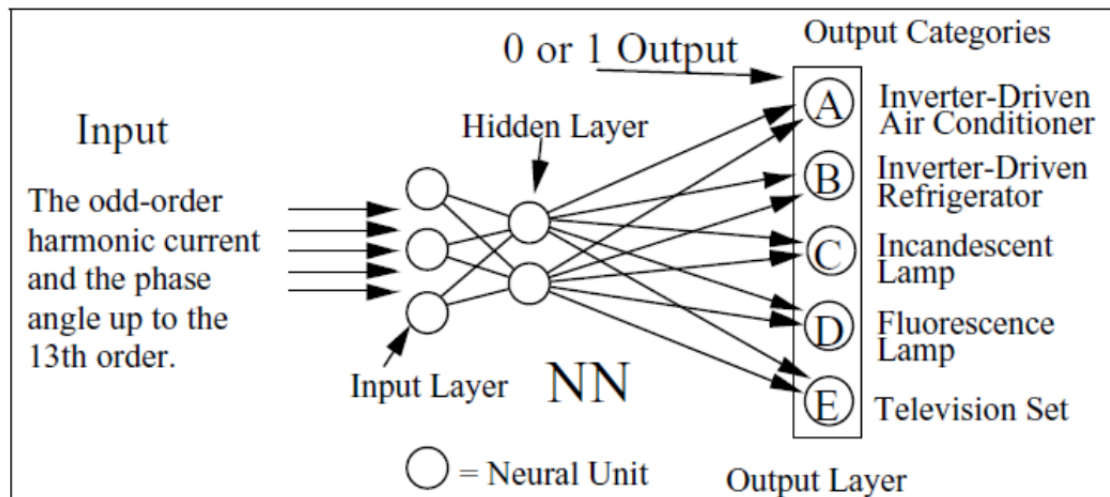


Figure 3.2 Multilayer perceptron designed for NILM system in (Yoshimoto *et al.*, 2000).

In 2006, D. Srinivasan *et al.* proposed a neural-network-based approach to nonintrusive harmonic source identification (Srinivasan *et al.*, 2006). Neural networks are trained to extract important features from the input current waveform to uniquely identify various types of appliances using their distinct harmonic signatures. In this work, several neural network based classification models including MLP, RBF network, and SVM with linear, polynomial, and RBF kernels were developed for signature extraction and device identification. Their results showed that MLPs and SVM were both able to determine the presence of appliances based on their harmonic signatures with high accuracy.

In 2008, H.-H Chang *et al.* proposed the use of neural network classifiers to evaluate back propagation and learning vector quantization for feature selection of load identification in a NILM system (Chang *et al.*, 2008). The NILM system uses an adaptive algorithm of the turn-on transient energy for start-up analysis to improve the efficiency of load identification and computational time. The testing recognition accuracy can be relatively high at 95.3% for back propagation classifier, in multiple operations.

3.3.2 Unsupervised Learning Based Approaches

Recently, researchers started to explore methods that can achieve disaggregated energy sensing without any a-priori information. Especially for the NILM systems that are installed in a target environment with a minimal setup cost as the training requirement for the supervised load identification algorithms is expensive or laborious. Therefore, unsupervised learning based NILM systems are needed for a wider applicability of usages (Zoha, 2012).

In (Gonçalves *et al.*, 2011), an unsupervised disaggregation of appliances using aggregated data was proposed. In this approach, a blind source separation technique was used to discern electrical appliances from the aggregated load data in an unsupervised fashion. The steady-state ΔP and ΔQ features were employed for clustering appliances.

In (Shao *et al.*, 2012), a temporal motif mining approach was proposed to unsupervised energy disaggregation. To identify individual appliances, power change events such as (+500 W, -500 W) were considered in contrast to power consumption.

Recently several variants of hidden Markov models have also been proposed to unsupervised NILM systems in (Kim *et al.*, 2011; Kolter and Johnson, 2011; Kolter and Jaakkola, 2012; Parson *et al.*, 2014).

3.4 Summary

In this chapter, we have reviewed several approaches for nonlinear load classification. Some techniques are based on signature analysis and some others are based on the principle of machine learning. For signature analysis based approaches, we presented them into three groups: steady-state signature based approaches, transient-state signature analysis based approaches and non-traditional appliance features based approaches. For machine learning based approaches, they have been classified into two groups: supervised learning based approaches and unsupervised based approaches.

Among the nonlinear loads classification approaches which have been reviewed, most of them belong to non-intrusive load monitoring. These approaches are related to the development of our proposed approaches for nonlinear loads classification presented in Chapter 5.

Chapter 4 : Harmonic Estimation Using Artificial Neural Networks

4.1 Introduction

In this chapter, we propose two new neural network–based approaches that have been developed for harmonic estimation of the distorted signals. The first new approach is based on a proposed linear MLP. The second new approach is a structure that is based on several typical MLPs.

In the first new approach (Nguyen and Wira, 2013a; Nguyen and Wira, 2013b), a linear MLP has been developed for estimating the harmonics of distorted signals. The linear MLP is able to estimate any periodic signal by expressing its output as a sum of harmonic components according to Fourier series. The network takes some specific harmonic elements with unit amplitudes as inputs and uses neurons that have linear activation functions. The measured signal serves as a reference and is compared to the network output. The amplitudes of the fundamental and high–order harmonics are deduced from the combination of the weights of the neurons. The linear MLP identifies the amplitudes of the fundamental component and high–order harmonic components with good precision even under noisy conditions.

In the second new approach (Nguyen and Wira, 2015), we propose another neural network approach based on the structure of MLPs for identifying current harmonics in power systems. The learning approach is based on several MLP, adopts the Fourier decomposition of a signal and a training set generated from harmonic waveforms is used to calculate the weights. After training, each MLP is able to identify two coefficients for each harmonic term of the input signal. The effectiveness of the new approach is evaluated by experiments. Results show that the proposed MLPs of the new approach enable to identify effectively the amplitudes of harmonic terms from the signals under noisy condition. Results are compared to other and recent MLP approaches. The new approach can be applied in harmonic compensation strategies by being implement in an active power filter to ensure the power quality in electrical power systems.

ANNs with their ability to learn from sample data have shown that they are excellent solutions for performing advanced digital signal processing tasks (Haykin, 1999). Therefore, several ANN approaches have been developed for harmonic identification (Wira *et al.*, 2010). They are based on different neural structures, and have to identify the amplitude and the phase of each higher–order harmonic of the current measured on a power line. Once estimated, they can be used to generate

compensation currents. This is achieved by a voltage–source inverter under the supervision of a control law. The controller produces a reference signal that takes into account the necessary harmonic components but phase–opposite. The inverter converts the reference signal into a high–intensity current that will be injected into the power line. This principle is represented by [Figure 1.2](#) in Chapter 1. The skills related to each block are also mentioned.

The ADALINE neural network (Widrow and Lehr, 1990) is the simplest learning approach for estimating harmonics. An ADALINE has only one layer and has one neuron per output. Each neuron of ADALINE gets multiple inputs and returns one output which is a weighted linear combination of the inputs. The Mean Square Error (MSE) is used for updating the weights during the training process (Haykin, 1999). For harmonic estimation, a signal is formalized in Fourier series and the corresponding harmonics with unit amplitudes are synthesized and used as inputs (Dash *et al.*, 1996). After learning and convergence, the coefficients of fundamental and harmonic components are represented by the weights of the ADALINE. Several successful variants have been developed since with different expression of the signal (Wira *et al.*, 2008; Wira and Nguyen, 2013).

The MLP is a layered learning structure where neurons are organized in layers. The data comes from a system and are transferred to an input layer and go through several hidden layers and at least through out of an output layer. This data–flow goes through all the nonlinear neurons of the layers from the input to the output of the network. MLPs have to be trained in order to calculate appropriate values for the weights and the backpropagation algorithm is the most well–known training algorithm (Haykin, 1999). The optimal weights are the ones that allow the network to provide outputs with the smallest error when compared to a target, i.e., to reduce a cost function. MLP have been proposed for estimating harmonic components in active filter schemes. In (Pecharanin *et al.*, 1994) for example, two MLPs are designed to estimate the 3rd, 5th and 7th harmonics. The backpropagation learning algorithm is used and results shows that the neural approach enables to detect them effectively.

In (Lin, 2007), satisfactory results have been achieved for harmonic detection by providing only half cycle sampled values of distorted waveforms to MLP–based approach. It must be remembered that harmonic detection with the Fourier transformation requires input data for more one cycle of the current waveform and requires time for the analysis in next coming cycle. A similar approach is developed in (Nascimento *et al.*, 2011). Here, one MLP is used for each parameter of an individual harmonic component. The MLPs use the same inputs and are trained to identify the load

current harmonic components in half-cycle of the fundamental component period. Some MLP can also be trained off-line, using previous knowledge obtained from load harmonic contents generated by simulation algorithms.

In (Tümay *et al.*, 2008), a conventional MLP with fully connected neurons is compared to a MLP with partial connected neurons. For this last neural network, hidden neurons are divided to two groups in the hidden layer. The neurons in each group of the hidden layer are connected with only one of the output neurons. As each output neuron is never connected with the same hidden neurons, each output is independent from the others. Results show that the partial-connected MLP is more effective in extracting the 3rd and 5th harmonic components of a current waveform.

Radial Basis Functions Neural Networks (RBFNNs) are similar to MLP networks. In RBFNNs, activation functions of hidden neurons are Radial Basis Functions (RBFs) and activation functions of output neurons are sums. Thus, outputs of a RBFNN are simple linear combinations of radial basis functions of the inputs. A typical RBFNN has one input layer, one hidden layer with RBF activation functions and one linear output layer. Such a RBFNN approach is proposed in (Chang *et al.*, 2010) for estimating the harmonic content of a signal. The learning allows the RBFNN to approximate the mapping between the samples of the signal and the amplitudes and the phase angles of each harmonic component. The RBFNN can be trained off-line before being used to estimate the harmonic components.

A Recurrent Neural Network (RNN) is a type of a dynamic neural network. Indeed, some inputs of the RNN are the outputs of neurons from its output layer, or sometime from hidden neurons. This network exhibits a dynamic temporal behavior because of the internal network states which are created by the feedback loops. An Elman RNN for harmonic estimation has been used in (Temurtas *et al.*, 2004). The results obtained with Elman's RNN are better than those obtained using the feed forward neural networks. The proposed resilient backpropagation algorithm provides also faster convergence than the standard and adaptive backpropagation.

The advantages of using neural approaches for estimating the harmonic content of a signal are the followings: They work with a good precision even under noisy conditions due to their generalization capabilities; they are adaptive and therefore can face parameter/system/environment changes by using online learning; and they can provide an output on every iteration which may be a faster response than with conventional techniques, i.e., harmonic detection with the Fourier transformation requires one complete cycle of the current waveform.

4.2 Background

4.2.1 Fourier Analysis

In the Fourier analysis, any periodic or distorted waveform or signal can be represented and estimated by a function f , as a sum of sine and cosine components with appropriate coefficient attached to each of these components. This function is also called a Fourier series,

$$f(t) = A_0 + \sum_{n=1}^{\infty} [A_n \cos(n\omega t) + B_n \sin(n\omega t)], \quad (4.1)$$

where A_0 is the DC component, i.e., the direct component of the signal. The term $A_n \cos(n\omega t) + B_n \sin(n\omega t)$ mathematically represents for the n -th harmonic component that composes the signal, and n is usually called the order of the harmonic component. Each n -th harmonic component is defined by 2 coefficients A_n and B_n . Thus, the term with $n=1$ is the fundamental component of the signal and terms with $n > 1$ representing harmonic components. In power system applications, the fundamental component represents the main part of a signal, i.e., the one with the highest amplitude or the one carrying the biggest energy or power.

In (4.1), t represents for the discrete time. Without any loss of generality, only discretized signals are considered in this work, $t = kT_s$ with the sampling interval T_s and the iteration number k . The fundamental angular frequency is $\omega = 2\pi/T$ where $T = 1/f_1$ stands for the period of the signal and f_1 is called the fundamental frequency of the signal, i.e., of its fundamental component.

In signal sampling and quantization, a sampling interval or sampling period T_s is defined as the time span between two successive samples and a sampling rate is therefore given by $f_s = 1/T_s$ samples per second (Hz). For example, if a sampling interval $T_s = 125\mu s$ (microseconds), the sampling rate is $f_s = 1/125\mu s = 8000$ samples per second (Hz).

To calculate the harmonic amplitudes and the relative phase angles, we rearrange the expression (4.1) and we have a well know result

$$f(t) = C_0 + \sum_{n=1}^{\infty} C_n \cos(n\omega t - \theta_n), \quad (4.2)$$

with C_n the harmonic amplitudes and θ_n the phase angles:

$$C_0 = A_0, C_n = \sqrt{A_n^2 + B_n^2}, \theta_n = \tan^{-1}\left(\frac{B_n}{A_n}\right). \quad (4.3)$$

Of course, an ideal power signal, i.e., a voltage or a current, will be only one sinusoidal term, the fundamental component. Practically, generated are superposed to the fundamental term with an additional noise $\eta(t)$. A signal from a power system therefore can thus be approximated by a limited sum (to $n = N$):

$$\hat{f}(t) = A_0 + \sum_{n=1}^N [A_n \cos(n\omega t) + B_n \sin(n\omega t)] + \eta(t). \quad (4.4)$$

Harmonic estimation or identification in this work is a process that estimates or identifies values of coefficients A_0 , A_n and B_n in (4.4).

4.2.2 The Multilayer Perceptron

An artificial neuron is a simple process unit which receives one or more inputs and sums them to produce an output. Usually, the sums of each node are weighted, and the sum is passed through a nonlinear function known as an activation function or a transfer function.

A MLP network is composed of neurons organized in layers, with those on one layer connected to those on the next layer (except for the last layer also called the output layer). The MLP architecture is thus structured into an input layer, one or more hidden layer of neurons (called hidden neurons), and one output layer of neurons (output neurons). Neurons belonging to adjacent layers are usually fully connected. The feedforward network is a MLP that allow only for a one directional signal flow, from the input to the output layer.

Some parameters of such a type of an ANN cannot be determined from an analytical analysis of the process under investigation. This is the case of the number of hidden layers and the number of neurons belonging to them. Consequently, they have to be determined experimentally according to the precision which is desired for the estimation. On the other hand, the number of inputs and outputs depends on the considered process or mapping to approximation.

MLPs must be trained in order to find appropriate or optimal values of weights. This is achieved by using probabilistic learning techniques and with data from the process under

investigation (Haykin, 1999). The training data consists of the input vectors and the corresponding desired output vectors. The pairs of input–output values $\mathbf{x}(1), \mathbf{y}(1), \mathbf{x}(2), \mathbf{y}(2), \dots, \mathbf{x}(Q), \mathbf{y}(Q)$ represents the learning data set, where Q is the number of examples in the training set. For a given input $\mathbf{x}(k)$, the MLP computes an estimated output vector $\hat{\mathbf{y}}(k)$ that must be as close as to the ideal desired output $\mathbf{y}(k)$. The difference $\mathbf{e}(k) = \mathbf{y}(k) - \hat{\mathbf{y}}(k)$ constitutes the estimation error for example k that is used by the training algorithm to correct the weights of the neurons. This is repeated for all the samples composing the training data set until the convergence is reached. After training process, the MLP is able to estimate the output values corresponding to a given input. In other words, the MLP has learned the multidimensional function $\mathbf{y} = \mathbf{F}(\mathbf{x})$.

MLPs are well suited for the functions approximation. Associated to the backpropagation learning rule, they are well–known as universal approximation machines (Haykin, 1999; Bishop, 1995).

4.3 Proposed Method 1 : A Linear MLP for Harmonic Estimation

The main idea of this approach is to use a linear MLP with the appropriate inputs and target outputs for step by step fitting a Fourier series. The harmonics, as Fourier series parameters, are calculated from the weights and biases of the network at the end of the training process.

4.3.1 Proposed Linear MLP

In this work, the objective is to estimate the amplitudes A_0, A_n and B_n in (4.4). So, we propose a linear MLP for this work. Once we have the amplitudes A_0, A_n and B_n , we can calculate the harmonic amplitudes C_n and the relative phases θ_n as the expressions in (4.3).

A linear MLP consists of a feedforward MLP with three layers of neurons. Its inputs are the values of the sine and cosine terms of all harmonic terms to be identified. There is only one output neuron in the output layer. A desired output is used for a supervised learning. This reference is the measured signal whose harmonic content must be estimated. All neuron of the network are with a linear activation function, i.e., identity function. The MLP is therefore linear and nonlinearities are introduced by the input vector. An example of a linear MLP with one hidden layer having 5 neurons is shown in [Figure 4.1](#).

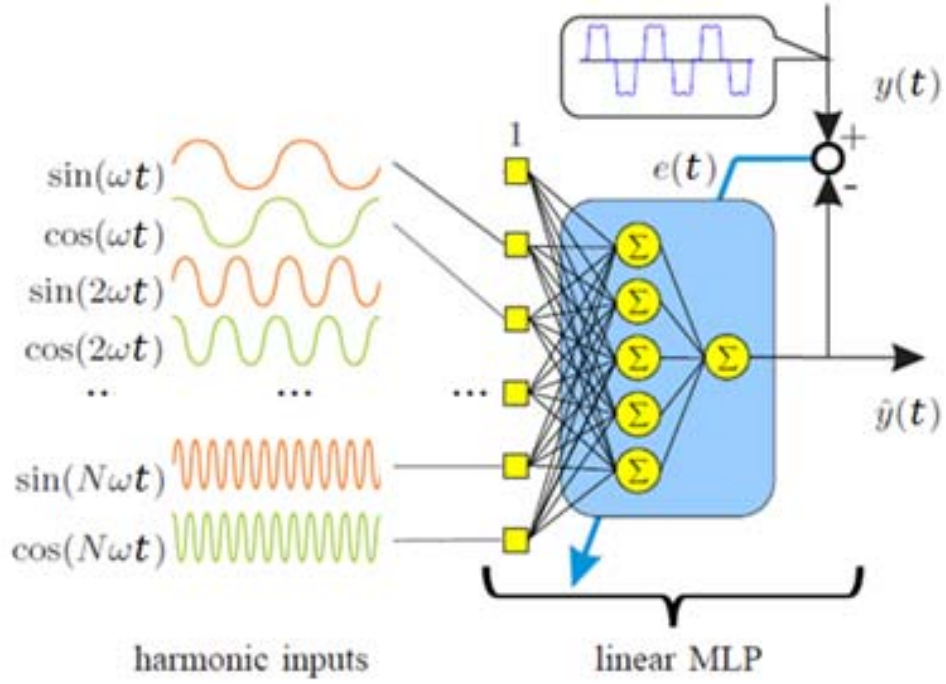


Figure 4.1 The linear MLP architecture for harmonic estimation.

In (4.5), $\hat{f}(t)$ is a weighted sum of sinusoidal terms and is therefore a linear relationship that can be fitted by a linear MLP taking sine and cosine terms with unit amplitudes as its inputs. Thus,

$$\begin{aligned}
 \hat{f}(t) &= A_0 + \sum_{n=1}^N [A_n \cos(n\omega t) + B_n \sin(n\omega t)] \\
 &= A_0 + [B_1 \quad A_1 \quad B_2 \quad A_2 \quad \dots \quad B_N \quad A_N] \begin{bmatrix} \sin(\omega t) \\ \cos(\omega t) \\ \sin(2\omega t) \\ \cos(2\omega t) \\ \dots \\ \sin(N\omega t) \\ \cos(N\omega t) \end{bmatrix} \\
 &= A_0 + [A_0 \quad B_1 \quad A_1 \quad B_2 \quad A_2 \quad \dots \quad B_N \quad A_N] \mathbf{x}
 \end{aligned} \tag{4.5}$$

with

$$\mathbf{x}(t) = [\sin(\omega t) \quad \cos(\omega t) \quad \sin(2\omega t) \quad \cos(2\omega t) \quad \dots \quad \sin(N\omega t) \quad \cos(N\omega t)]^T \tag{4.6}$$

can be estimated by a linear MLP with only hidden layer with M hidden neurons and with one output neuron. The linear MLP takes R inputs, $R = 2N$, N is the number of harmonics to be identified.

At instant t , the output of the i -th neuron $\hat{y}_i(t)$ ($i = 1, \dots, M$) is

$$\begin{aligned}
\hat{y}_i(t) &= \begin{bmatrix} w_{i,1} & w_{i,2} & \dots & w_{i,R-1} & w_{i,R} \end{bmatrix} \mathbf{x}(t) + b_i \\
&= \begin{bmatrix} w_{i,1} & w_{i,2} & \dots & w_{i,R-1} & w_{i,R} \end{bmatrix} \begin{bmatrix} \sin(\omega t) \\ \cos(\omega t) \\ \dots \\ \sin(N\omega t) \\ \cos(N\omega t) \end{bmatrix} + b_i \\
&= w_{i,1} \sin(\omega t) + w_{i,2} \cos(\omega t) + \dots + w_{i,R-1} \sin(N\omega t) + w_{i,R} \cos(N\omega t) + b_i
\end{aligned} \tag{4.7}$$

and the output of the output neuron $\hat{y}(t)$ is

$$\begin{aligned}
\hat{y}(t) &= \left(\sum_{i=1}^M w_{o,i} \hat{y}_i(t) \right) \\
&= w_{o,1} \hat{y}_1(t) + w_{o,2} \hat{y}_2(t) + \dots + w_{o,M-1} \hat{y}_{M-1}(t) + w_{o,M} \hat{y}_M(t) \\
&= \begin{bmatrix} w_{o,1} & w_{o,2} & \dots & w_{o,M-1} & w_{o,M} \end{bmatrix} \begin{bmatrix} \hat{y}_1(t) \\ \hat{y}_2(t) \\ \dots \\ \hat{y}_{M-1}(t) \\ \hat{y}_M(t) \end{bmatrix}
\end{aligned} \tag{4.8}$$

with

$w_{i,j}$ is the weight of i -th hidden neuron connected to the j -th input,

$w_{o,i}$ is the weight of the output neuron connected to the i -th hidden neuron,

and b_i is the bias of the i -th hidden neuron.

In this work, this linear MLP has only one output neuron. So, the output $\hat{y}(t)$ of the output neuron is also the output of this linear MLP. From (4.7) and (4.8), the network output therefore rewrites:

$$\begin{aligned}
\hat{\mathbf{y}}(t) &= \begin{bmatrix} w_{o,1} & w_{o,2} & \dots & w_{o,M-1} & w_{o,M} \end{bmatrix} \begin{bmatrix} \hat{y}_1(t) \\ \hat{y}_2(t) \\ \dots \\ \hat{y}_{M-1}(t) \\ \hat{y}_M(t) \end{bmatrix} \\
&= \begin{bmatrix} w_{o,1} \\ w_{o,2} \\ \dots \\ w_{o,M-1} \\ w_{o,M} \end{bmatrix}^T \begin{bmatrix} b_1 + w_{1,1} \sin(\omega t) + w_{1,2} \cos(\omega t) + \dots + w_{1,R-1} \sin(N\omega t) + w_{1,R} \cos(N\omega t) \\ b_2 + w_{2,1} \sin(\omega t) + w_{2,2} \cos(\omega t) + \dots + w_{2,R-1} \sin(N\omega t) + w_{2,R} \cos(N\omega t) \\ \dots \\ b_{M-1} + w_{M-1,1} \sin(\omega t) + w_{M-1,2} \cos(\omega t) + \dots + w_{M-1,R-1} \sin(N\omega t) + w_{M-1,R} \cos(N\omega t) \\ b_M + w_{M,1} \sin(\omega t) + w_{M,2} \cos(\omega t) + \dots + w_{M,R-1} \sin(N\omega t) + w_{M,R} \cos(N\omega t) \end{bmatrix} \\
&= w_{o,1} b_1 + w_{o,1} w_{1,1} \sin(\omega t) + w_{o,1} w_{1,2} \cos(\omega t) + \dots + w_{o,1} w_{1,R-1} \sin(N\omega t) + w_{o,1} w_{1,R} \cos(N\omega t) \\
&+ w_{o,2} b_2 + w_{o,2} w_{2,1} \sin(\omega t) + w_{o,2} w_{2,2} \cos(\omega t) + \dots + w_{o,2} w_{2,R-1} \sin(N\omega t) + w_{o,2} w_{2,R} \cos(N\omega t) + \dots \\
&+ w_{o,M-1} b_{M-1} + w_{o,M-1} w_{M-1,1} \sin(\omega t) + w_{o,M-1} w_{M-1,2} \cos(\omega t) \\
&+ \dots + w_{o,M-1} w_{M-1,R-1} \sin(N\omega t) + w_{o,M-1} w_{M-1,R} \cos(N\omega t) \\
&+ w_{o,M} b_M + w_{o,M} w_{M,1} \sin(\omega t) + w_{o,M} w_{M,2} \cos(\omega t) + \dots + w_{o,M} w_{M,R-1} \sin(N\omega t) + w_{o,M} w_{M,R} \cos(N\omega t) \\
&= \left(\sum_{i=1}^M w_{o,i} w_{i,1} \right) \sin(\omega t) + \left(\sum_{i=1}^M w_{o,i} w_{i,2} \right) \cos(\omega t) \\
&+ \dots \\
&+ \left(\sum_{i=1}^M w_{o,i} w_{i,R-1} \right) \sin(N\omega t) + \left(\sum_{i=1}^M w_{o,i} w_{i,R} \right) \cos(N\omega t) \\
&+ \left(\sum_{i=1}^M w_{o,i} b_i \right). \tag{4.9}
\end{aligned}$$

From the above expression, we propose two new terminologies for the linear MLP. The first is called the “weight combination” and the second is called the “bias combination”.

Definition 1 (The weight combination)

The weight combination of the linear MLP, \mathbf{c}_{weight} is a row-vector (with R elements) that is a linear combination of the hidden weights with the output weight which writes:

$$\mathbf{c}_{weight} = \begin{bmatrix} c_{weight(1)} & \dots & c_{weight(R)} \end{bmatrix} = \mathbf{w}_o^T \mathbf{W}_{hidden} \tag{4.10}$$

where

\mathbf{w}_o is the weight vector of the output neuron (with M elements)

$$\mathbf{w}_o = \begin{bmatrix} w_{o,1} \\ w_{o,2} \\ \dots \\ w_{o,M-1} \\ w_{o,M} \end{bmatrix} \quad (4.11)$$

and

\mathbf{W}_{hidden} is a $M \times R$ weight matrix of all neurons of the hidden layer

$$\mathbf{W}_{hidden} = \begin{bmatrix} w_{1,1} & w_{1,2} & \dots & w_{1,R-1} & w_{1,R} \\ w_{2,1} & w_{2,2} & \dots & w_{2,R-1} & w_{2,R} \\ \dots & \dots & \dots & \dots & \dots \\ w_{M-1,1} & w_{M-1,2} & \dots & w_{M-1,R-1} & w_{M-1,R} \\ w_{M,1} & w_{M,2} & \dots & w_{M,R-1} & w_{M,R} \end{bmatrix}. \quad (4.12)$$

Definition 2 (The bias combination)

The bias combination of the linear MLP, c_{bias} , is a linear combination of all bias of hidden neurons with the weights of output neuron which writes:

$$c_{bias} = \mathbf{w}_o^T \mathbf{b}_{hidden} \quad (4.13)$$

where \mathbf{b}_{hidden} is the bias vector of the hidden layer

$$\mathbf{b}_{hidden} = \begin{bmatrix} b_1 \\ b_2 \\ \dots \\ b_{M-1} \\ b_M \end{bmatrix} \quad (4.14)$$

According to these two definitions, the linear MLP output $\hat{y}(t)$ can be expressed with the weight combination \mathbf{c}_{weight} and the bias combination c_{bias} and with network input $\mathbf{x}(t)$ from (4.6):

$$\hat{y}(t) = \mathbf{c}_{weight} \mathbf{x}(t) + c_{bias}. \quad (4.15)$$

In order to update the weights, the output $\hat{y}(t)$ of the linear MLP needs to be compared to the measured signal $y(t)$. After learning and convergence, the weights \mathbf{c}_{weight} and the bias c_{bias}

converge to their optimal values, respectively \mathbf{c}_{weight}^* and c_{bias}^* . Due to the linear characteristic of the expression, \mathbf{c}_{weight}^* converges to

$$\mathbf{c}_{weight}^* \rightarrow [B_1 \quad A_1 \quad B_2 \quad A_2 \quad \dots \quad B_N \quad A_N] \quad (4.16)$$

and c_{bias}^* converge to:

$$c_{bias}^* \rightarrow A_0 \quad (4.17)$$

At the end, the signal $y(t)$ is thus estimated by the linear MLP with optimal values of \mathbf{c}_{weight}^* and c_{bias}^* . Furthermore, the amplitudes of the harmonic terms are obtained from the weight combination (4.16). And, the DC value of the signal is obtained from the bias combination (4.17). After convergence, the coefficients come from the appropriate element of \mathbf{c}_{weight}^* and c_{bias}^* , i.e.,

$$A_0 = c_{bias}^* \quad (4.18)$$

and the A_n and B_n from $c_{weight(j)}^*$ for $1 \leq j \leq R$:

$$c_{weight(j)}^* = \sum_{i=1}^M (w_{o,i}^* w_{i,j}^*). \quad (4.19)$$

The harmonic amplitudes C_n and the relative phase angles θ_n are calculated from $A_0, A_1, B_1, \dots, A_N, B_N$ as in (4.3).

Linear activation functions have been used for the neurons of the MLP so that the mathematical expression of the network output looks like a sum of harmonic terms if sinusoidal terms have been provided as the inputs at the same time. Indeed, the output of the linear MLP has therefore the same expression as a Fourier series. As a consequence, the neural weights of the linear MLP have a physical representation: Combined according to the two previous definitions, they correspond to the amplitudes of the harmonic components.

Discussion

Generally, MLPs are efficient in approximating nonlinear functions as a black-box. A black-box model is an approach of which there is no a priori information available. After learning, an MLP is able to provide a precise output for a given input, but it is not possible to get from it a set of

parameters to describe the function is that estimated, i.e., the weights of the MLP are not interpretable.

However, the linear MLP proposed in the previous section for estimating harmonics is different. In this approach, the nonlinearities are not introduced by the neural net itself (as usual) but by the inputs. Indeed, its inputs express the harmonics supposed to be present in the signal. Because of the linear activation functions, the output of the linear MLP is a weighted linear combination of the inputs. The weights are degrees of freedom of the network and, once trained, they represent a weighted linear combination of the harmonics. The amplitudes of the harmonics can thus be obtained directly from the weights which can be considered as interpretable. This approach and its mathematical developments can easily be generalized with more than one hidden layer.

The linear MLP handles only one signal. This means that the output of the linear MLP is for one signal in which harmonics have to be estimated. This means that the neuron in the hidden layer belongs to this unique output. The above proposed scheme clearly shows that one linear MLP represents only one Fourier series. So for estimating harmonics of a three phase current signal required three linear MLP networks with the same inputs.

Most approaches based on MLP, RNN or RBFNN do not learn on-line for self-adaptation and to enhance performances. However, ADALINE-based approaches are able to learn on-line. It is also the case of the proposed approach which is simple network. The linear MLP is not based on several MLP working in parallel, or on one per harmonic. It fits a Fourier series with a linear weighted combination of unit harmonic inputs. The linear activation function of its neurons allows an easy learning and fast convergence. An interactive learning (Wilamowski, 2011) can be used instead of the conventional backpropagation.

For practical issues, computational costs of neural approaches should be considered. The computational complexity of neural network architectures can be evaluated by the number of weights involved. Estimating N harmonics is achieved with an input vector of $R = 2N$ elements or $R = 2N + 1$ elements if including the DC component. A linear MLP with one hidden layer of M neurons requires $(2N + 1)M + M + 1$ weights for estimating N harmonics while an ADALINE needs only $2N + 1$ weights. These considerations include the biases.

For example, for $N = 10$ harmonics and $M = 5$ hidden neurons, this amounts to $(2N + 1)M + M + 1 = (2 \times 10 + 1) \times 5 + 5 + 1 = 111$ weights respectively for the linear MLP and $2N + 1 = 2 \times 10 + 1 = 21$ weights for the ADALINE. The ADALINE is the simplest architecture

because it associates only one weight for one input. Efficient linear MLPs, i.e., with good performances and reasonable number hidden neurons and appropriate inputs in order to be compliant to real-time applications. The linear MLP can therefore perform estimations of the harmonics at high speed.

4.3.2 Results of Harmonic Identification in Electrical Power System

Context of this Study

The effectiveness of the linear MLP in estimating harmonics is evaluated with several digital signals. Comparisons between the linear MLP approach and an ADALINE-based approach (Dash *et al.*, 1996) are also proposed in terms of performance, of computational costs, and of robustness against noise.

All these approaches are well suited for power system applications where typical nonlinear loads generate very low even harmonics and where triple harmonics can be ignored in three-phase circuits (Arrillaga and Watson, 2003). As a consequence, appropriate input terms can be specified for the network. Once identified, the harmonic terms can be compensated individually according to the adopted strategy, i.e., full or selective harmonic compensation, Power Factor Correction (PFC), unbalance compensation, and so on. It is obvious that the dimension of the weight vector to be updated each iteration depends on the number of harmonics to be estimated.

In order to identify the harmonic terms of the following signals, a linear MLP with one hidden layer is chosen. Initially, the weight have random values, i.e., \mathbf{W}_{hidden} , \mathbf{w}_o , \mathbf{b}_{hidden} , b_o are randomly chosen in $[-1, +1]$ and the Levenberg-Marquardt learning rule is used with a learning rate of 0.7. After a few sampling steps, the training soon converges and the value of the error diminishes to an acceptably small value. At the beginning, the ADALINE is also initially untrained with $w \in [-1, +1]$. Its learning is the α -LMS (Least Mean Squares) with learning rate of 0.25.

A sine wave with harmonics of ranks 3, 5, 7

We propose to identify the harmonic content of a typical signal composed of a fundamental frequency ($f = 50\text{Hz}$, $\omega = 2\pi f$) on which harmonics of ranks 3, 5, 7 have been added as well as a uniformly distributed noise $\eta(t)$:

$$s(t) = \sin(\omega t) + \frac{1}{3} \sin(3\omega t) + \frac{1}{5} \sin(5\omega t) + \frac{1}{7} \sin(7\omega t) + \eta(t). \quad (4.20)$$

This signal is referenced in the discrete time by t with a sampling time $T_s = 0.0002$ second and 4000 samples are used.

The first step consists in choosing the inputs of the neural approaches, i.e., the harmonic terms that are supposed to be in the signal. For this, an input vector $\mathbf{x}(t) = [\sin(i\omega t) \quad \cos(i\omega t)]$ has been created with harmonic orders $i = \{1, 2, 3, 4, 5, 6, 7, 8, 9, 10\}$ and with $i = \{1, 2, 3, 5, 7, 11, 13, 17, 19, 23\}$. In the following, these two input vectors have been abbreviated by \mathbf{x}_{1-10} and \mathbf{x}_{1-23} respectively. Of course, these two input vectors still depend on the time t and are both composed of 20 elements (sine and cosine for each harmonic rank). If we know the harmonics that are present in the signal for estimating their amplitudes, then they must be precisely specified in the input vectors of both neural approaches.

In the case given by (4.20), knowing that $s(t)$ is only composed of a DC component, of harmonics of rank 3, 5, and 7 in phase to a fundamental term with $f = 50$ Hz allows to define $\mathbf{x}(t) = [1 \quad \sin(i\omega t)]$ with $i = \{1, 3, 5, 7\}$ as the input and to use lower computational costs. The values of the coefficients A_0 , A_n and B_n are estimated by learning. After convergence, the amplitudes of the harmonic terms are obtained from the weight of the networks.

In the first test, a null noise is considered, i.e., $\eta(t) = 0, \forall t$. After learning, the estimation error each individual amplitude is of order 10^{-14} with an ADALINE and of order 10^{-10} with a linear MLP with 3 hidden neurons, and both of them with 20 inputs (\mathbf{x}_{1-10}). The same configuration, but with 40 inputs ($i = \{1, 2, \dots, 20\}$) for the linear MLP and the ADALINE, leads to approximate the signal with errors of the same range. The MSE (Mean Square Error) of the estimation is used as a measure of overall performance. The resulting MSE is less than $2 \cdot 10^{-20}$ whatever the previous neural estimator. The estimated coefficients therefore perfectly represent the harmonic content of (4.20). Both approaches are precise in identifying the harmonic terms of such type of signals without noise.

The robustness against noise has been evaluated by adding more noise is measured by the Signal-to-Noise Ratio (SNR) expressed in dB. Thus, a ratio higher than 1 indicates more signal than noise and a ratio $SNR_{dB} = 0$ means that the amplitudes of the signal and of the noise are the

same. The harmonic content of the signal is estimated by a linear MLP with 3 hidden neurons and by an ADALINE. Results are presented in Table 4.1 for several values of SNR and with \mathbf{x}_{1-10} as the input vector. The performance of the linear MLP depends on its initial condition, i.e., initial weight values. Therefore, 10 learning phases with different initial weights of the linear MLP have been conducted and resulting minimal, maximal and mean values of the MSE have been noted down. As can be seen, the linear MLP provides better estimations than the ADALINE and is more effective when the noise is important.

SNR (dB)	MSE			
	ADALINE	linear MLP (min)	linear MLP (max)	linear MLP (mean)
46	8.3802e-06	7.1659e-06	7.1725e-06	7.1703e-06
32	2.1815e-04	1.8277e-04	1.8291e-04	1.8282e-04
26	8.0347e-04	7.3262e-04	7.3353e-04	7.3315e-04
12	2.0427e-02	1.8066e-02	7.2878e-02	7.2834e-02
6	8.3833e-02	7.2795e-02	7.2878e-02	7.2834e-02
4	1.1974e-01	1.1319e-01	1.1336e-01	1.1325e-01
2	2.0367e-01	1.8242e-01	1.8285e-01	1.8269e-01
0	3.3146e-01	2.8624e-01	2.8680e-01	2.8650e-01

Table 4.1 Performance comparison between ADALINE and linear MLP with \mathbf{x}_{1-10}

The values in Table 4.1 are obtained with \mathbf{x}_{1-10} . They can be compared to the performance obtained with \mathbf{x}_{1-23} . A MSE of $7.0992 \cdot 10^{-6}$ is obtained for the linear MLP and $8.5268 \cdot 10^{-6}$ for the ADALINE in the case $SNR_{dB} = 46$. Additionally, the MSE is then $2.9260 \cdot 10^{-6}$ for the linear MLP and $3.4156 \cdot 10^{-1}$ for the ADALINE in the same case of $SNR_{dB} = 0$. The linear MLP is also more robust than the ADALINE with a more specific input vector. Besides, this can be seen on Figure 4.2 where the original signal with a high level of noise ($SNR_{dB} = 46$) and the estimations from the linear MLP and the ADALINE are represented over 2 periods of time. The original signal without any noise is also plotted to show the precision of the estimated signals. Furthermore, this figure shows the spectrum histograms obtained by the two neural approaches using inputs \mathbf{x}_{1-10} or \mathbf{x}_{1-23} .

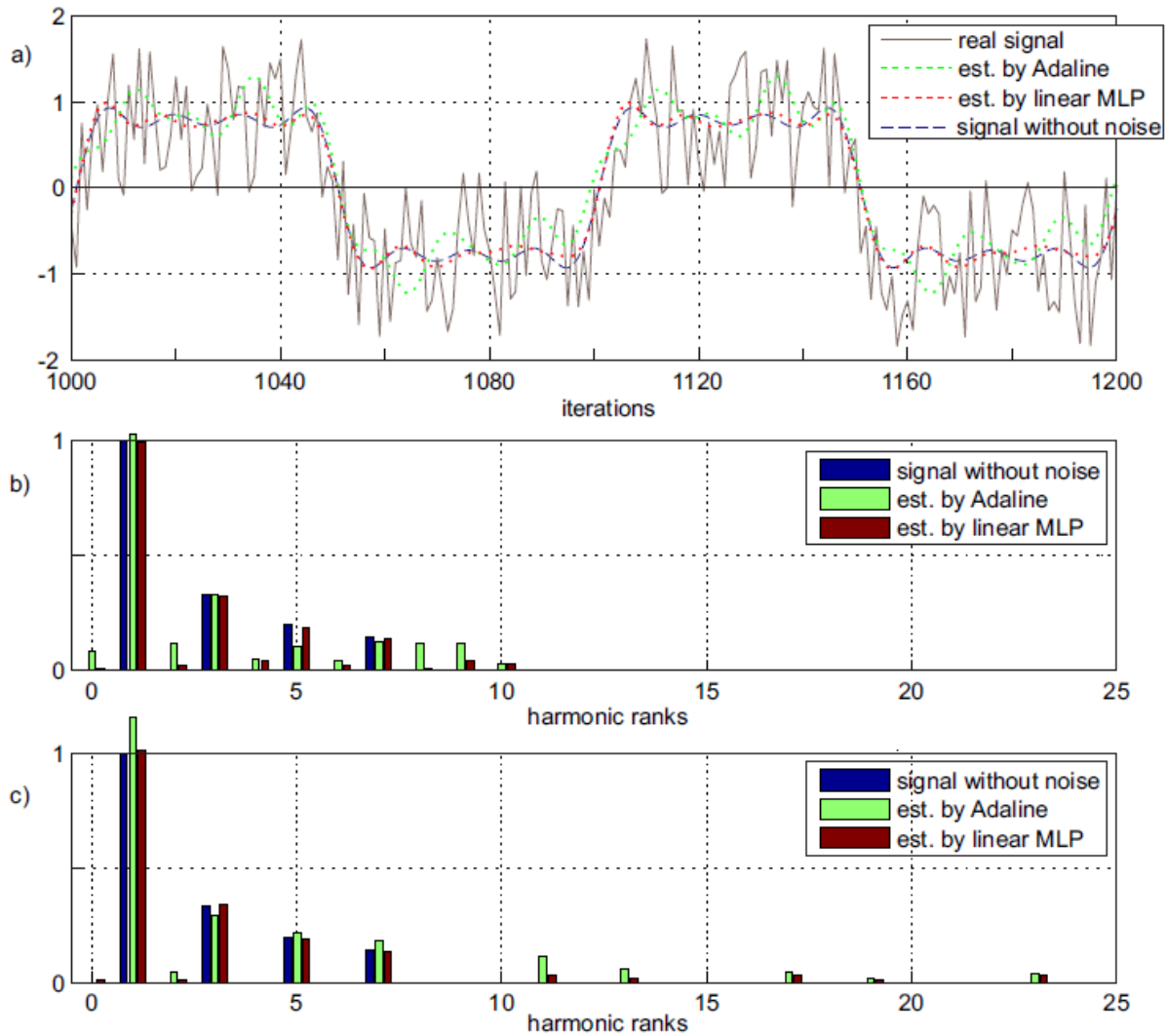


Figure 4.2 Performance of a linear MLP (with 3 hidden neurons) and an ADALINE in identifying the harmonics of the noisy sine wave $s(t)$ with harmonics of rank 3, 5 and 7, a) real constructed signals (with \mathbf{x}_{1-10}), b) normalized spectrum histograms with by \mathbf{x}_{1-10} , and c) normalized spectrum histograms with \mathbf{x}_{1-23} .

According more elements in the input vector or more neurons in the hidden layer does not necessarily make the error decreasing. A linear MLP taking into account 10 harmonics is able to estimate these types of signal even under noisy conditions. Knowing the present harmonics allows to precisely specifying the inputs in order to obtain their amplitude and allows to reduce the computational complexity and to reach a faster convergence. Additional results obtained with other signals show that with the appropriate inputs, the linear MLP is perfectly able to estimate the Fourier series with a better precision than with an ADALINE.

A real current measured on a nonlinear load

The efficiency of the linear MLP in estimating harmonics has been evaluated on a typical current measured on a real nonlinear load power device (characterized by $f = 50 \text{ Hz}$, 380 V , 20 A). For this, 4000 samples are used with $T_s = 6.0000e - 005$ second .

Generally, power system signals present a limited number of specific harmonics. A specific input vector like \mathbf{x}_{1-23} is convenient for estimating the current distortions with the neural approaches. The signal is measured and analyzed with a linear MLP. Its performance is compared to an ADALINE with the same input vector and under the same conditions. Results and comparison to the ADALINE are represented by Figure 4.3. The MSE with a linear MLP with 17 hidden neurons is $4.35 \cdot 10^{-2} \text{ A}$. This has been obtained by trial and error. Numerous tests have been conducted with 2 to 30 hidden neurons. The MSE is smaller $4.40 \cdot 10^{-2} \text{ A}$ in all cases. This is equivalent to an error of 0.18% for the current on the range of 24 A .



Figure 4.3 Estimation of the harmonic terms of a current from a real nonlinear load with a linear MLP and an ADALINE. a) Real and constructed signals b) Estimated spectrum histograms

In order to compare, the MSE obtained with an ADALINE is 1.1931 A with 20 inputs and is 0.1093 A with an ADALINE with 60 inputs, i.e., with up to harmonic of rank 30. The linear MLP is therefore more precise than the ADALINE-based approach in identifying the amplitudes of the

harmonic terms. Both implementations, of the linear MLP and of the ADALINE, are compliant to the real constraint of the sampling period.

4.3.3 Results in Estimating Harmonics of Biomedical Signals

Context of this Study

An ECG (Electrocardiography) is a recording of the electrical activity of the heart and is used in the investigation of heart diseases. For this, the conventional approach generally consists in detecting the P, Q, R, S, and T deflection (Rangayyan, 2002) which can be achieved by digital analyses of slopes, amplitudes, and widths (Pan and Tompkins, 1985). Other well-known approaches use independent components analysis (for example for fetal electrocardiogram extraction) or time–frequency methods like the S–transform (Moukadem *et al.*, 2013).

Our objective is to develop an approach that is general and therefore able to process various types of biomedical and non–stationary signals. Its principle is illustrated by Figure 4.4. Generic and relevant features are first extracted. They are the harmonic terms and statistical moments and will be used to categorize the signals in order to help the diagnosis of abnormal phenomena and diseases.

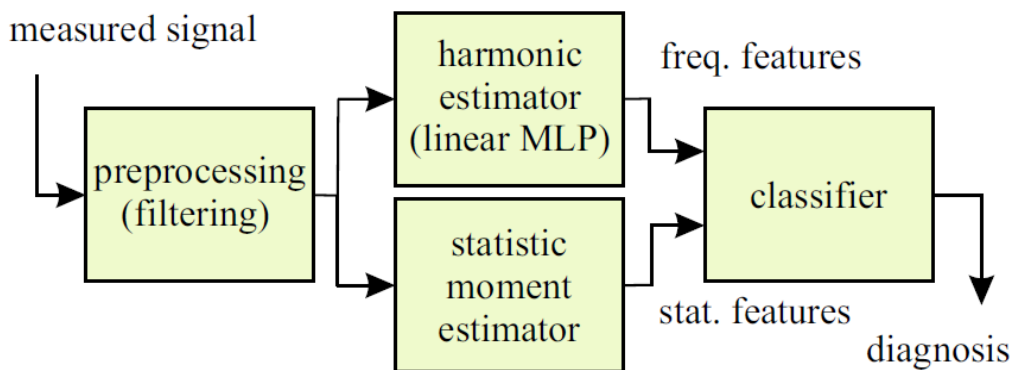


Figure 4.4 General principle for characterizing ECG records.

The following study focuses on the harmonic terms extraction from ECG. A harmonic term is a sinusoidal component of a periodic wave or quantity having a frequency that is an integer multiple of the fundamental frequency. It is therefore a frequency component of the signal. We want to estimate the main frequency components of biomedical signals, and especially non–stationary signals. Neural approaches are therefore used. They have been applied successfully for estimating the harmonic currents of power system (Ould Abdeslam *et al.*, 2007; Wira *et al.*, 2008).

Estimating harmonics can be achieved with ADALINE (Dash *et al.*, 1996) whose mathematical model directly assumes the signal to be a sum of harmonic components. As a result, the weights of the ADALINE represent the coefficients of the terms in the Fourier series (Wira *et al.*, 2008; Vázquez *et al.*, 2001; Wira and Nguyen, 2013). MLP based approaches have also been proposed for estimating harmonics. In (Lin, 2007), a MLP is trained off–line with testing patterns generated with different random magnitude and phase angle properties that should represent possible power line distortions as inputs. The outputs are the corresponding magnitude and phase coefficient of the harmonics. This principle has also been applied with RBF neural network in (Chang *et al.*, 2010) and feed forward and RNN in (Temurtas *et al.*, 2004).

In these studies, the neural approaches are not on–line self–adapting. The approach introduced therefore is simple and compliant with real–time implementations.

Experiments and Results in Estimating Harmonics of ECG

The effectiveness of linear MLP is illustrated in estimating the frequency content of ECG signals from the MIT–BIT Arrhythmia database (Moody and Mark, 1996). A linear MLP with initial weights is chosen. The fundamental frequency of the signal is on–line extracted from the ECG signal with zero–crossing technique based on the derivative of the signal. Results are presented in [Figure 4.5a](#).

In this study, tracking the frequency is also used to detect abnormal heart activities. If the estimated frequency is within a specific and adaptive range, it means that the heart activity is normal. This range is represented on [Figure 4.5b](#) by a red area. It is centered on the mean value of the range (corresponding to the orange square on [Figure 4.5b](#), then the fundamental frequency is not updated and data will not be used for the learning of the linear MLP.

Based on the estimated main frequency, sinusoidal signals are generated to synthesize the input vector \mathbf{x}_{1-20} to take into account harmonics of ranks 1 to 20 at each sample time t . The desired output of the network is the digital ECG with a sampling period $T_s = 2.8 \text{ ms}$. The Levenberg–Marquardt algorithm (Bishop, 1995) with a learning rate of 0.7 is used to train the network and allows to compute the values of the coefficients A_0, A_n, B_n of (4.16). The amplitudes of the harmonic terms are obtained from the weights after convergence.

Results over three periods of time for the record 104 are shown on [Figure 4.6](#) with 3 hidden neurons and \mathbf{x}_{1-20} for the input. The estimated signal is represented in [Figure 4.6a](#) and its frequency

content on Figure 4.6b. This figure provides comparisons to an ADALINE (with the same input) and FFT calculated over the range 0–50 Hz. Harmonics obtained by the neural approaches are multiples of the fundamental frequency $f_o = 1.2107$ Hz while FFT calculates all frequencies directly. It can be seen that the estimation of the linear MLP is very close to the one obtained by the FFT.

The MSE (Mean Square Error) of the estimation is used as a measure of overall performance. The resulting MSE is less than $1.6 \cdot 10^{-3}$ with the linear MLP with 3 hidden neurons. The MSE represents $1.4 \cdot 10^{-3}$ with the FFT and $10.2 \cdot 10^{-3}$ with the ADALINE. The estimated coefficients obtained with the linear MLP therefore perfectly represent the harmonic content of ECG. Results are similar for other signals from the database.

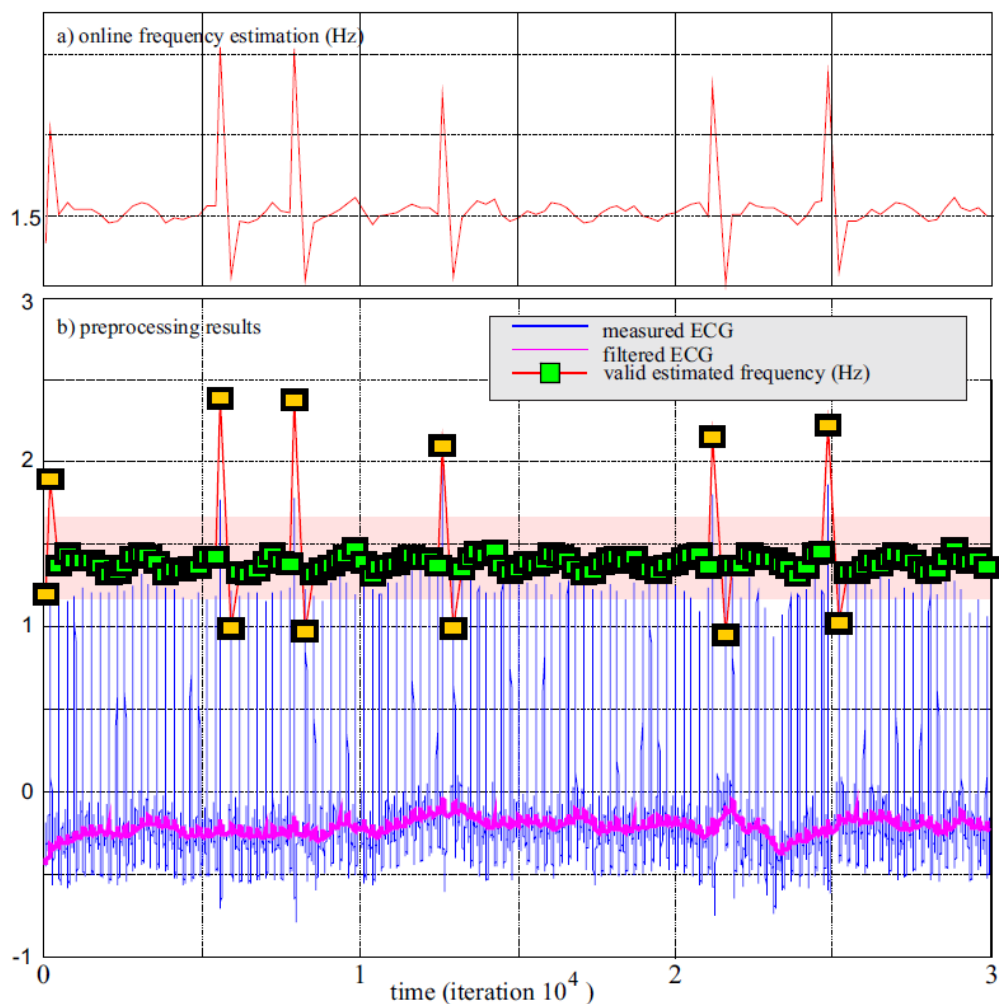


Figure 4.5 On-line fundamental tracking of an ECG.

Additional results with an input vector \mathbf{x}_{1-40} that take into account harmonics of ranks 1 to 40 and with more hidden neurons are presented in Table 4.2. The linear MLP approach is the best compromise in terms of performance and computational costs evaluated by the number of weights. The computing time required by a linear MLP with 3 hidden neurons is less than for the FFT.

Harmonic Estimator	Input vector	Number of neurons	Number of weights	MSE
FFT	0 to 50 Hz	–	–	0.0014
linear MLP	\mathbf{x}_{1-20}	3+1	127	0.0016
linear MLP	\mathbf{x}_{1-40}	3+1	247	0.0016
linear MLP	\mathbf{x}_{1-20}	6+1	253	0.0016
linear MLP	\mathbf{x}_{1-40}	6+1	493	0.0016
ADALINE	\mathbf{x}_{1-20}	1	41	0.0102
ADALINE	\mathbf{x}_{1-40}	1	81	0.0105

Table 4.2 Performance comparison between the linear MLP, ADALINE and conventional FFT in estimating the harmonic content of an ECG.

The robustness against noise has been evaluated by adding noise to the signal. Even with a signal-to-noise ratio up to 10 dB, the harmonic content of ECG is estimated by a linear MLP with 3 hidden neurons with a MSE less than $2 \cdot 10^{-3}$ compared to $4 \cdot 10^{-3}$ for the FFT and to $8 \cdot 10^{-3}$ for the ADALINE.

The linear MLP has been applied to the other records of the MIT-BIH database for training and validation. The MSE calculated after the initial phase of learning is in all cases less than $2.5 \cdot 10^{-3}$ with 3 hidden neurons.

The linear MLP is a very generic approach that performs efficient frequency feature extraction even under noisy conditions. One by product of this approach is that it is capable to generically handle various types of signals. The benefit of using a hidden layer, i.e., using a linear MLP, is that it allows more degrees of freedom than an ADALINE. For an ADALINE, the degrees for freedom represent the amplitudes of the harmonics. The weight adaption has direct influence on their values. The ADALINE is therefore more sensitive to outliers and noise. On the other hand, with

more neurons, the amplitudes come from a combination of weights and are not the weight values. The estimation error is thus shared out over several neurons by the learning algorithm. This explains why the linear MLP works better than the ADALINE in this particular application where signals are noisy and non-stationary.

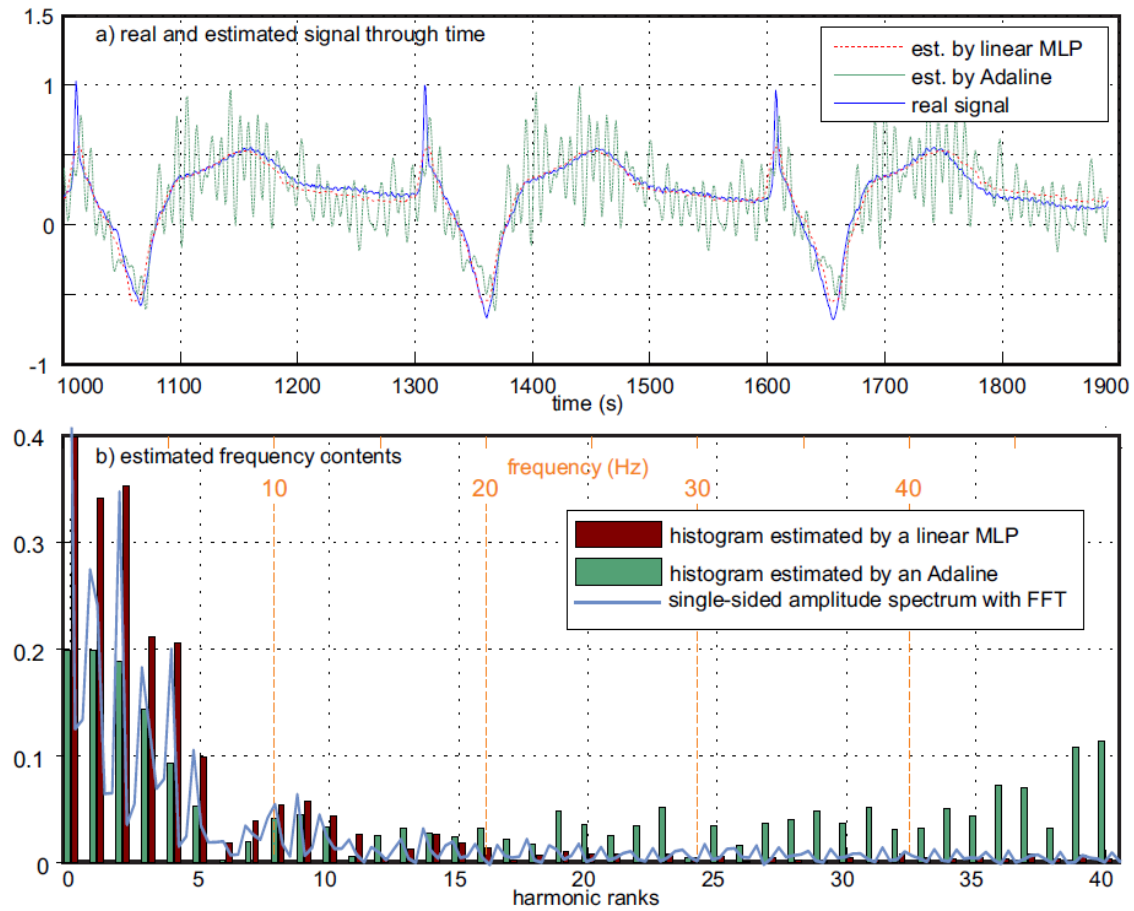


Figure 4.6 Performances of a linear MLP with 3 hidden neurons, an ADALINE and the FFT in identifying harmonics of an ECG.

4.3.4 The linear MLP with one hidden neuron compared to an ADALINE

In this section, we discuss about the linear MLP with one hidden neuron that is compared to an ADALINE. In Section 4.3.1, we proposed a linear MLP architecture for harmonics identification in a power system. So how is this architecture when it has only one neuron in its hidden layer? In this work, we step-by-step make the transformation from a linear MLP with one neuron in its hidden layer to an ADALINE.

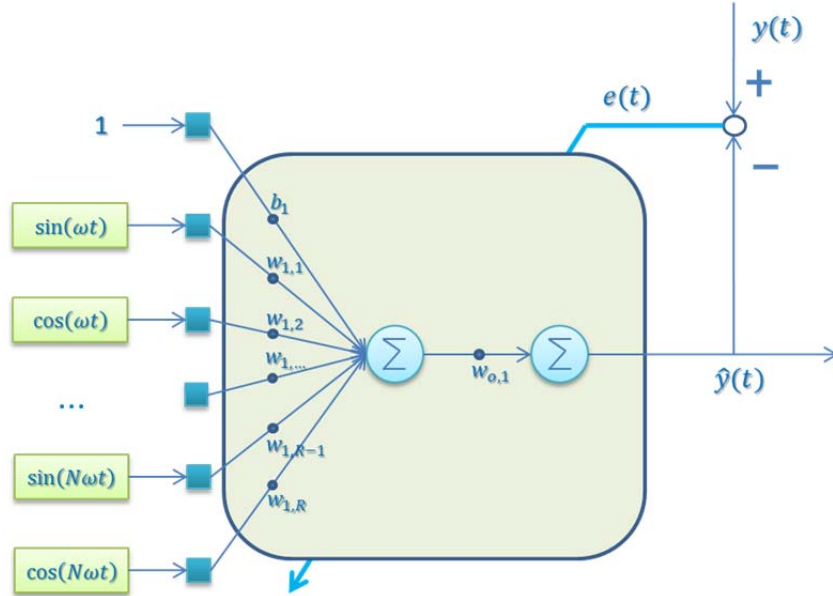


Figure 4.7 A linear MLP with one hidden neuron for harmonic identification

In **Figure 4.7**, we have architecture of a linear MLP with only one neuron in its hidden layer. This linear MLP is designed for harmonic identification with an input vector \mathbf{x} at the instance time t as follows

$$\mathbf{x}(t) = [\sin(\omega t) \quad \cos(\omega t) \quad \dots \quad \sin(N\omega t) \quad \cos(N\omega t)]^T = \begin{bmatrix} \sin(\omega t) \\ \cos(\omega t) \\ \dots \\ \sin(N\omega t) \\ \cos(N\omega t) \end{bmatrix}. \quad (4.21)$$

This MLP takes R inputs, $R = 2N$, N is the number of harmonics to be identified. Let a weight vector be \mathbf{w}_1 that contains the weights of the neuron in hidden layer of this model and b_1 is the bias of this neuron as follows:

$$\mathbf{w}_1 = [w_{1,1} \quad w_{1,2} \quad \dots \quad w_{1,R-1} \quad w_{1,R}]. \quad (4.22)$$

In vector \mathbf{w}_1 , $w_{1,j}$ is the weight of the hidden neuron connected to the input j -th input ($j = 1, \dots, R$). At instant t , the output of the only-one hidden neuron $\hat{y}_1(t)$ is

$$\begin{aligned}
\hat{y}_1(t) &= \begin{bmatrix} w_{1,1} & w_{1,2} & \dots & w_{1,R-1} & w_{1,R} \end{bmatrix} \mathbf{x}(t) + b_1 \\
&= \begin{bmatrix} w_{1,1} & w_{1,2} & \dots & w_{1,R-1} & w_{1,R} \end{bmatrix} \begin{bmatrix} \sin(\omega t) \\ \cos(\omega t) \\ \dots \\ \sin(N\omega t) \\ \cos(N\omega t) \end{bmatrix} + b_1 \\
&= w_{1,1} \sin(\omega t) + w_{1,2} \cos(\omega t) + \dots + w_{1,R-1} \sin(N\omega t) + w_{1,R} \cos(N\omega t) + b_1.
\end{aligned} \tag{4.23}$$

Therefore, the output of the network or the output neuron $\hat{y}(t)$ is

$$\begin{aligned}
\hat{y}(t) &= \sum_{i=1}^M w_{o,i} \hat{y}_i(t) = \sum_{i=1}^1 w_{o,i} \hat{y}_i(t) = w_{o,1} \hat{y}_1(t) = \hat{y}_1(t) w_{o,1} \\
&= (w_{1,1} \sin(\omega t) + w_{1,2} \cos(\omega t) + \dots + w_{1,R-1} \sin(N\omega t) + w_{1,R} \cos(N\omega t) + b_1) w_{o,1} \\
&= w_{1,1} w_{o,1} \sin(\omega t) + w_{1,2} w_{o,1} \cos(\omega t) + \dots + w_{1,R-1} w_{o,1} \sin(N\omega t) + w_{1,R} w_{o,1} \cos(N\omega t) + b_1 w_{o,1} \\
&= b_1 w_{o,1} + w_{1,1} w_{o,1} \sin(\omega t) + w_{1,2} w_{o,1} \cos(\omega t) + \dots + w_{1,R-1} w_{o,1} \sin(N\omega t) + w_{1,R} w_{o,1} \cos(N\omega t) \\
&= \begin{bmatrix} b_1 w_{o,1} & w_{1,1} w_{o,1} & w_{1,2} w_{o,1} & \dots & w_{1,R-1} w_{o,1} & w_{1,R} w_{o,1} \end{bmatrix} \begin{bmatrix} 1 \\ \sin(\omega t) \\ \cos(\omega t) \\ \dots \\ \sin(N\omega t) \\ \cos(N\omega t) \end{bmatrix}.
\end{aligned} \tag{4.24}$$

From the above expression, we can construct a network with only one neuron that has a weight vector for the same above inputs as following expression:

$$\mathbf{w} = \begin{bmatrix} b_1 w_{o,1} & w_{1,1} w_{o,1} & w_{1,2} w_{o,1} & \dots & w_{1,R-1} w_{o,1} & w_{1,R} w_{o,1} \end{bmatrix}. \tag{4.25}$$

In vector \mathbf{w} , $b_1 w_{o,1}$ is the bias of the network and $w_{1,j} w_{o,1}$ ($j = 1, \dots, R$) is the weight of the neuron of the network connected to the j -th input. The following figure shows the architecture of this network in detail.

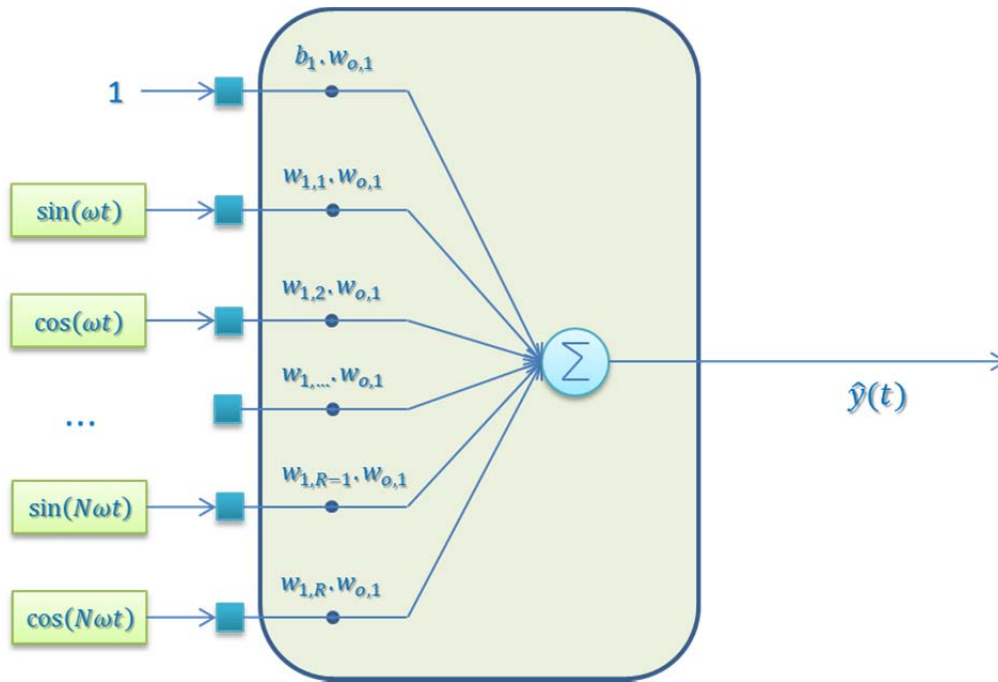


Figure 4.8 A one–neuron neural network reduced from the linear MLP with one neuron in hidden layer for harmonic identification.

We continue reducing the weight elements in weight vector \mathbf{w} simpler with following expressions:

$$\begin{aligned}
 w_0 &= b_1 w_{o,1}, \\
 w_1 &= w_{1,1} w_{o,1}, \\
 w_2 &= w_{1,2} w_{o,1}, \\
 &\dots \\
 w_{R-1} &= w_{1,R-1} w_{o,1}, \\
 w_R &= w_{1,R} w_{o,1}.
 \end{aligned} \tag{4.26}$$

We now have the new interface of the weight vector \mathbf{w} with elements $w_0, w_1, w_2, \dots, w_{R-1}, w_R$ as follows:

$$\mathbf{w} = [w_0 \quad w_1 \quad w_2 \quad \dots \quad w_{R-1} \quad w_R]. \tag{4.27}$$

So, we have an equivalent ADALINE that is showed in following figure.

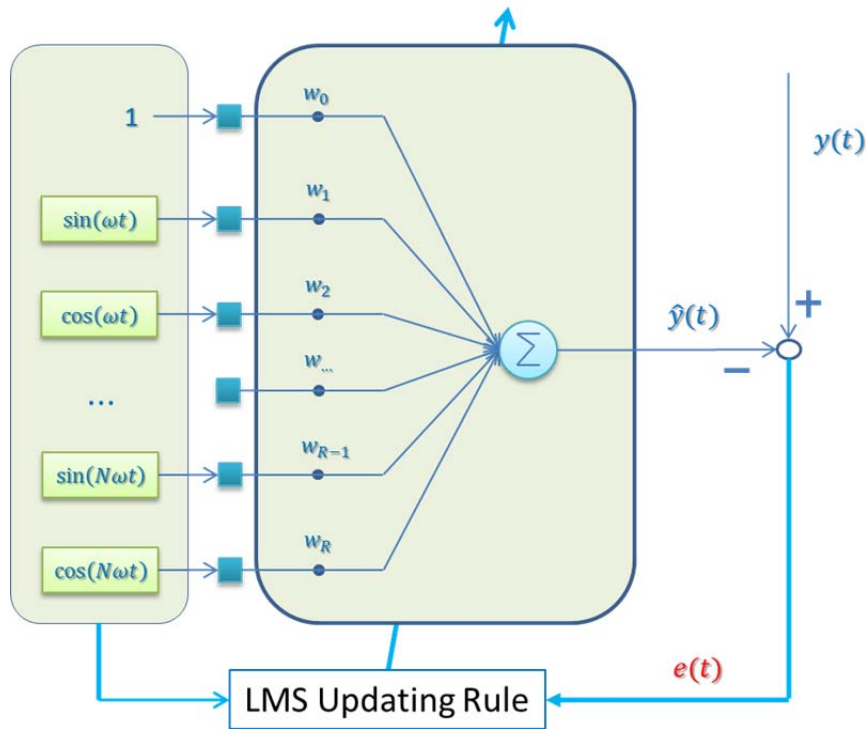


Figure 4.9 An ADALINE using LMS rule for harmonic identification.

In the end, we can say that the linear multilayer perceptron architecture in case with only one hidden neuron is like an ADALINE architecture. We are able to apply the LMS rule for this model and we get the same results.

4.4 Proposed Method 2 : A Multiple MLP for Harmonic Estimation

In this work, we propose an adaptive and intelligent harmonic content estimator by means of a neural approach based on MLPs. This neural network has advantages in nonlinear classification and pattern recognition and is very useful for solving technical problems. Here, it is used to provide a more effective solution for the power system harmonics identification problem.

The proposed approach in this section relies on several MLP with a low number of neurons. Each of them is dedicated to estimate the parameters of a specific harmonic component supposed to present in a disturbed signal. In the proposed methodology, the MLPs in the multiple MLP are trained to identify the load current harmonic components, in half-cycle of the fundamental component period. Together, the MLPs allow to directly estimating the coefficients of harmonic terms in the Fourier series in (4.1). These harmonic components are then used to determine the reference current used for the selective compensation.

4.4.1 Proposed Multiple MLP

In order to generate the compensation current of an active power filter, a precise estimation of harmonic components of the line current is required to provide a reference for the generation algorithm. The method proposed hereafter uses a parallel MLP structure as an alternative tool to harmonic content identification, with limited computational effort when compared to traditional methods.

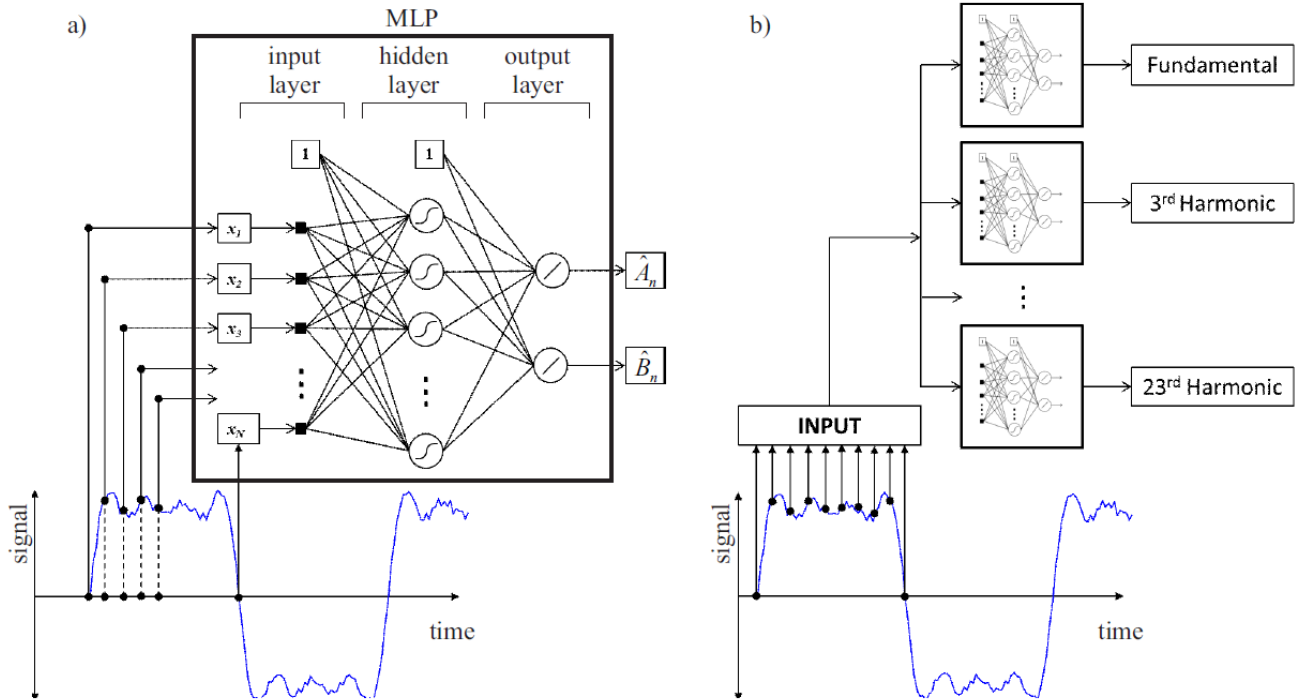


Figure 4.10 Proposed MLP architecture for estimating harmonic distortions, a) principle for one harmonic component, and b) with several MLP in parallel for each harmonic component.

We propose a structure based on several MLPs with appropriated inputs and outputs in order to solve the harmonic identification problem. After training, the MLPs are able to directly identify the harmonic components of an on-line current.

According to the Fourier analysis, any periodic or distorted waveform or signal can be represented by a function that is also called a Fourier series in (4.1). We propose a learning approach to estimate the coefficients, A_n and B_n , of each the n -th harmonic component. A MLP thus is designed with one hidden layer composed of several nonlinear neurons and two linear outputs corresponding to the two above coefficients.

The main idea of this approach is to use two outputs of each MLP in order to directly identify the values of two coefficients. This is achieved for each harmonic component which is supposed to

be present in the signal. Several MLPs are thus implemented in parallel, one for each harmonic. Figure 4.10 illustrates the block diagram representation of the methodology used in this work.

Every MLP gets the sampled values of the first half-cycle of the fundamental period of the distorted signal as inputs. All the MLPs therefore use the same inputs:

$$\mathbf{x}(t) = [x_1(t) \quad x_2(t) \quad x_3(t) \quad \dots \quad x_N(t)]^T \quad (4.28)$$

where the elements of $\mathbf{x}(t)$ are consecutive samples of the measured disturbed signal in half-cycle of its fundamental component period. In order to estimate A_n and B_n of the harmonic of rank n , the MLP uses the following target values

$$y_n(t) = [A_n \quad B_n]^T. \quad (4.29)$$

The MLP used for estimating n -th harmonic of must thus be trained with a data set

$$\Psi = \{\mathbf{x}(t), \mathbf{y}_n(t)\} \quad (4.30)$$

to identify the load current harmonic components in half-cycle of the fundamental component period. Each MLP learns a mapping between samples of the disturbed current and the coefficients of its corresponding harmonic component. The harmonic components are thus calculated or approximated directly from the outputs of the trained MLPs, \hat{A}_n and \hat{B}_n .

The adaptation of the weights and bias in the MLP is based, first, on the computation of the error between the expected values of the coefficient and those estimated by the ANN, and secondly, on the execution of the Levenberg–Marquardt backpropagation algorithm. The steps for adjustment of these weights are detailed in (Trenn, 2008). The sigmoidal activation function is used for the neurons in the hidden layer and the linear function is employed for the output neurons. After the learning and convergence,

$$\begin{bmatrix} \hat{A}_n & \hat{B}_n \end{bmatrix} \rightarrow [A_n \quad B_n] \quad (4.31)$$

for each of the MLP dedicated to the n -th harmonic.

For the proposed methodology, the harmonic identification ANN structure is trained off-line, using a set of training data generated by Fourier analysis of calculated load currents. These current

signals are all reconstructed from the first 23 harmonic components. This means that 23 MLPs of small sizes (only 1 hidden layer, with less than 10 neurons, and 2 output neurons) are implemented in parallel. The computational effort associated with the adjustment of the weights is therefore limited.

4.4.2 Experiments and Results

Identification process and context

The performance of the proposed estimation approach using the MLPs is examined through simulation tests. The system model was implemented in the MATLAB/Simulink environment. The objective is to detect the amplitudes of the harmonic components caused by nonlinear loads.

Some experiments are proposed thereafter. In a first experiment, a signal with harmonic components of ranks 3, 5 and 7 is used as a typical simple test. In a second experiment, a real current signal measured on a nonlinear load is used. For both experiments, results obtained with the proposed approach are compared to those obtained with the neural approach from (Nascimento *et al.*, 2011). Both approaches have been implemented and tested under the same conditions, with the same training set.

A set of 51 amplitude samples of the disturbed load current signal is obtained, in half-cycle of the fundamental component signal, and used as inputs to the neural architecture composed of parallel MLPs. They all receive the same sequence of current signal samples. The structure of each optimized neural estimator has 9 neurons in one intermediate (hidden) layer and 2 output neurons which produces for its respective harmonic component the values \hat{A}_n and \hat{B}_n . So, $(51+1) \times 9 + (9+1) \times 2 = 488$ weights will be used to estimate one harmonic component.

For being able to compare the proposed approach to the one from (Nascimento *et al.*, 2011) in terms of resources and costs, we chose to design it with a similar or close number of neurons. In this approach, 2 MLPs are dedicated to fully estimate one harmonic component, and we thus chose 51 inputs, 5 hidden neurons and 1 output neuron for each of them. This approach thus needs $2 \times ((51+1) \times 5 + 5 + 1) = 532$ weights to estimate one harmonic component.

The MLPs of both neural approaches are firstly trained off-line with the same training set before being used online. This training set is made of data representing normalized distorted waveforms that are randomly generated from the amplitude fundamental waveform and from

harmonics of ranks 3, 5, 7, 11, 13, 17, 19, and 23. This allows to compose $\Psi = \{\mathbf{x}(t), \mathbf{y}_n(t)\}$ with $n \in \{3, 5, 7, 11, 13, 17, 19, 23\}$ for the training process. Attention has been paid for generating of the data set in order to obtain representative values of real disturbed signal from power lines. Figure 4.11 shows a training performance example, i.e., for the learning of the 23rd harmonic with a MLP. It should be noticed, that this is a severe case, because the amplitude of the 23rd harmonic component is small compared to the amplitude of the fundamental component (usually less than 4%). With only 12 neurons, a MLP is able to converge quickly even under noisy conditions.

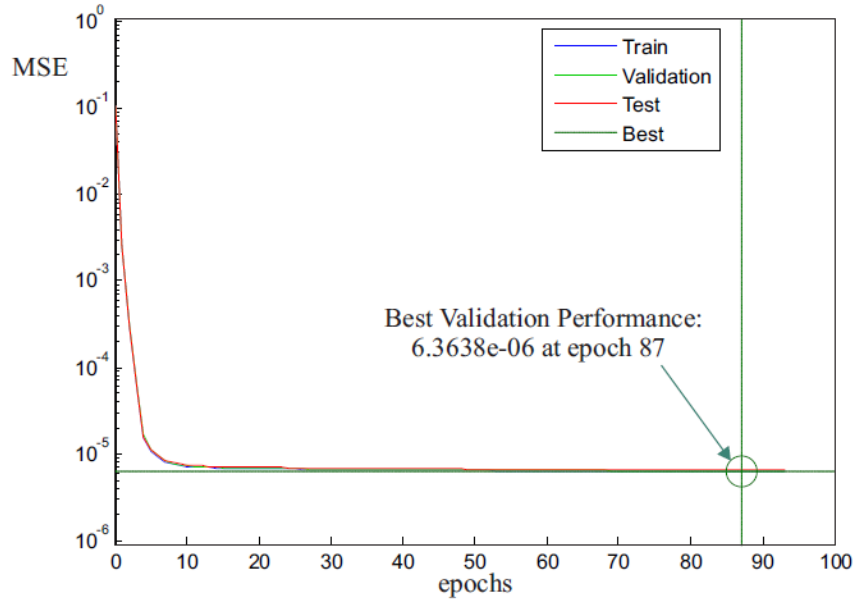


Figure 4.11 Training performance of the proposed neural approach in detecting harmonic of rank 23.

Experiment 1: With a pure signal containing only 3rd, 5th and 7th harmonics

In this experiment, a signal with harmonic components of rank 3, 5, and 7 in addition to the fundamental component is considered:

$$s(t) = \sin(\omega t) + \frac{1}{3} \sin(3\omega t) + \frac{1}{5} \sin(5\omega t) + \frac{1}{7} \sin(7\omega t) + \eta(t), \quad (4.32)$$

with $f_1 = 50$ Hz and $T_s = 0.2$ microsecond. $\eta(t)$ is a uniformly distributed noise chosen to obtain a Signal-to-Noise Ratio (SNR) of 32 dB. This expression is used to generate the 4000 samples of Ψ .

The proposed approach is used estimate the coefficients \hat{A}_n and \hat{B}_n . They are then used to calculate the corresponding harmonic components. All harmonics and fundamental components

are then used for reconstructing the signal. This reconstructed signal can be compared to the original one by calculating the MSE (min, max, and mean values). Results are given in Table 4.3 and are compared to the approach of (Nascimento *et al.*, 2011).

MLP approaches	Minimal MSE	Maximal MSE	Mean MSE
Proposed MLP approach (with 11 neurons/harmonic, i.e., 488 weights)	0.0592	0.0680	0.0635
MLP approach from (Nascimento <i>et al.</i> , 2011) (with 12 neurons, i.e., 532 weights)	0.0896	0.1049	0.0965

Table 4.3 Performances of MLP approaches in estimating the harmonic content of signal with only 3rd, 5th and 7th harmonics.

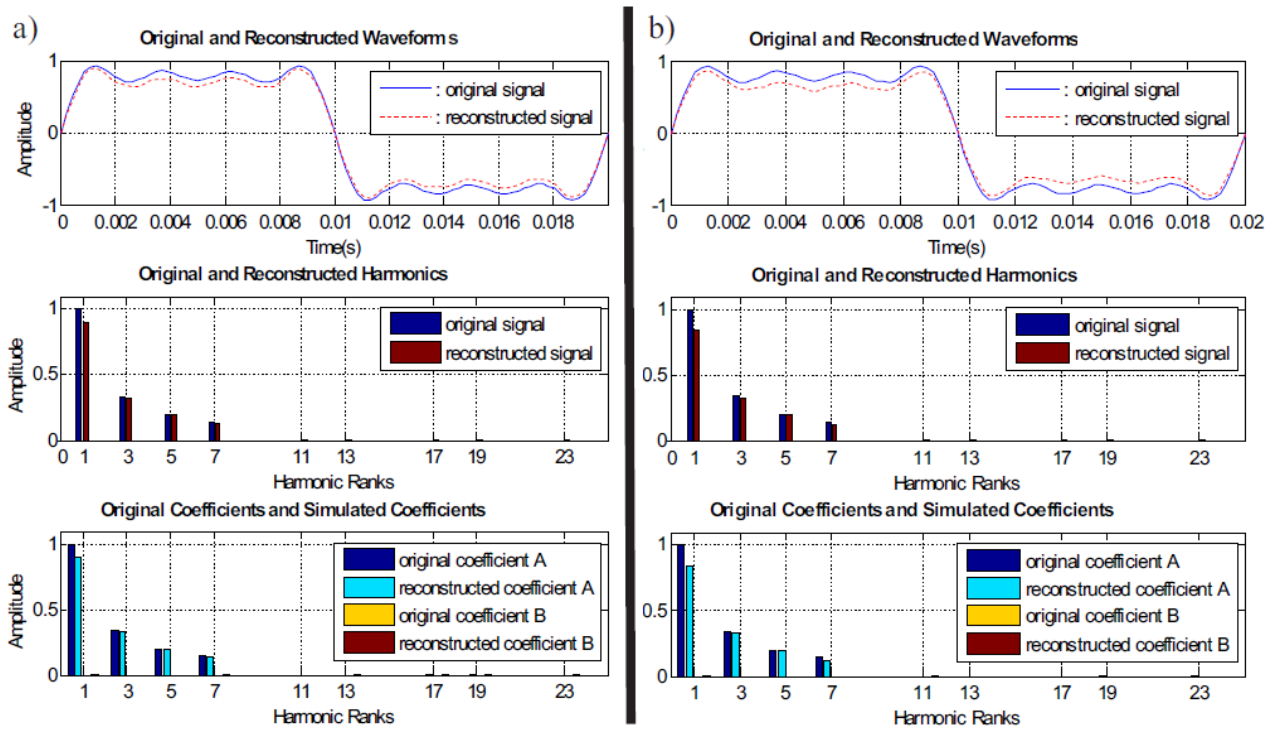


Figure 4.12 Harmonic identification of a sine wave with harmonic of ranks 3, 5, 7. a) with the proposed approach b) with the approach of (Nascimento *et al.*, 2011)

Figure 4.12 also shows the reconstructed signals obtained from the two approaches and the original one given by (4.32). After convergence, the MSE between the original and the reconstructed signal with the proposed approach is 0.065 over one period. With the same conditions, the approach of (Nascimento *et al.*, 2011) yields a MSE of 0.100 over one period. The estimation of the amplitude and the approximation of the signal are better with the proposed

method with less number of weights than the other method. As one can see, the proposed method exhibits generalizing capabilities and is robust against noise.

Experiment 2: With a typical current measured on a real nonlinear load power device

In the following experiment, a typical current that is measured on a nonlinear load device characterized by $f_1 = 50$ Hz, 380 V, 20 A and $T_s = 0.2$ microsecond is considered. The proposed neural approach is used to estimate the amplitudes from the harmonic components found in this current.

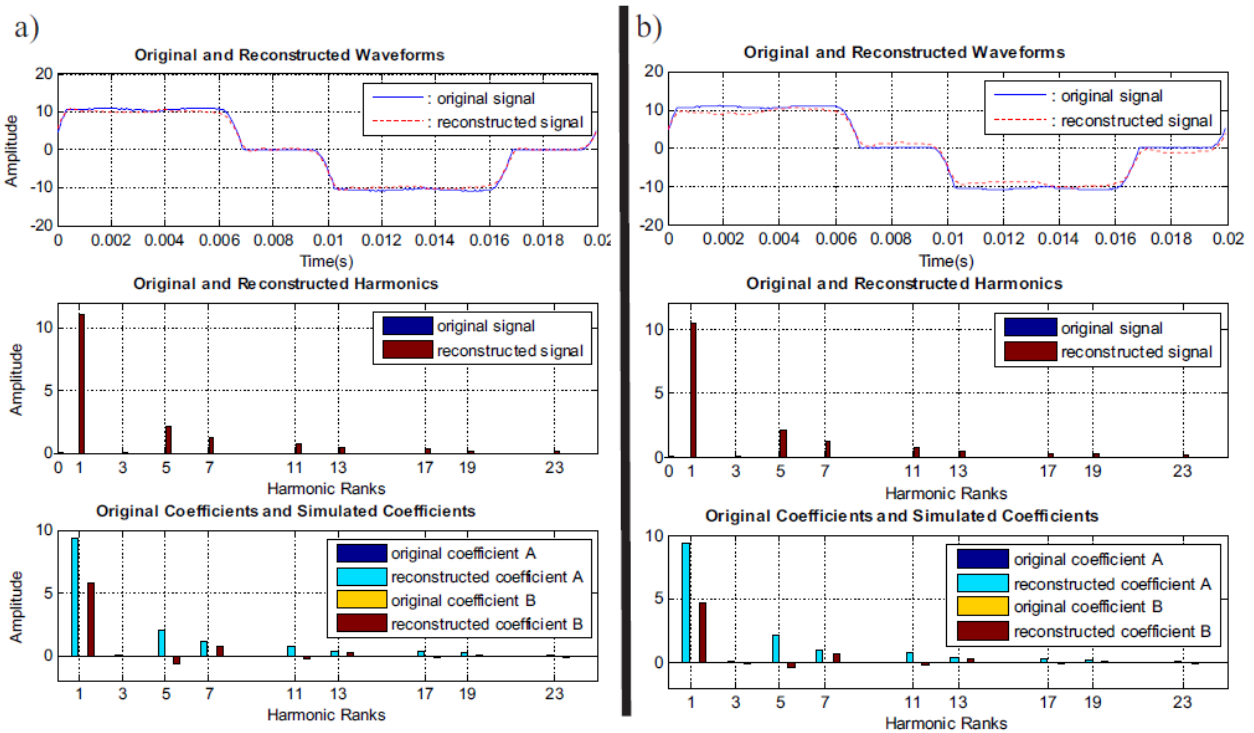


Figure 4.13 Experimental results of harmonic identification of a current measured from a real nonlinear load, a) with the proposed approach, b) with the approach of (Nascimento et al., 2011).

Figure 4.13 illustrates the results of the ANN harmonic content estimation as well as showing the target value. Table 4.4 shows the MSE between estimated and target values. Figure 4.13 and Table 4.4 also show and compare the results obtained with the approach from (Nascimento *et al.*, 2011). The original coefficients A_n and B_n for this signal are not available because of it is a measured signal but they can be calculated with any frequency analysis method. The error relative to the original signal is calculated to determine the network effectiveness in the harmonic estimation process. After learning and convergence, the MSE is thus 0.455 A with the proposed method and 1.016 A with the other method over one period of the current. This represents

respectively less than 2.3% and 5% of the current. Of course, these errors may be related to the number of inputs used by the ANNs, i.e., are dependent of sampling process.

MLP approaches	Minimal MSE	Maximal MSE	Mean MSE
Proposed MLP approach (with 11 neurons/harmonic, i.e., 488 weights)	0.4507	0.5025	0.4778
MLP approach from (Nascimento et al., 2011) (with 12 neurons, i.e., 532 weights)	0.9805	1.0148	1.0035

Table 4.4 Performances of MLP approaches in estimating the harmonic content of a real nonlinear load current

Additional experiments have been conducted. The proposed neural method has been tested in a single-phase system, considering nonlinear loads popular in industrial applications. The results have shown that MLP-based method was able to determine the expected harmonic content in half-cycle source voltage. Therefore, the requirements for harmonic determination were satisfied.

4.5. Summary

In this chapter, two original MLP based approaches have been introduced for the harmonic estimation problem. The first method is based on a new linear MLP that is able to learn on-line for fitting a Fourier series. The second method is a structure with several MLPs that are trained off-line and this structure is able to estimate harmonics of the distorted signal after learning. The effectiveness of these approaches is evaluated by the experiments with generated and real measured signals under different noisy conditions.

In the first approach, a linear multi-layer perceptron (MLP) has been proposed to learn and estimate signals by fitting a Fourier series. The linear MLP estimates any periodic signal by expressing it as a sum of harmonic terms. The proposed neural network takes generated unit harmonic elements for its inputs and uses neurons with linear activation functions. The measured signal is used as a reference that is compared to its own output. This error allows to find out the optimal weights and thus to determine the amplitudes of the harmonics. Due to the architecture of the linear MLP, the amplitudes can be written as a combination of the weights of neurons after learning. Estimating harmonic is illustrated on synthetic and experimental signals and the results compared to those of the well-known ADALINE. These results show that the linear MLP

identifies the amplitudes of the fundamental and higher-order harmonics with a good precision even under noisy conditions. The linear MLP is able to adapt itself for estimating individually harmonics of nonlinear load currents, whose amplitudes and relative phase angle are subject to unpredictable changes.

In the second approach, a new neural architecture based on MLPs for estimating the harmonic contents of electrical power signals has been proposed. In this approach, several MLPs with a reduced number of neurons are used in parallel. Indeed, the MLPs are dedicated for each individual harmonic component which is supposed to be present in the disturbed signal. As a result, the number of neurons and weights used in the proposed model is less than with other neural techniques. In order to investigate the performance of this identification method, the study has been accomplished using simulation tests. The results of the identification approach, compared to other similar methods, are found satisfactory by assuring good estimating performances and high robustness against noise. The results showed that the new approach works effectively in estimating each individual harmonic component. Furthermore, this approach is able to identify harmonic contents with only a half of the fundamental period of the signal even under noisy conditions.

Both of these proposed approaches will effectively improve the performances of active power filter schemes for compensating harmonics in power systems.

Chapter 5 : Electric Appliances Classification Using Artificial Neural Networks

5.1 Introduction

In this chapter, we present three machine learning approaches that have been developed for nonlinear load classification in a power system. The first proposed approach is based on a binary output multilayer perceptron. The second proposed approach is based on a structure of multiple binary output multilayer perceptrons. The third approach is based on a structure of multiple support vector machines.

In first proposed approach method, a simple multilayer layer perceptron has been developed for nonlinear load classification in a power system. The proposed multilayer perceptron is able to identify nonlinear loads which are ON or OFF based on extracting the harmonic features from the distorted waveform in power system. In this approach, the network is trained with a generated training set. As a typical multilayer perceptron, this network is based on supervised training. A data training set was generated with harmonic amplitudes as inputs and targets (value 0 for OFF or value 1 for ON) for training this network before using it.

In the second proposed approach, we propose another new neural network approach based on the structure of MLPs for classifying nonlinear loads in a power system. The learning approach is based on several binary–output multilayer perceptrons. After training, each multilayer perceptron is able to identify an electrical appliance is “ON” or “OFF” in power system. The difference of this method and the first method is to use more many multilayer perceptrons. This structure is trained by the same generated training set above.

In the third proposed approach, a structure of multiple support vector machines was proposed. This proposed structure consists of N support vector machines. The number N is the number of appliances we need to identify them “ON” or “OFF” in a power system. Because the support vector machines in this structure are supervised learning system, we use the same above generated training set to train this structure before we use it to classify nonlinear devices.

Finally, [Figure 5.1](#) shows our strategy for the problem nonlinear load classification. There two steps to classify electric appliances from the distorted signal from power system. The first step is harmonic identification or estimation which has been presented in Chapter 2 and Chapter 4 with our proposed methods. The second step is the nonlinear load classification itself that will be

present thereafter. We proposed three models to address this problem. Two of the proposed methods are based on multilayer perceptron network techniques. The third proposed method is designed with several support vector machines also called SVM.

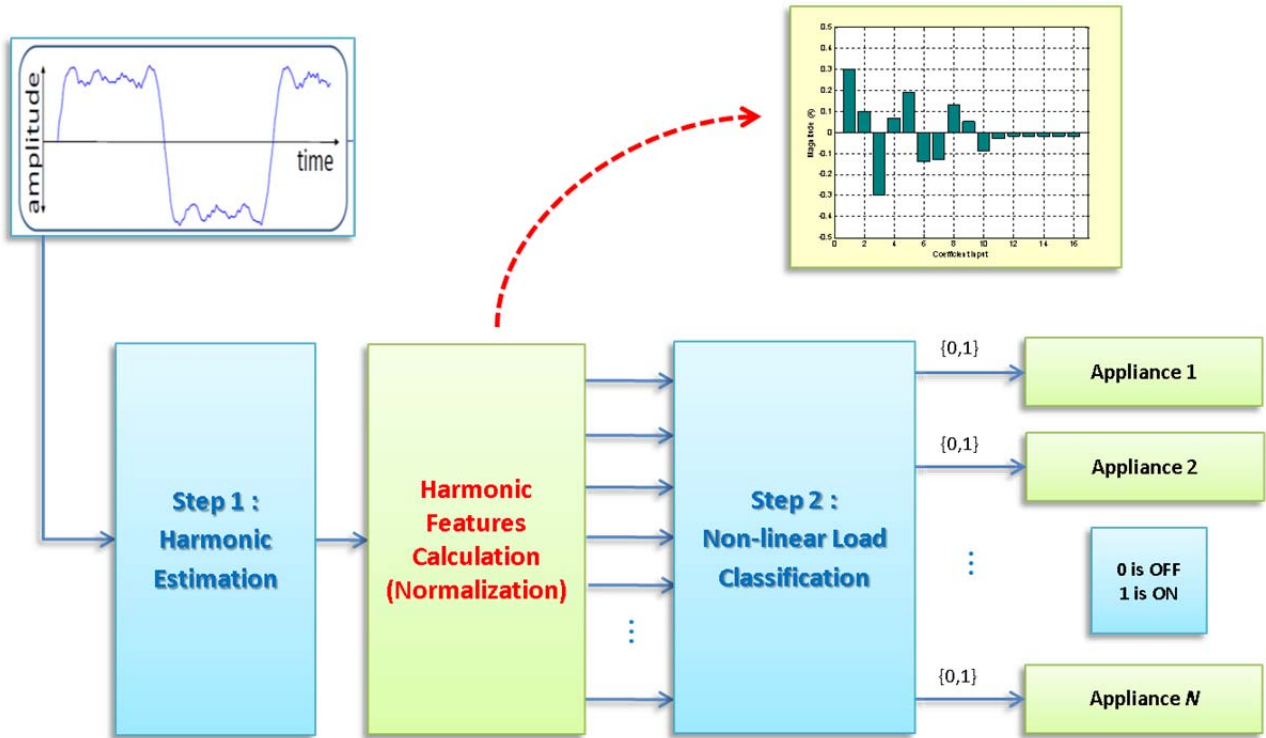


Figure 5.1 Electric appliances classification by harmonic features with 2 steps.

5.2 Proposed Methods for Nonlinear load classification

5.2.1 Proposed Model 1 : A Binary–Output MLP

The first proposed method for solving the problem of nonlinear load classification is based on a multilayer perceptron with normalized harmonic amplitudes as inputs. As a typical multilayer perceptron, this neural network uses several sigmoid neurons in the hidden layer and linear neurons in the output layer. The MLP learning architecture is represented by Figure 5.2.

The number of neurons in the output layer of the MLP network depends to the number of appliances we want to identify from the distorted input signal. Each output neuron, the neuron in the output in this network, will provide the values 0 or 1 that correspond to the states ON or OFF of each appliance to consume current from in power system. We name this method the binary–output multilayer perceptron, or Model 1.

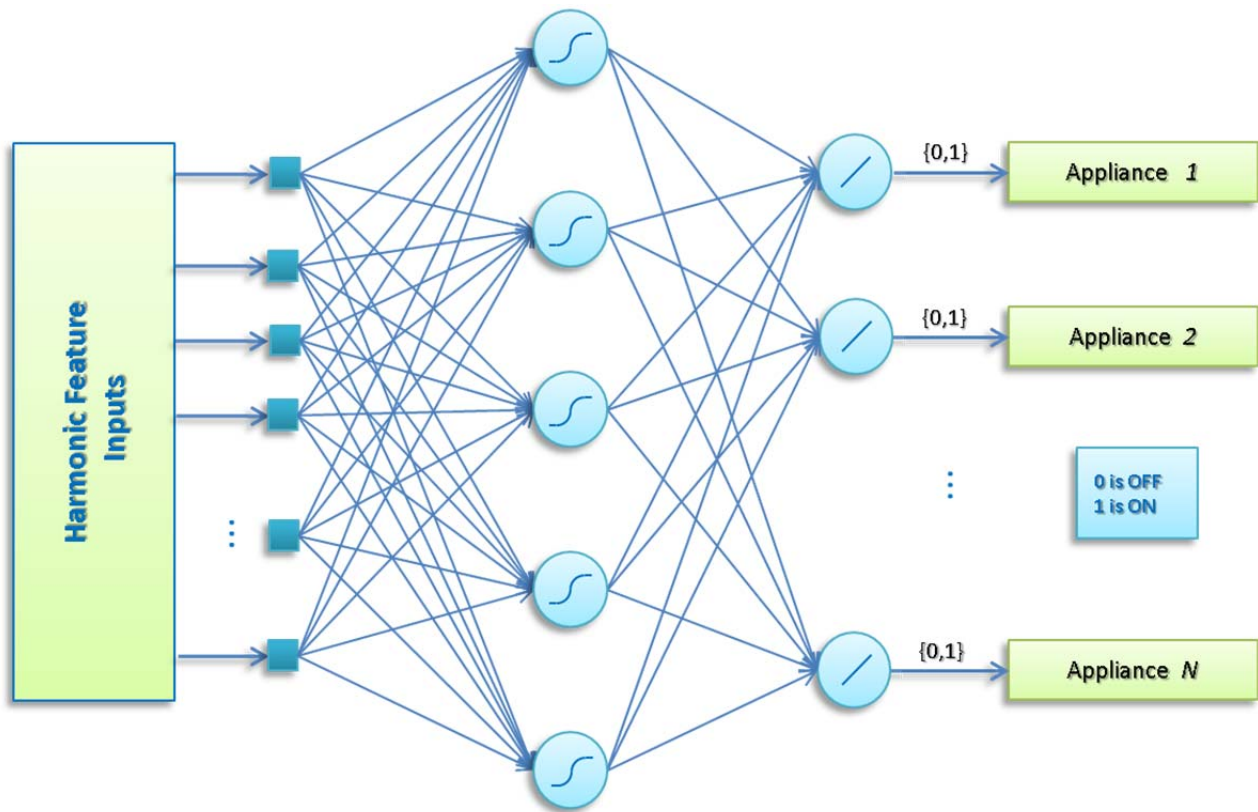


Figure 5.2 Proposed Model 1 – A Binary-Output MLP for Nonlinear Load Classification.

The main idea of this method is to use only one multilayer perceptron with multiple output neurons. After training, this network is able to classify nonlinear loads from the harmonics features that were extracted from a distorted waveform of a power system. From the outputs of this network, we are able to know each device in a power system is ON working or OFF.

5.2.2 Proposed Model 2 : A Multiple Binary–Output MLP

In the second proposed method, we use several binary–output multilayer perceptrons to solve the same problem of the first proposed method. In this approach, we proposed a structure with several multilayer perceptrons. Each multilayer perceptron has the same inputs as harmonic features and one binary output as in following figure. The output of each multilayer perceptron exports the values 0 or 1. In this structure, each multilayer perceptron will be trained with the same training data set then the above mentioned method. And after learning, each network will calculate and answer if the appliance is switched ON or OFF in the system. We name this method the “Multiple Binary–Output Multilayer Perceptron” or Model 2.

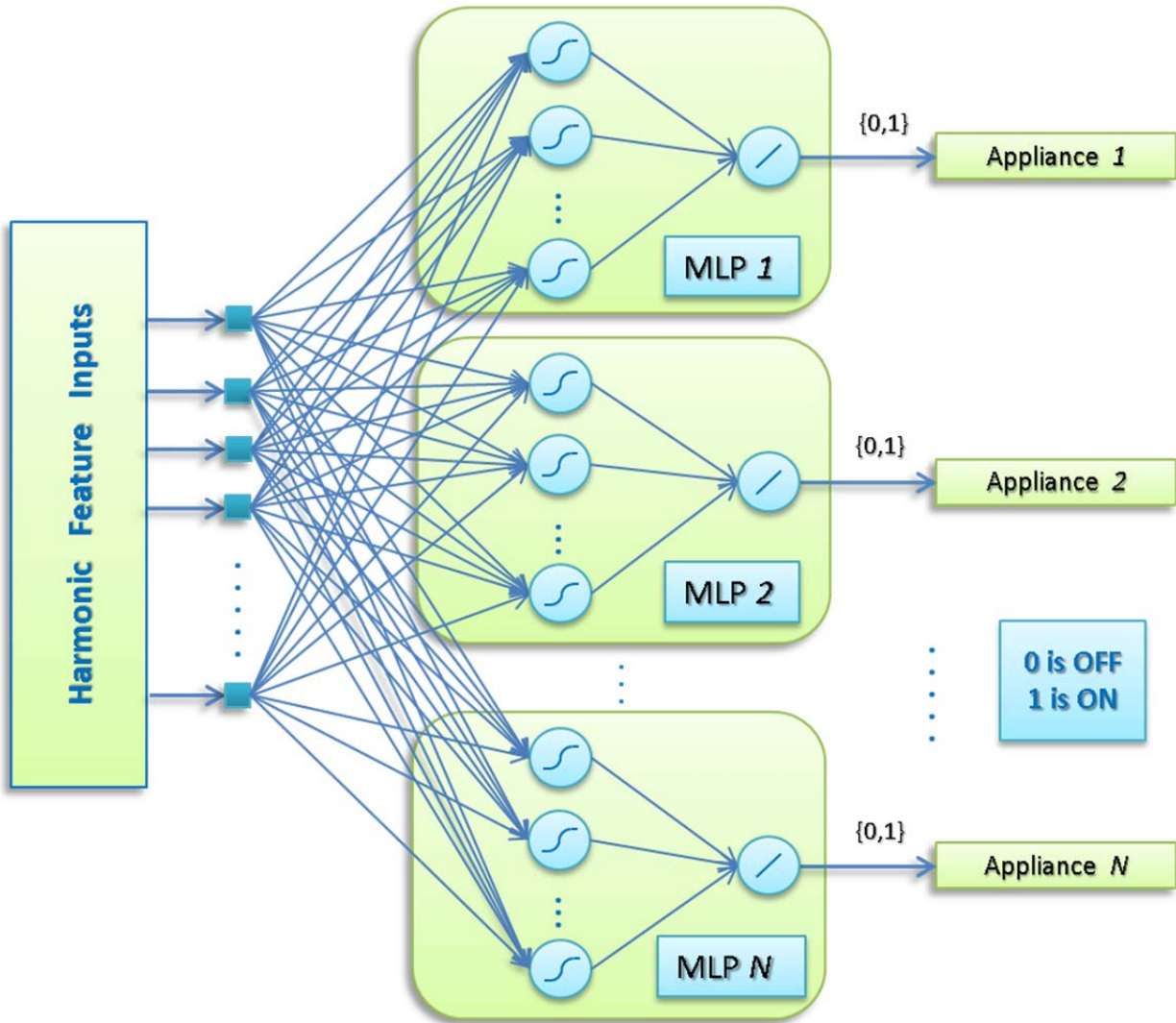


Figure 5.3 Proposed Model 2 – A Multiple Binary–Output MLP for Nonlinear Load Classification

5.2.3 Proposed Model 3 : A Multiple Support Vector Machine

In machine learning, the support vector machine is a supervised learning model that is typically used to categorize data and to recognize patterns. For a given training data set with known categories, a support vector machine is able to assign to each data sample point in a high dimensional space. After learning, the optimized hyper–planes corresponding to the support vectors are able to classify each input from the data set into two subsets.

In this method, the structure of the support vector machines is used for classifying non–linear loads in order to decide according from the harmonic content provided as the input if appliances are switched ON or OFF and are consuming current from the power system. One has to note that a basic support vector machine only deals with two classes. So we use one support vector for each

non-linear load that is supposed to be connected in the power system. We name this method the Multiple Support Vector Machine or Model 3.

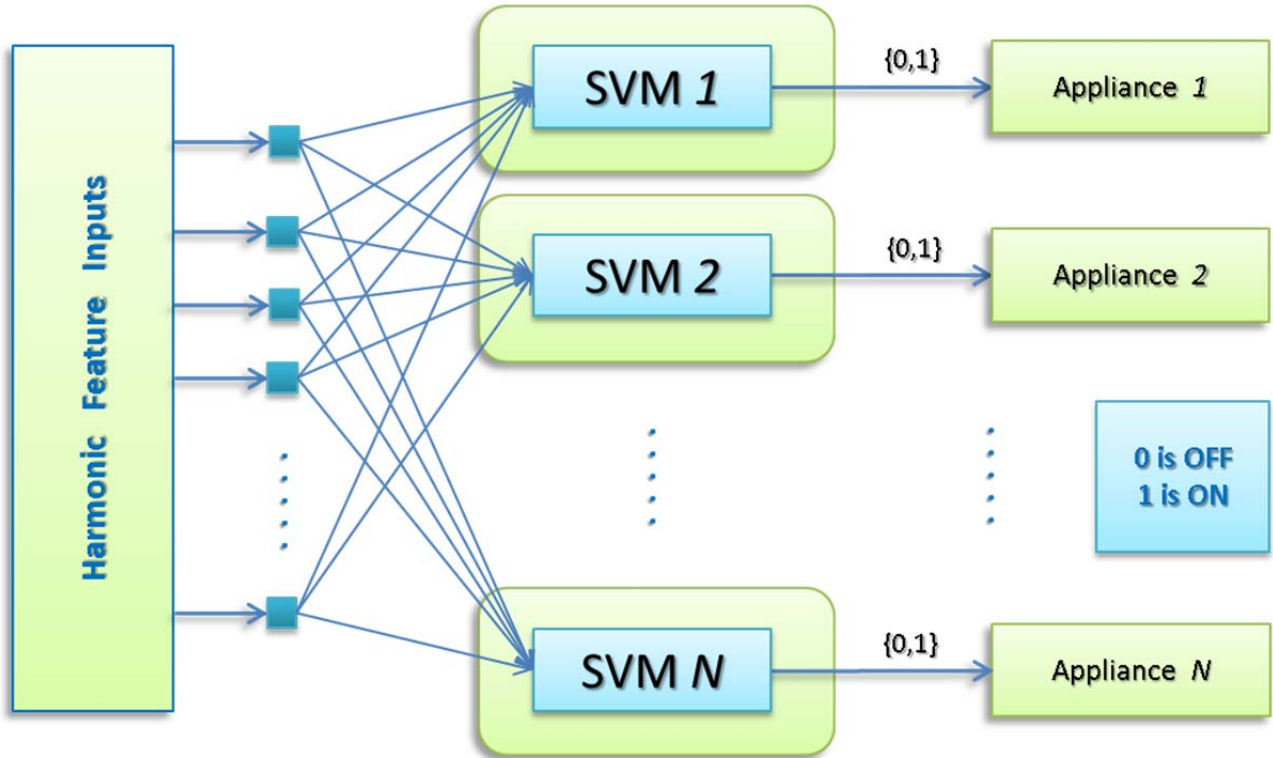


Figure 5.4 Proposed Model 3 – A Multiple SVM for Nonlinear Load Classification

5.3 Experimental Setup

In this section, we present some computer experiments of three proposed methods in order to evaluate their performances. Results in classifying nonlinear loads absorbing current in a power system are investigated. The performances of our three proposed methods for nonlinear load classification using multilayer perceptrons and support vector machines is examined through computer simulation tests. The system model was implemented in the MATLAB environment. The objective of these tests is to identify electrical appliances existing in the system from the harmonic features extracted (identified/estimated) from the distorted waveform of a power system. In following experiment we use the three above methods for the nonlinear load classification problem. All three methods use the same estimated harmonic features from distorted waveform signals their input. We called them the harmonic feature input.

In this experiment, a harmonic feature input is a tuple of normalized magnitudes of harmonic coefficients estimated or identified from a distorted waveform current. These harmonic coefficients are calculated by our proposed harmonic estimation methods, one based on a linear MLP and one based on a structure of multiple MLP that we proposed and presented in the Chapter 4 of this thesis.

In model 1, the binary–output multilayer perceptron, we use only one multilayer perceptron to implement the classifier for nonlinear load classification. The inputs of this network are the normalized harmonic coefficients that have been identified from the distortion waveform current measured from the power system. The output neurons correspond to the appliances/devices that we want to classify from the distorted waveform current of the power system. This network has only one hidden layer. The number of hidden neurons is between the number of network inputs and the number of network outputs.

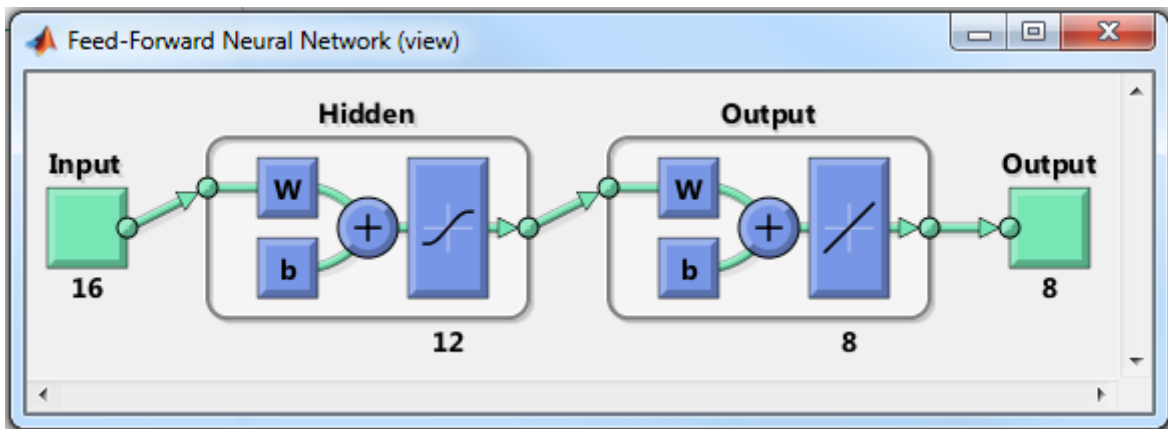


Figure 5.5 A MLP implemented in MATLAB for model 1

Figure 5.5 shows a configuration of the nonlinear load classifier implemented in MATLAB for model 1 with 16 inputs according to 16 normalized harmonic coefficient magnitudes, 12 hidden neurons in the hidden layer and 8 output neurons in the output layer according to 8 appliances/devices to be classified. This MLP is trained offline before being used online. The training algorithm for this MLP is the Levenberg–Marquardt algorithm.

In model 2, the multiple binary–output multilayer perceptrons, a structure of several MLPs is used to implement the classifier. The number of multilayer perceptrons used in this structure corresponds to the number of appliances that need to be identified (to detect if they are switched ON or OFF) from the distorted waveform current from the power system. Each multilayer perceptron receives the same harmonic feature inputs as in model 1. Each MLP network contains

one output neuron that is associated to an appliance or a device in the system. In this structure, each MLP has only one hidden layer and the number of hidden neurons in each MLP is between 1 and number of network inputs.

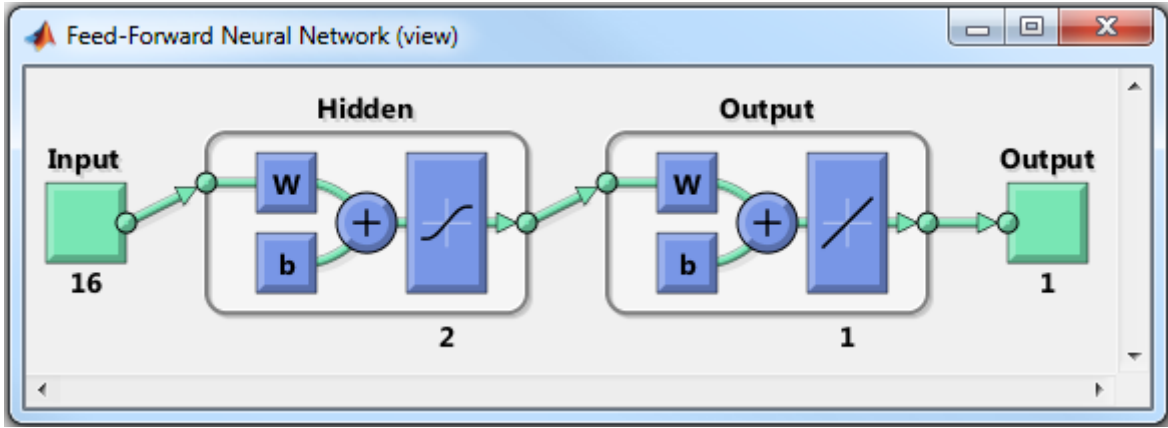


Figure 5.6 A MLP implemented in MATLAB for the multiple MLP in model 2.

In [Figure 5.6](#), a multilayer perceptron is implemented in the MATLAB environment for the structure of model 2 with 16 inputs according 16 normalized harmonic coefficient magnitudes, 2 hidden neurons in their hidden layers, and 1 output neuron in their output layers. All of the multilayer perceptrons in this method are trained offline by the Levenberg–Marquardt algorithm before being used online.

In model 3, the multiple support vector machine, we configure the number of support vector machines according to the number of appliances/devices supposed to be present in the power system. Each support vector machine receives the same harmonic feature inputs as in model 1 and in model 2. Each support vector machine contains one output according to an appliance. The number of support vectors (in each of SVM) has been optimized in the MATLAB environment when trained offline. The kernel function of these support vector machines is the Gaussian radial basis function kernel.

In the following experiment, we use the three proposed methods to identify of 8 kinds of home appliances. The home appliances that are connected in the power system are a monitor, computer, fluorescent lamp, television, battery charger, fan, fridge, and light bulb. The power system harmonic coefficients data of these 8 home appliances are from (Srinivasan et al., 2006). Their names and their photos are listed in [Table 5.1](#). In order to evaluate 3 above proposed methods, we use 16 measured harmonic coefficient magnitudes of 8 appliances in (Srinivasan et al., 2006) for

this experiment. The harmonic ranks of distortion waveforms are 1, 3, 5, 7, 9, 11, 13 and 15. Magnitudes of 16 harmonic coefficients (harmonic signatures) of 8 appliances are showed in [Figure 5.7](#). If the amplitude value of a harmonic component is negative, this can simply be considered as a component with a positive amplitude but phase-opposite to the main component of the signal, i.e., the component corresponding to the fundamental frequency.

Distorted current waveforms contain numerous harmonics and the current Total Harmonic Distortion (THD) is a relevant measure of the amount of distortion in the current's wave shape (Arrillaga and Watson, 2003): The higher the current THD value, the greater the distortion. So, the current THD is a general indicator that is commonly used to evaluate the quality a current waveform or to express the energy-efficiency of a power system. For example, the Federal Energy Management Program in the USA, which issues energy-efficiency guidelines for federal buildings, specifies THD of 20% or less. So, utilities should only include electronic circuits that produce distorted currents with a THD of less than 20% in their energy-efficiency programs.

All three above proposed models for this experiment are off-line learning systems. They are trained off-line by the same training data set before being used online. In order to achieve the full experiment, we need to prepare and to generate two distinct data sets. The first data set is the training data set for the offline training of the 3 proposed learning methods. The second data set is the test set that is used for the validation of the responses obtained with the 3 trained methods. Thus for this experiment, all the data sets have been generated from precise values for the magnitudes of the higher-order harmonics on which some small random fluctuations have been added for the 8 appliances introduced in [Table 5.1](#). This has been done for the harmonic of ranks 1, 3, 5, 7, 9, 11, 13 and 15. These ranks are the most relevant and important in power systems. It is well known that harmonics that are odd triple multiples of the fundamental frequency (3rd, 9th, 15th, 21st, ...) have the greatest potential impact on electrical systems because this current flows on the neutral conductor and might overload it. The ANSI C82.11 standard also sets limits for odd triple multiples and other harmonics.

The exact values of the amplitudes used to generate the data sets are provided in [Table 5.2](#). With the generated the data sets, 8 different appliances are available for training the learning methods, and 8 other appliances can be used for the validation tests.









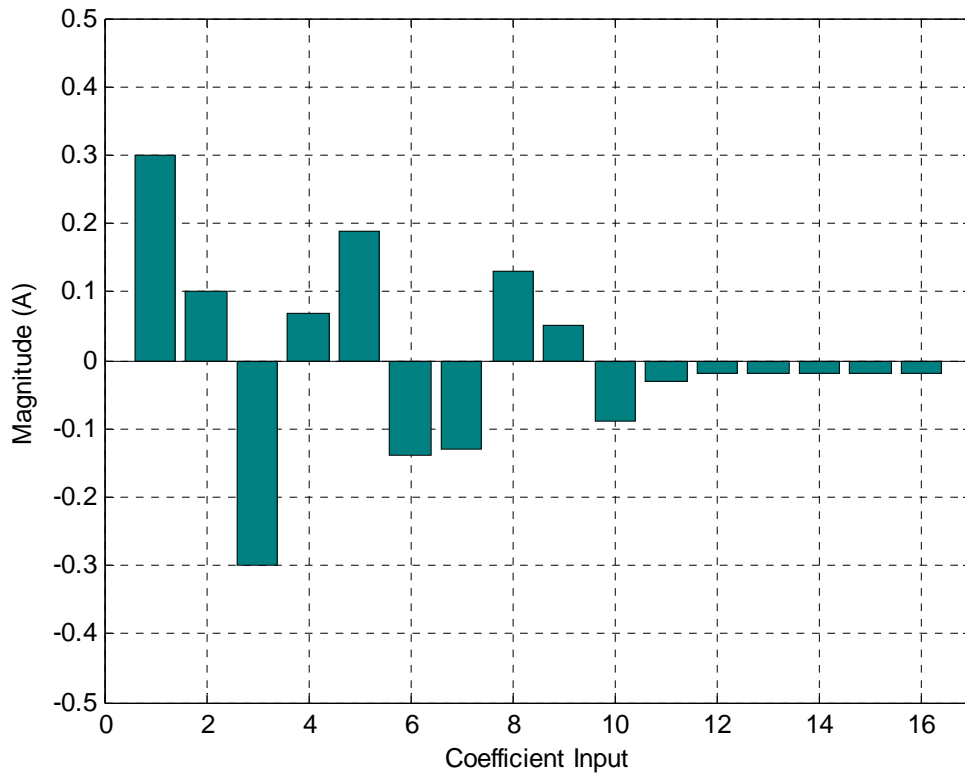
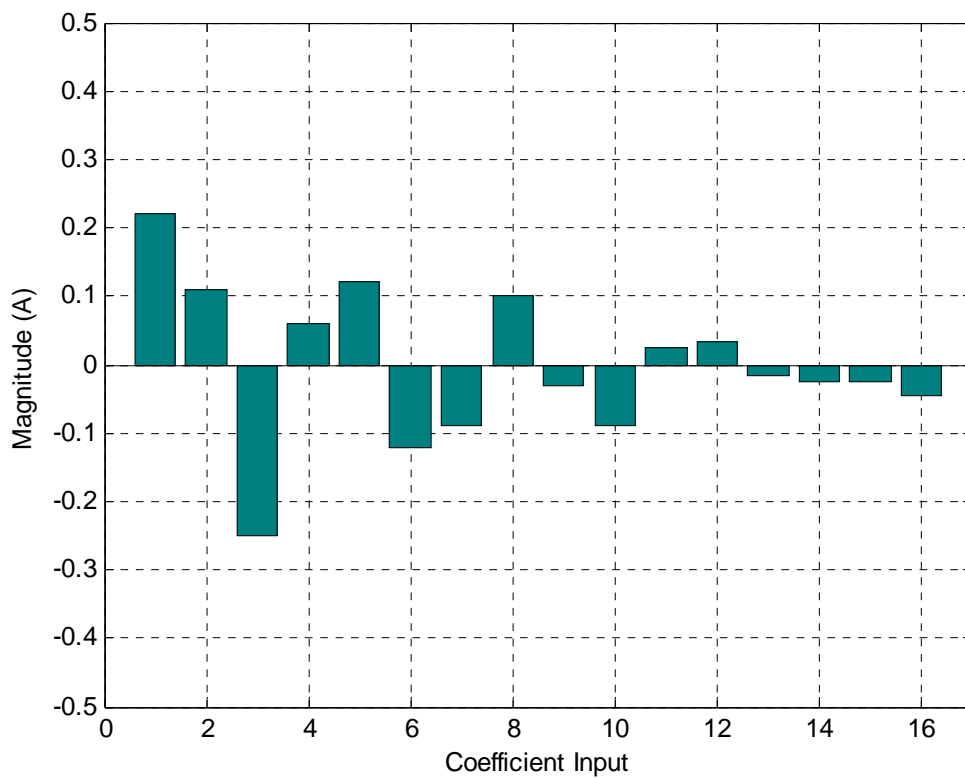
N°	Appliance Name	Appliance	Description
1	Monitor THD = 151.99 %		Solid-state electronic devices have been shown to be the largest contributor to distortion due to the switching of diode bridges producing a discontinuous current, which then causes a distorted sine wave.
2	Computer THD = 169.74 %		Solid-state electronic devices have been shown to be the largest contributor to distortion due to the switching of diode bridges producing a discontinuous current, which then causes a distorted sine wave. For a computer, the current consumption can vary according to the processing activity of the microprocessor.
3	Fluorescent Lamp THD = 116.99 %		High-frequency electronic ballasts for fluorescent lighting systems, also called solid-state ballasts, are promoted for providing significant energy savings over magnetic ballasts. They can generate short inrush currents as high as 100 times the nominal operating levels. The electronic part is a switching circuit with the purpose to generate the light out of a low pressure fluorescent lamp. So, the electronic circuit must perform four main functions: a) Provide a start-up voltage across the end electrodes of the lamp. B) Maintain a constant current when the lamp is operating in the steady state. c) Assure that the circuit will remain stable, even under fault conditions. d) Comply with the applicable domestic and international regulations (PFC, THD, RFI, and safety).
4	Television THD = 173.23 %		There different types of television sets, i.e., with a LED screen, a LCD screen, a plasma screen or even with a conventional cathode ray tube... but they are all based on solid-state electronic devices producing discontinuous currents.
5	Battery Charger THD = 127.16 %		Battery chargers can contain several converters starting at least with an AC-DC switching circuit and generally ending with a control circuit producing a regulated DC voltage output.
6	Fan THD = 49.74 %		Device with is only an electric motor.
7	Fridge THD = 138.91 %		Systems with PFC capacitors and motors are considered to be “linear loads” with acceptable (negligible) distortion levels. This device does not consume energy continuously, i.e., all the time, but only in a periodically way.
8	Light Bulb THD = 14.69 %		Theoretically a pure resistive appliance.

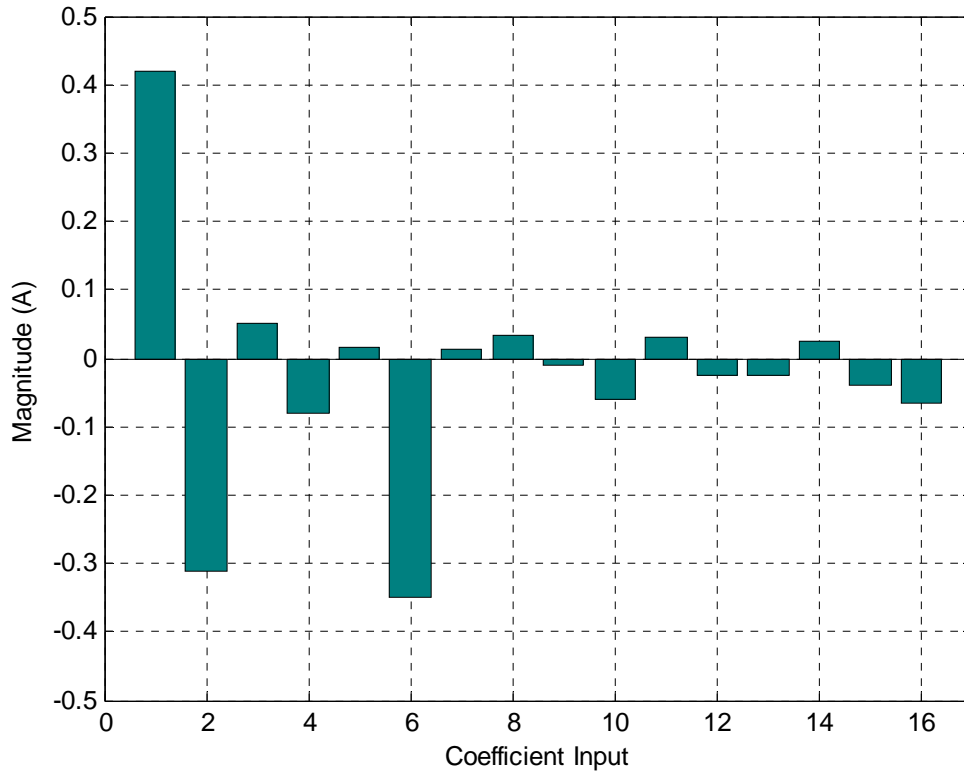
Table 5.1 List of home appliance types used in the experiment



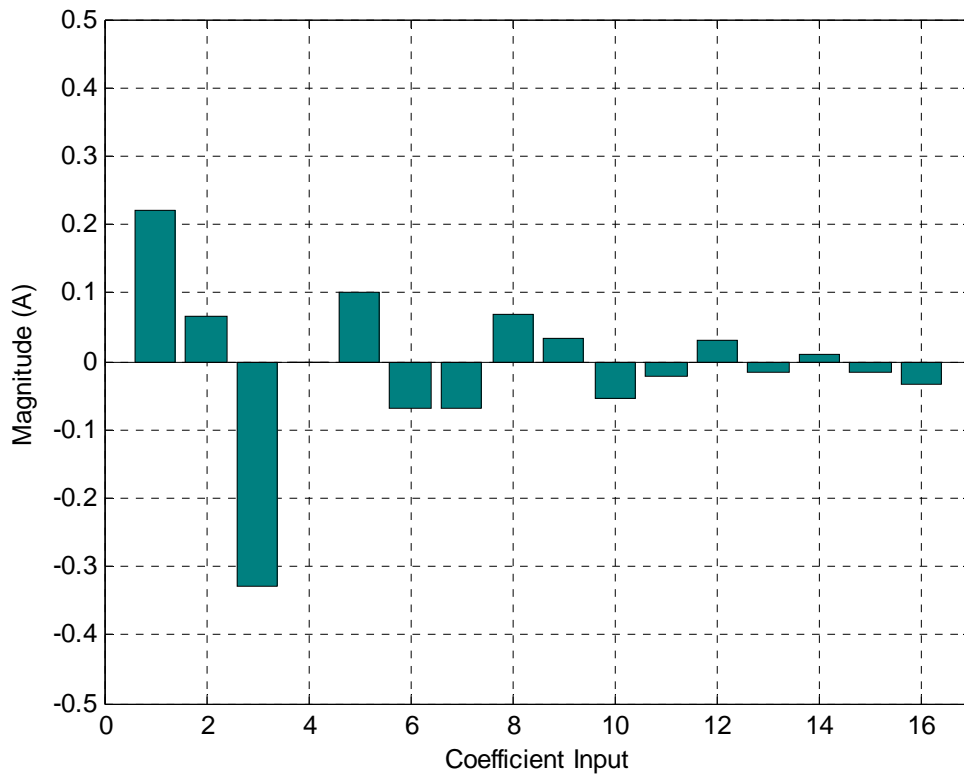
a) Harmonic signature of a monitor



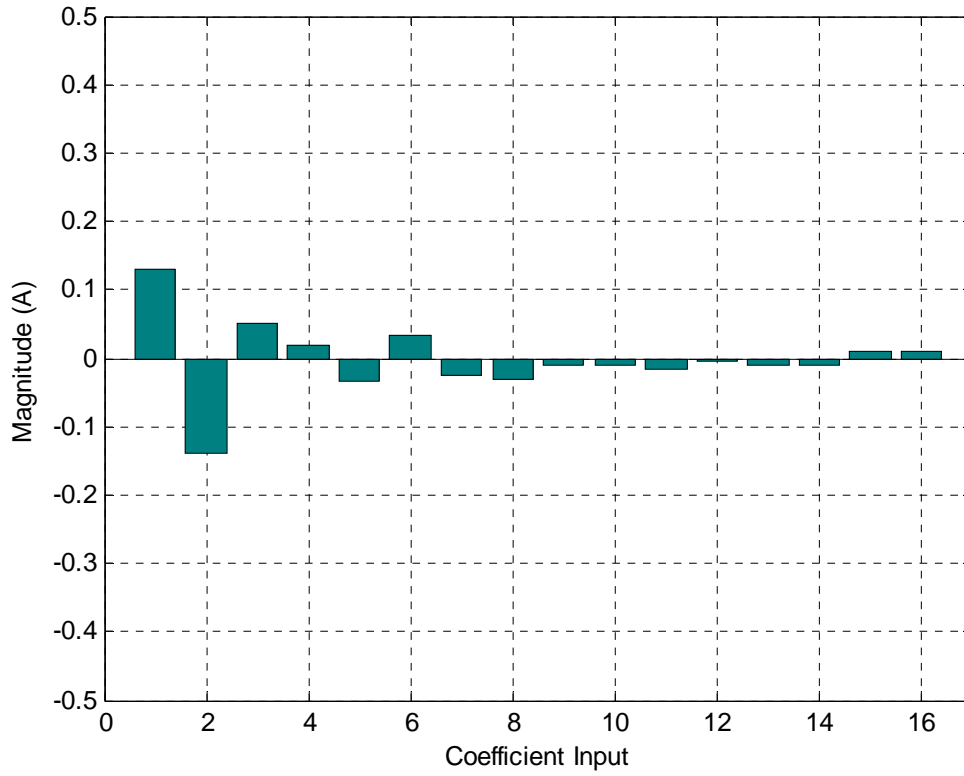
b) Harmonic signature of a computer



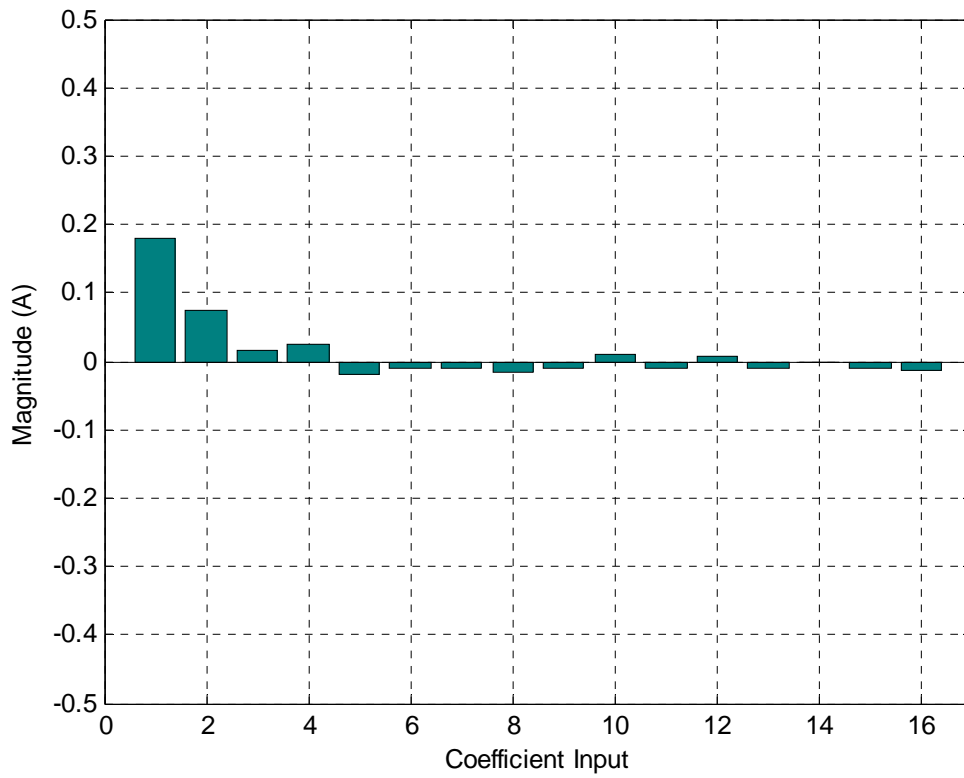
c) Harmonic signature of a fluorescent lamp



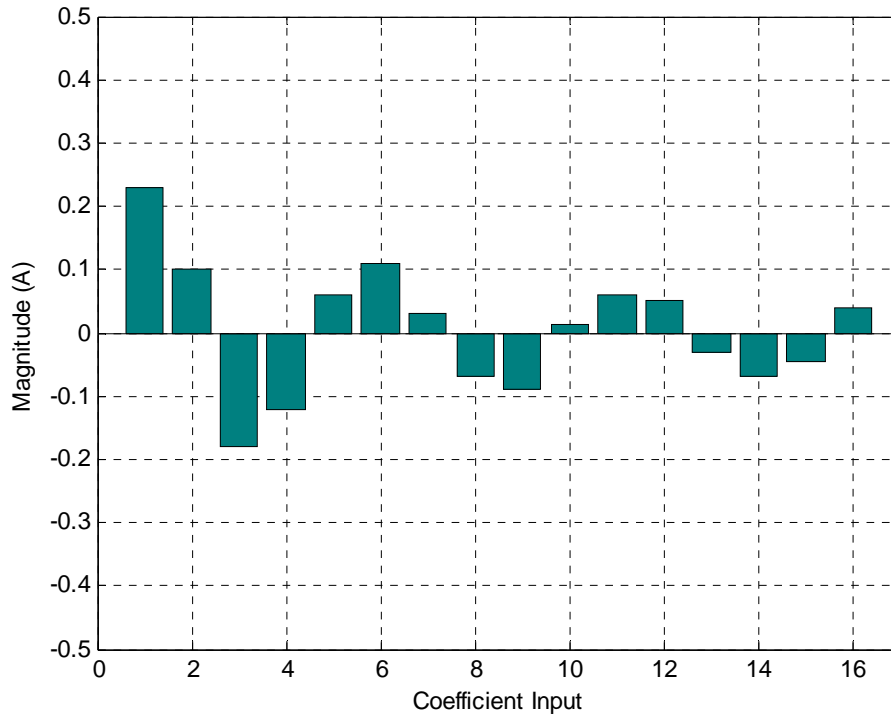
d) Harmonic signature of a television set



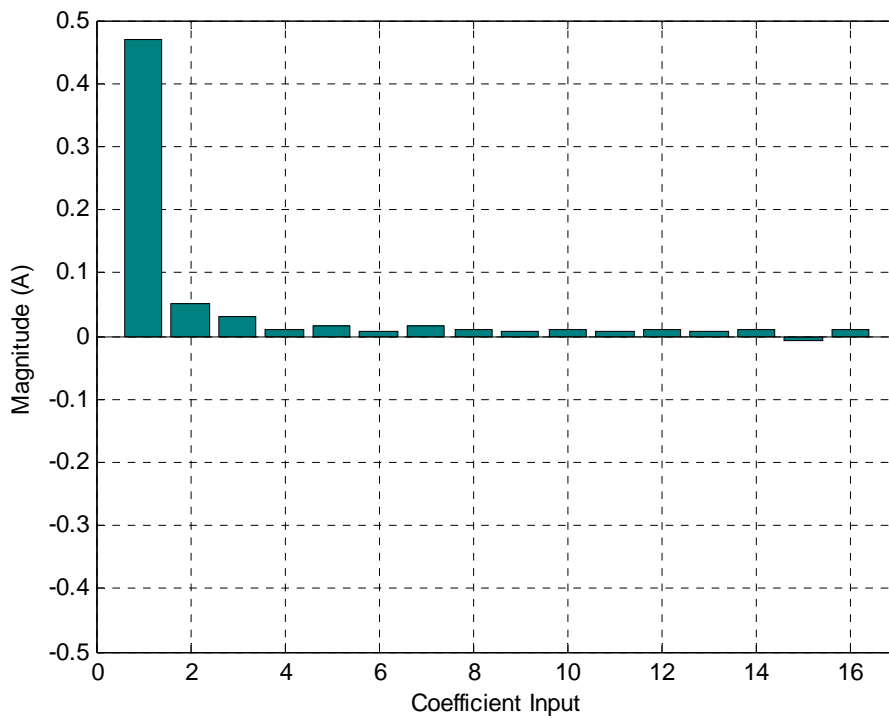
e) Harmonic signature of a battery charger



f) Harmonic signature of a fan



g) Harmonic signature of a fridge



h) Harmonic signature of a light bulb

Figure 5.7 Harmonic coefficient magnitude signatures of 8 home appliances in the system. a) Monitor, b) CPU, c) Fluorescent lamp, d) Television, e) Battery charger, f) Fan, g) Fridge, h) Light bulb from (Srinivasan *et al.*, 2006).

Figure 5.7 shows the magnitudes (in A) of current harmonic signature (coefficients of harmonic ranks of 1, 3, 5, 7, 9, 11, 13, and 15) of 8 home appliances used in this experiment. The values at the odd columns (1, 3, 5, 7, 11, 13, 15) are the magnitudes of coefficients A_n in (4.4) of harmonic terms $n = 1, 3, 5, 7, 9, 11, 13, 15$. The values at the even columns (2, 4, 6, 8, 10, 12, 14, 16) are the magnitudes of coefficients B_n in (4.4) of harmonic terms $n = 1, 3, 5, 7, 9, 11, 13, 15$. We use this information to generate 2 groups of 8 appliances. The first group of 8 home appliances is used to generate 256 waveforms as $2^8 = 256$ combinations of status ON or OFF of 8 devices in the system. As the same way, we generate the validation set from the second group of 8 other home appliances.

The additional information to generate the current data sets (the training dataset and the validation dataset) is as follows. We propose the fundamental frequency is $f = 50$ Hz. The signals in the generated data sets are referenced in the discrete time by t with a sampling time $T_s = 0.0002$ second. 101 samples are generated for a fundamental cycle for each generated signal waveform in the generated data sets. The experimental tests are tested with the MATLAB R2013 environment on a computer with a processor of type Intel(R) Core(TM) 2 Quad CPU Q9550 at 2.83 GHz, with 4 GB of RAM and Microsoft(R) Windows 7 Professional as the operating system.

Harmonic	Coefficients	Magnitude (A) Fluctuation (A)	Home Appliances							
			Monitor	CPU	Fluorescent lamp	TV set	Battery charger	Fan	Fridge	Light bulb
1	A_1	Magnitude	0.3	0.22	0.42	0.22	0.13	0.18	0.23	0.47
		Fluctuation	0.04	0.08	0.025	0.03	0.015	0.03	0.03	0
	B_1	Magnitude	0.1	0.11	-0.31	0.065	-0.14	0.075	0.1	0.05
		Fluctuation	0.02	0.02	-0.08	0.025	-0.015	0.025	0.01	0
3	A_3	Magnitude	-0.3	-0.25	0.05	-0.33	0.05	0.017	-0.18	0.03
		Fluctuation	-0.03	-0.06	0.03	-0.16	0.02	0.017	-0.015	0
	B_3	Magnitude	0.07	0.06	-0.08	0	0.02	0.025	-0.12	0.01

		Fluctuation	0.01	0.02	-0.02	0	0.015	0.01	-0.015	0.005
5	A_5	Magnitude	0.19	0.12	0.017	0.1	-0.035	-0.02	0.06	0.015
		Fluctuation	0.03	0.04	0.017	0.01	-0.01	-0.01	0.005	0.005
	B_5	Magnitude	-0.14	-0.12	-0.35	-0.07	0.035	-0.01	0.11	0.008
		Fluctuation	-0.005	-0.02	-0.015	-0.005	0.025	-0.01	0.02	0.005
7	A_7	Magnitude	-0.13	-0.09	0.012	-0.07	-0.025	-0.009	0.03	0.015
		Fluctuation	-0.03	-0.03	0.012	-0.005	-0.01	-0.009	0.015	0.005
	B_7	Magnitude	0.13	0.1	0.035	0.07	-0.03	-0.015	-0.07	0.01
		Fluctuation	0.005	0.02	0.02	0.005	-0.015	-0.01	-0.005	0.005
9	A_9	Magnitude	0.05	-0.03	-0.009	0.035	-0.01	-0.01	-0.09	0.008
		Fluctuation	0.025	-0.03	-0.009	0.01	-0.01	-0.005	-0.015	0.005
	B_9	Magnitude	-0.09	-0.09	-0.06	-0.055	-0.01	0.01	0.012	0.01
		Fluctuation	-0.005	-0.02	-0.015	-0.005	-0.01	0.005	0.012	0.005
11	A_{11}	Magnitude	-0.03	0.025	0.03	-0.022	-0.015	-0.01	0.06	0.008
		Fluctuation	-0.01	0.02	0.02	-0.005	-0.005	-0.005	0.005	0.005
	B_{11}	Magnitude	-0.02	0.035	-0.025	0.03	-0.005	0.007	0.05	0.01
		Fluctuation	0.005	0.02	-0.02	0.005	-0.005	0.007	0.015	0.005
13	A_{13}	Magnitude	-0.02	-0.015	-0.025	-0.015	-0.009	-0.009	-0.03	0.008
		Fluctuation	-0.02	-0.01	-0.015	-0.005	-0.009	-0.009	-0.015	0.005
	B_{13}	Magnitude	-0.02	-0.025	0.025	0.01	-0.011	0	-0.07	0.01
		Fluctuation	-0.005	-0.025	-0.009	0.005	-0.005	0	-0.02	0.005
15	A_{15}	Magnitude	-0.02	-0.025	-0.04	-0.015	0.01	-0.01	-0.045	-0.008
		Fluctuation	-0.005	-0.01	-0.015	-0.005	0.01	-0.005	-0.02	-0.005
	B_{15}	Magnitude	-0.02	-0.045	-0.065	-0.035	0.01	-0.012	0.04	0.01
		Fluctuation	-0.005	-0.02	-0.015	-0.01	0.01	-0.012	0.01	0

Table 5.2 The magnitudes and fluctuations of coefficients A_n and B_n of n -th harmonics ($n = 1, 3, 5, 7, 9, 11, 13, 15$) of 8 appliances used to generate the training dataset and the validation set in the experimental tests.

In this experiment, there are 3 main tests. In the first test, we test the 3 proposed methods with the harmonic signatures identified by a linear MLP that we have proposed in chapter 4. In the second test, the 3 proposed models are evaluated with the harmonic signature estimated the multiple MLP also proposed in chapter 4. Finally, we have also evaluate the 3 proposed methods by using signals with an additional noise where the signal-to-noise ratio (SNR) varies from 46 dB to 0 dB.

5.4 Experimental Results

5.4.1 Experimental Result 1: Test with harmonic signatures extracted by the linear MLP harmonic estimator

In this test, we use the load harmonic signatures extracted by the linear MLP that we proposed in Chapter 4 to evaluate our 3 proposed classification methods. These harmonic signatures are extracted from above mentioned validation set. One should remember that in the following:

- Model 1 is the binary-output MLP,
- Model 2 is the multiple binary-output MLP,
- Model 3 is the multiple SVM.

There are 3 steps in this test. In the first step, we do experiment with 21 configurations of Model 1 in order to choose the best configuration for Model 1. To do this we change the number of hidden neurons in Model 1 from 2 to 22. In the second step, we do experiment with 5 configurations of Model 2 in order to choose the best configuration for Model 2. In the third step, after we have the best configuration of Model 1 and the best configuration of Model 2, we do experiment to evaluate 3 models (Model 1, Model2, and Model 3).

The best configurations of Model 1 and Model 2 are selected in [Table 5.3](#) and in [Table 5.4](#). For Model 1, we used the same training set with current generated waveforms to train 21 configurations of Model 1 with the number of hidden neurons increasing from 2 to 22. After training, we use the validation set to validate these 21 configurations of Model 1. We also do the same thing with 5 configurations of Model 2 with the number of hidden neurons changing from 2 to 6. The best configurations are selected from the configurations having the best result or the highest accuracy.

Number of hidden neurons	Accuracy (%) of The Binary-Output MLP (Model 1: with only 1 MLP with 8 binary outputs) The number of hidden neurons changes from 2 to 22.								
	Monitor	CPU	Fluo. lamp	TV set	Battery charger	Fan	Fridge	Light bulb	8 Appl.s
2	77.65	55.29	47.06	53.73	64.31	50.59	72.55	88.63	63.73
3	89.02	55.69	76.08	49.02	60.78	56.47	90.20	74.12	68.92
4	84.31	80.78	91.76	58.82	49.02	54.51	95.69	79.22	74.26
5	79.61	72.94	63.53	73.73	73.73	85.10	81.57	68.63	74.85
6	64.31	68.24	87.06	68.24	72.55	75.29	81.57	81.18	74.80
7	79.22	94.12	79.61	68.24	89.02	77.65	87.45	83.92	82.40
8	58.04	69.02	98.04	96.47	69.41	79.22	85.49	75.29	78.87
9	60.78	73.73	89.41	98.04	74.51	66.27	84.31	75.69	77.84
10	61.96	74.90	100	96.08	80.00	72.16	85.10	72.16	80.29
11	63.14	77.65	90.59	96.08	60.78	78.82	84.71	66.27	77.25
12	83.53	65.10	90.20	96.08	66.67	79.22	85.49	75.69	80.25
13	58.82	78.04	95.69	96.47	78.04	67.06	99.61	76.86	81.32
14	62.35	92.55	98.43	97.65	84.31	87.06	94.90	79.61	87.11
15	62.75	68.63	90.98	73.33	63.53	79.22	88.24	76.08	75.34
16	74.51	87.45	98.04	80.78	97.65	88.63	95.69	80.39	87.89
17	57.65	69.80	99.61	78.43	70.59	84.71	85.49	83.53	78.73
18	58.82	76.86	96.08	96.47	75.29	78.43	89.80	76.86	81.08
19	61.18	80.39	95.29	96.47	68.24	85.49	95.29	78.43	82.60
20	59.22	78.43	99.61	69.41	70.59	79.22	90.20	76.86	77.94
21	64.31	89.80	99.22	79.61	84.71	83.14	97.65	87.84	85.78
22	69.80	83.92	97.25	73.33	69.80	85.88	90.20	78.43	81.08
Best Configuration	Best at 89.02% with 3 hidden neurons	Best at 94.12% with 7 hidden neurons	Best at 99.61% with 17 or 20 hidden neurons	Best at 97.65% with 14 hidden neurons	Best at 97.65% with 16 hidden neurons	Best at 88.63% with 16 hidden neurons	Best at 99.61% with 13 hidden neurons	Best at 88.63% with 2 hidden neurons	Best at 87.89% with 16 hidden neurons

Table 5.3 Accuracy comparison of the configurations of the binary-output MLP (Model 1) with the number of hidden neurons changes from 2 to 22

Table 5.3 shows values of the accuracy (%) of configurations of Model 1. To identify the monitor, the best configuration is with 3 hidden neurons at the accuracy 89.02 %. To identify the

CPU, the best configuration is with 7 hidden neurons at the accuracy 94.12 %. To identify the fluorescent lamp, the best configuration is with 17 or 20 hidden neurons at the accuracy 99.61 %. To identify the TV set, the best configuration is with 14 hidden neurons at the accuracy 97.65 %. To identify the battery charger, the best configuration is with 16 hidden neurons at the accuracy 97.65 %. To identify the fan, the best configuration is with 16 hidden neurons at the accuracy 88.63 %. To identify the fridge, the best configuration is with 13 hidden neurons at the accuracy 99.61 %. To identify the light bulb, the best configuration is with 2 hidden neurons at the accuracy 88.63 %. And the best configuration for Model 1 to identify 8 these home appliances is chosen with 16 hidden neurons at the highest accuracy 87.89 %.

Number of hidden neurons	Accuracy (%) of The Multiple Binary-Output MLP (Model 2: with 8 MLPs with only 1 binary output) The number of hidden neurons of each MLP changes from 2 to 6.								
	Monitor	CPU	Fluo. lamp	TV set	Battery charger	Fan	Fridge	Light bulb	8 Appl.s
2	57.25	74.90	91.37	97.65	60.00	78.43	99.61	83.14	80.29
3	56.47	73.73	92.94	96.08	59.61	78.82	84.71	75.29	77.21
4	63.53	92.94	96.08	97.25	60.39	78.82	90.98	77.25	82.16
5	58.43	91.76	92.55	96.08	74.51	78.43	92.94	78.04	82.84
6	61.57	73.73	97.25	74.51	73.33	88.63	85.49	80.78	79.41
Best Configuration	Best at 63.53% with 4 hidden neurons	Best at 92.94% with 4 hidden neurons	Best at 97.25% with 6 hidden neurons	Best at 97.65% with 2 hidden neurons	Best at 97.65% with 5 hidden neurons	Best at 88.63% with 6 hidden neurons	Best at 99.61% with 2 hidden neurons	Best at 83.14% with 2 hidden neurons	Best at 82.84% with 5 hidden neurons

Table 5.4 Accuracy comparison of the configurations of Model 2 with the number of hidden neurons changes from 2 to 6

Table 5.4 shows values of the accuracy (%) of configurations of Model 2. To identify the monitor, the best configuration is with 4 hidden neurons at the accuracy 63.53 %. To identify the CPU, the best configuration is with 4 hidden neurons at the accuracy 92.94 %. To identify the fluorescent lamp, the best configuration is with 6 hidden neurons at the accuracy 97.25 %. To identify the TV set, the best configuration is with 2 hidden neurons at the accuracy 97.65 %. To identify the battery charger, the best configuration is with 5 hidden neurons at the accuracy 74.51

%. To identify the fan, the best configuration is with 6 hidden neurons at the accuracy 88.63 %. To identify the fridge, the best configuration is with 2 hidden neurons at the accuracy 99.61 %. To identify the light bulb, the best configuration is with 2 hidden neurons at the accuracy 83.14 %. And the best configuration for Model 2 to identify 8 these home appliances is chosen with 5 hidden neurons at the highest accuracy 82.84 %.

Appliance	Accuracy (%)		
	Binary-Output MLP (Model 1) Best Configuration (16 hidden neurons)	Multiple Binary-Output MLP (Model 2) Best Configuration (5 hidden neurons in each MLP)	Multiple SVM (Model 3) Optimized Configuration
Monitor	74.51	58.43	96.86
CPU	87.45	91.76	97.25
Fluorescent lamp	98.04	92.55	99.22
Television	80.78	96.08	93.73
Battery charger	97.65	74.51	96.08
Fan	88.63	78.43	90.59
Fridge	95.69	92.94	99.22
Light bulb	80.39	78.04	100
8 appliances	87.89	82.84	96.62
Performance Time (for 256 waveforms)	0.3188 seconds	0.1414 seconds	0.0850 seconds
Training Time (for 256 waveforms)	2.2106 seconds	13.1119 seconds	0.7476 seconds

Table 5.5 Accuracy comparison of classification of 3 models

In [Table 5.5](#), the comparison of classification accuracy and performance time of 3 models is showed. The result shows that the multiple SVM based approach (Model 3) is the best approach with the best accuracy at 96.62%, the fastest training time 0.7476 seconds, the fastest performance time 0.0850 seconds on 256 harmonic signatures of the training set and the validation set.

5.4.2 Experimental Result 2: Test with harmonic signatures extracted by the multiple MLP harmonic estimator

In this test, we use the load harmonic signatures extracted by the multiple MLP-based proposed harmonic estimator that we proposed in chapter 4 to evaluate our 3 proposed classification methods in this chapter. These harmonic signatures are extracted from above validation set.

There are three steps in this test as we do in the first test. The best configurations of Model 1 and Model 2 are selected in [Table 5.6](#) and in [Table 5.7](#). For Model 1, we used the same training set with current generated waveforms to train 21 configurations of Model 1 with the number of hidden neurons increasing from 2 to 22. After training, we use the validation set to validate these 21 configurations of Model 1. We also do the same thing with 5 configurations of Model 2 with the number of hidden neurons changing from 2 to 6. The best configurations are selected from the configurations having the best result or the highest accuracy.

[Table 5.6](#) shows values of the accuracy (%) of configurations of model 1. To identify the monitor, the best configuration is with 3 hidden neurons at the accuracy 85.49 %. To identify the CPU, the best configuration is with 7 hidden neurons at the accuracy 96.47 %. To identify the fluorescent lamp, the best configuration is with 10 hidden neurons at the accuracy 100 %. To identify the TV set, the best configuration is with 9 or 14 hidden neurons at the accuracy 98.43 %. To identify the battery charger, the best configuration is with 16 hidden neurons at the accuracy 97.25 %. To identify the fan, the best configuration is with 5 hidden neurons at the accuracy 83.92 %. To identify the fridge, the best configuration is with 13 hidden neurons at the accuracy 99.22 %. To identify the light bulb, the best configuration is with 21 hidden neurons at the accuracy 87.06 %. And the best configuration for Model 1 to identify 8 these home appliances is chosen with 16 hidden neurons at the highest accuracy 87.60 %.

Number of hidden neurons	Accuracy (%) of The Binary-Output MLP (Model 1 with only 1 MLP with 8 binary outputs) The number of hidden neurons changes from 2 to 22.								
	Monitor	CPU	Fluo. lamp	TV set	Battery charger	Fan	Fridge	Light bulb	8 Appl.s
2	76.86	59.22	47.84	52.55	64.71	49.80	74.12	83.53	63.58
3	85.49	56.47	82.35	48.63	61.96	56.86	87.45	72.55	68.97
4	84.31	80.78	92.94	58.43	45.88	54.51	96.86	74.12	73.48
5	80.00	72.16	58.43	74.51	71.37	83.92	81.96	68.24	73.82
6	64.31	72.55	89.02	69.80	70.59	73.73	79.22	71.37	73.82
7	76.86	96.47	79.22	67.06	93.33	70.59	87.06	82.35	81.62
8	59.22	65.10	97.65	96.47	59.22	75.69	89.80	77.25	77.55
9	60.78	73.33	89.80	98.43	72.94	65.49	85.10	68.63	76.81
10	60.78	75.29	100	96.47	70.59	75.69	86.27	71.37	79.56
11	65.88	81.18	90.98	96.47	73.33	74.90	86.67	66.27	79.46
12	85.49	63.92	91.76	96.47	78.82	76.47	87.84	77.25	82.25
13	60.00	80.00	95.29	96.86	72.55	64.31	99.22	77.25	80.69
14	61.96	93.33	97.65	98.43	74.90	82.35	96.08	78.43	85.39
15	67.45	67.06	93.73	74.90	76.08	78.04	89.80	77.65	78.09
16	70.59	91.37	98.43	84.71	97.25	83.14	94.90	80.39	87.60
17	58.43	70.59	99.61	80.78	60.78	83.53	86.67	75.69	77.01
18	59.22	76.47	95.69	96.47	71.76	72.55	91.37	76.86	80.05
19	61.96	83.14	95.29	96.47	77.65	81.96	96.08	78.43	83.87
20	59.61	80.39	99.61	70.20	61.57	75.29	92.16	73.73	76.57
21	65.49	90.98	98.43	80.00	77.25	78.04	98.04	87.06	84.41
22	67.84	86.67	97.65	72.94	79.61	82.35	91.37	78.43	82.11
Best Configuration	Best at 85.49% with 3 or 12 hidden neurons	Best at 96.47% with 7 hidden neurons	Best at 100% with 10 hidden neurons	Best at 98.43% with 9 or 14 hidden neurons	Best at 97.25% with 16 hidden neurons	Best at 83.92% with 5 hidden neurons	Best at 99.22% with 13 hidden neurons	Best at 87.06% with 21 hidden neurons	Best at 87.60% with 16 hidden neurons

Table 5.6 Accuracy comparison of The Binary-Output MLP (Model 1) with the number of hidden neurons changes from 2 to 22

Number of hidden neurons	Accuracy (%) of The Multiple Binary-Output MLP (Model 2 with 8 MLPs with only 1 binary output) The number of hidden neurons of each MLP changes from 2 to 6.								
	Monitor	CPU	Fluo. lamp	TV set	Battery charger	Fan	Fridge	Light bulb	8 Appl.s
2	58.43	73.73	92.16	98.82	72.94	74.51	99.22	82.75	81.57
3	56.86	73.33	94.12	96.08	73.33	74.51	85.49	76.86	78.82
4	62.35	94.90	94.90	97.65	73.33	74.90	94.90	77.25	83.77
5	59.22	91.76	93.73	96.47	84.71	74.51	94.90	78.82	84.26
6	61.96	72.94	97.25	75.69	63.53	86.27	87.84	80.39	78.24
Best Configuration	Best at 62.35% with 4 hidden neurons	Best at 99.90% with 4 hidden neurons	Best at 97.25% with 6 hidden neurons	Best at 98.82% with 2 hidden neurons	Best at 84.71% with 5 hidden neurons	Best at 86.51% with 6 hidden neurons	Best at 99.22% with 2 hidden neurons	Best at 82.75% with 2 hidden neurons	Best at 84.26% with 5 hidden neurons

Table 5.7 Accuracy comparison of The Multiple Binary-Output MLP (Model 2) with the number of hidden neurons changes from 2 to 22

Table 5.7 shows values of the accuracy (%) of configurations of Model 2. To identify the monitor, the best configuration is with 4 hidden neurons at the accuracy 63.35%. To identify the CPU, the best configuration is with 4 hidden neurons at the accuracy 94.90%. To identify the fluorescent lamp, the best configuration is with 6 hidden neurons at the accuracy 97.25%. To identify the TV set, the best configuration is with 2 hidden neurons at the accuracy 98.82%. To identify the battery charger, the best configuration is with 5 hidden neurons at the accuracy 84.71%. To identify the fan, the best configuration is with 6 hidden neurons at the accuracy 86.27%. To identify the fridge, the best configuration is with 2 hidden neurons at the accuracy 99.22 %. To identify the light bulb, the best configuration is with 2 hidden neurons at the accuracy 82.75%. And the best configuration of Model 2 to identify 8 these home appliances is chosen with 5 hidden neurons at the highest accuracy 84.26 %.

Appliance	Accuracy (%)		
	Binary-Output MLP (Model 1) Best Configuration (16 hidden neurons)	Multiple Binary-Output MLP (Model 2) Best Configuration (5 hidden neurons in each MLP)	Multiple SVM (Model 3) Optimized Configuration
Monitor	70.59	59.22	97.25
CPU	91.37	91.76	95.69
Fluorescent lamp	98.43	93.73	96.86
Television	84.71	96.47	96.08
Battery charger	97.25	84.71	92.16
Fan	83.14	74.51	88.24
Fridge	94.90	94.90	99.22
Light bulb	80.39	78.82	97.65
8 appliances	87.60	84.26	95.39
Performance Time (For 256 waveforms)	0.3161 seconds	0.1381 seconds	0.0850 seconds
Training Time (For 256 waveforms)	2.2106 seconds	13.1119 seconds	0.7476 seconds

Table 5.8 Comparison of classification accuracy of 3 models

In Table 5.8, the comparison of classification accuracy and performance time of the 3 models is showed. The result shows that the multiple SVM-based approach (Model 3) is the best approach with the best accuracy at 95.39%, the fastest training time 0.7476 seconds, the fastest performance time 0.0850 seconds on 256 harmonic signatures of the training set and the validation set.

5.4.3 Experimental Result 3: Test with noised signals

In this test, we use noised signals to evaluate the 3 models. The level of noise is measured by the Signal-to-Noise Ratio (SNR) expressed in dB. Thus, a ratio higher than 1 indicates more signal than noise and a ratio $SNR_{dB} = 0$ means that amplitudes of the signal and of the noise are the same. The harmonic signatures are identified from data set by the linear MLP harmonic estimator and by the multiple MLP harmonic estimator. And we use these harmonic signatures to evaluate our 3 proposed classification models.

SNR (dB)	MSE					
	Linear MLP Harmonic Estimator			Multiple MLP Harmonic Estimator		
	min	max	mean	min	max	mean
46	3.1441e-07	8.2251e-05	2.1842e-05	1.1016e-05	3.7896e-02	6.1805e-03
32	6.1842e-06	1.8472e-03	5.6073e-04	4.8868e-05	3.9136e-02	9.0113e-03
26	2.5987e-05	9.0071e-03	2.2487e-03	1.9041e-04	8.8435e-02	1.8694e-02
12	6.8682e-04	3.0212e-01	5.7250e-02	2.2919e-03	1.6740e+00	3.1598e-01
6	3.5989e-03	1.1024e+00	2.3279e-01	8.2662e-03	5.3199e+00	1.1653e+00
4	4.3379e-03	1.9103e+00	3.6622e-01	1.3135e-02	1.0605e+01	1.7818e+00
2	7.1617e-03	2.3321e+00	5.7390e-01	3.2216e-02	1.6139e+01	2.6503e+00
0	1.0212e-02	4.0231e+00	9.3867e-01	4.8900e-02	2.3067e+01	4.0771e+00

Table 5.9 MSE comparison between Linear MLP Harmonic Estimator and Multiple MLP harmonic estimator on noised signals with signal-to-noise ratio from 46dB to 0dB.

Table 5.9 shows and compares the MSE between the linear MLP-based Harmonic Estimator and the multiple MLP based harmonic estimator. The minimal, maximal and mean values of MSE of 2 harmonic estimators/identifiers are showed. The result shows that the linear MLP identify harmonics from noised signals more precise than multiple MLP Harmonic Estimator.

In Table 5.10, the comparison of accuracy and performance time of the 3 proposed models. The result shows that the multiple SVM based approach (Model 3) with the linear MLP-based Harmonic Estimator is the best approach for nonlinear load classification.

SNR (dB)	Accuracy (%) and Performance Time (seconds)					
	Linear MLP Harmonic Estimator			Multiple MLP Harmonic Estimator		
	One MLP Classifier (Model 1)	Multiple MLP Classifier (Model 2)	Multiple SVM Classifier (Model 3)	One MLP Classifier (Model 1)	Multiple MLP Classifier (Model 2)	Multiple SVM Classifier (Model 3)
46	87.84 %	82.70 %	96.47 %	86.91 %	83.77 %	94.26 %
	0.3195 seconds	0.1384 seconds	0.0857 seconds	0.3224 seconds	0.1435 seconds	0.0830 seconds
32	86.57 %	82.45 %	95.44 %	80.83 %	78.43 %	75.98 %
	0.3158 seconds	0.1438 seconds	0.0846 seconds	0.3216 seconds	0.1415 seconds	0.0885 seconds
26	84.56 %	81.32 %	91.67 %	69.22	69.26	55.74
	0.3472 seconds	0.1460 seconds	0.0882 seconds	0.3332 seconds	0.1491 seconds	0.0916 seconds
12	68.87 %	68.87 %	54.31 %	56.27 %	57.79 %	49.80 %
	0.3366 seconds	0.1445 seconds	0.0879 seconds	0.3314 seconds	0.1443 seconds	0.0926 seconds
6	62.50 %	62.01 %	49.80 %	51.86 %	51.86 %	49.80 %
	0.3253 seconds	0.1391 seconds	0.0857 seconds	0.3578 seconds	0.1481 seconds	0.0945 seconds
4	59.41 %	59.17 %	49.80 %	53.19 %	53.97 %	49.80 %
	0.3790 seconds	0.1576 seconds	0.1010 seconds	0.3369 seconds	0.1454 seconds	0.0870 seconds
2	58.82 %	59.66 %	49.80 %	50.93 %	53.73 %	49.80 %
	0.3371 seconds	0.1524 seconds	0.0922 seconds	0.3349 seconds	0.1489 seconds	0.0925 seconds
0	56.08 %	57.65 %	49.80 %	51.13 %	52.45 %	49.80 %
	0.3385 seconds	0.1469 seconds	0.0915 seconds	0.3372 seconds	0.1449 seconds	0.0912 seconds

Table 5.10 Accuracy and performance time comparison of 2 harmonic estimators/identifiers and of 3 proposed classifiers with noised signals with signal-to-noise ratio from 46 dB to 0 dB

5.4.4 Discussion and comparison of classification accuracy

The results obtained by our proposed methods can be compared to other existing neural methods. As an example, we will compare the performance of Model 3, i.e. the multiple SVM which presents the best performance over the 3 proposed classifiers, to another SVM approach in terms of classification accuracy. Indeed, the previous test results demonstrate that the best solution for electric appliances identification have been obtained with the linear MLP and the multiple SVM with RBF kernels. The work in (Srinivasan *et al.*, 2006) uses a FFT harmonic estimator and a SVM-approach with RBF kernels to identify the electric appliances. Comparing the classification accuracy has been achieved and results are presented in Table 5.11. In this table, our results have been taken from Table 5.5 and from Table 5.8.

Appliance	Accuracy (%)		
	SVM with RBF kernel From Table III in (Srinivasan <i>et al.</i> , 2006) Classification Accuracy When Using Mathematically Created Training Set (with FFT Harmonic Estimator)	Multiple SVM with RBF kernel Our Approaches	
		From Table 5.5 (with Linear MLP Harmonic Estimator)	From Table 5.8 (with Multiple MLP Harmonic Estimator)
Monitor	98.70 %	96.86 %	97.25 %
CPU	75.00 %	97.25 %	95.69 %
Fluorescent lamp	99.90 %	99.22 %	96.86 %
Television	78.50 %	93.73 %	96.08 %
Battery charger	70.30 %	96.08 %	92.16 %
Fan	68.40 %	90.59 %	88.24 %
Fridge	99.90 %	99.22 %	99.22 %
Light bulb	94.50 %	100 %	97.65 %

Table 5.11 Accuracy comparison of classification of 2 SVM with RBF kernel approaches

If we use the linear MLP harmonic estimator for our SVM approach, the accuracy are in the range between 90.59 % (for the electric fan) and 100% (for the light bulb) while the accuracy of the approach in (Srinivasan *et al.*, 2006) are in the range between 68.40 % (for the electric fan) and 99.90% (for the fluorescent lamp or of fridge). Both approaches used mathematically created

training sets. Our approach gives better results in term of robustness: It can be seen that the lowest value of the classification accuracy has been achieved with the linear MLP harmonic estimator associated with the multiple SVM that has been proposed in this thesis.

This difference in term of classification accuracy might come from the harmonic estimation step. In our approach, we used our proposed linear MLP for harmonic identification which is more efficient compared to the FFT used in (Srinivasan *et al.*, 2006). Our SVM approach also shows better results when associated with the multiple MLP harmonic estimator. Its accuracy is in the range between 88.24 % (for the electric fan) and 99.22 % (for the fridge). These show that our classifier which is based on a SVM with RBF kernels approaches with the two proposed harmonic estimators (the linear MLP harmonic estimator and the multiple MLP harmonic estimator) are robust in classifying electric appliances.

5.5 Summary

In this chapter, we have proposed three off-line learning based approaches for nonlinear load classification in a power system. There are two approaches based on multilayer perceptron technique and one approach based on a support vector machine technique. For the first approach, we proposed a binary-output multilayer perceptron. In the second approach, we propose a multiple binary-output MLP. In third approach, we proposed a multiple SVM. All the 3 models are used for identifying appliances consuming or not current from a power system. They all use as their inputs the estimated harmonic features, i.e., the amplitude and the angles of the harmonic components of ranks 1, 3, 5, 7, 9, 11, 13 and 15. The 2 proposed approaches for harmonic identification that have been introduced in Chapter 4 are used to estimate the harmonic signatures of 8 typical nonlinear loads.

In order to evaluate the performance of the 3 models, the experiments have been conducted and the experimental results are also presented in this chapter. The 3 models are also evaluated with some noisy signals. From the results, we can deduce that the approach based on a multiple SVM (Model 3) shows the best performance.

Chapter 6 : Conclusions

6.1 Proposed Methods for Harmonic Estimation

Since a couple of decades, the number of electrical nonlinear load devices has increased continually in domestic and industrial installations. The unwanted harmonic generated by nonlinear loads or devices yield many problems in power systems. Therefore, harmonic identification approaches are more important than ever for power quality issues. Technical solutions like active power filter can use harmonic identification approaches in order to compensate and eliminate harmonic distortions. In this thesis, we have introduced two new approaches based on MLPs for estimating power system harmonics.

In the first approach, we proposed and developed a linear MLP for identifying on-line harmonics. The linear MLP adapts its parameters with a learning process and is able to estimate the amplitude and the phase angle of each harmonic term. Furthermore, the linear MLP is able estimate any periodic signal by expressing its output as a sum of harmonic components according to Fourier series. The network takes some specific harmonic elements with unit amplitudes generated as inputs and uses neurons that have linear activation functions. The measured signal serves as a reference and is compared to the network output. The amplitudes of the fundamental and high-order harmonics are deduced from the combination of the weights of the neurons. The linear MLP identifies the amplitudes of the fundamental component and high-order harmonic components with good precision even under noisy conditions (Nguyen and Wira, 2013a; Nguyen and Wira, 2013b).

In the second approach, we proposed another MLP technique based approach for identifying current harmonics in power systems. A structure of several nonlinear MLPs is proposed and used as a pattern recognition solution for the harmonic identification task. After training, each MLP of this structure is able to identify 2 coefficients related to each harmonic term contained in the input signal. The effectiveness of this new approach is evaluated by experiments. Results show that the proposed MLPs approach is able to identify effectively the amplitudes of the harmonic terms from the signals under noisy condition. Results are compared to one obtained by the linear MLP and to recent MLP approaches (Nguyen and Wira, 2015).

These proposed methods have been introduced and presented in Chapter 4. The approaches are able to identify individually each harmonic term of signals from power systems. They have been

successfully validated by experimental tests. They can be inserted in an active power filters to ensure the power quality in power systems.

6.2 Proposed Methods for Electric Appliances Classification

In order to apply our proposed methods in the field of NILM, we also proposed and developed 3 approaches for non-linear load appliance classification in power systems. These approaches were presented in Chapter 5. Two MLP-based approaches and one SVM-based approach were proposed for this objective.

In first approach, a simple MLP has been developed to identify nonlinear appliances connected to the power system and consuming or not energy. Based on the harmonic features extracted from the distorted waveform in a power system, the method is able to detect which appliances are switched on. The network is trained offline with a training data set. After training, the network is perfectly able to identify the nonlinear appliances, i.e., switched ON and thus consuming and disturbing the power quality.

In second approach, we propose a specific structure of MLPs for classifying nonlinear appliances in a power system. The learning approach is based on several binary-output multilayer perceptrons. After training, each multilayer perceptron is able to identify an electrical appliance in the power system, i.e. if they are switched ON or OFF. The difference of this method compared to the first method is that it uses many multilayer perceptrons. This structure is trained with the same training data set generated from signals measured on a power system where 8 different appliances have be inserted like in (Srinivasan et al., 2006).

In third approach, a structure of multiple support vector machines was proposed. This proposed structure consists of N support vector machines. The number N is the number of appliances we need to identify in a power system. Because support vector machines are supervised learning systems, we use the same training set to train it in order to classify the nonlinear devices.

The 3 approaches have been implement and evaluated by several computer experiments. The results show that the proposed SVM technique based method performs faster and leads to a better precision compared to the two MLP-based approaches.

6.3 Limitations and Future Work

In this thesis, 2 proposed approaches for harmonic estimation and 3 proposed approaches for nonlinear appliances classification have been developed. The proposed methods have been evaluated by experimental tests with some good results. In the other hand, the proposed approaches have some limitations. Indeed, for the harmonic identification problem, the 2 proposed methods are only convenient to time-domain signal analysis. For the non-linear load appliance classification problem, the proposed methods are only based on frequency features. Some new indicators could be chosen and used if they are relevant of the power quality and/or of the types of load connected in the power system.

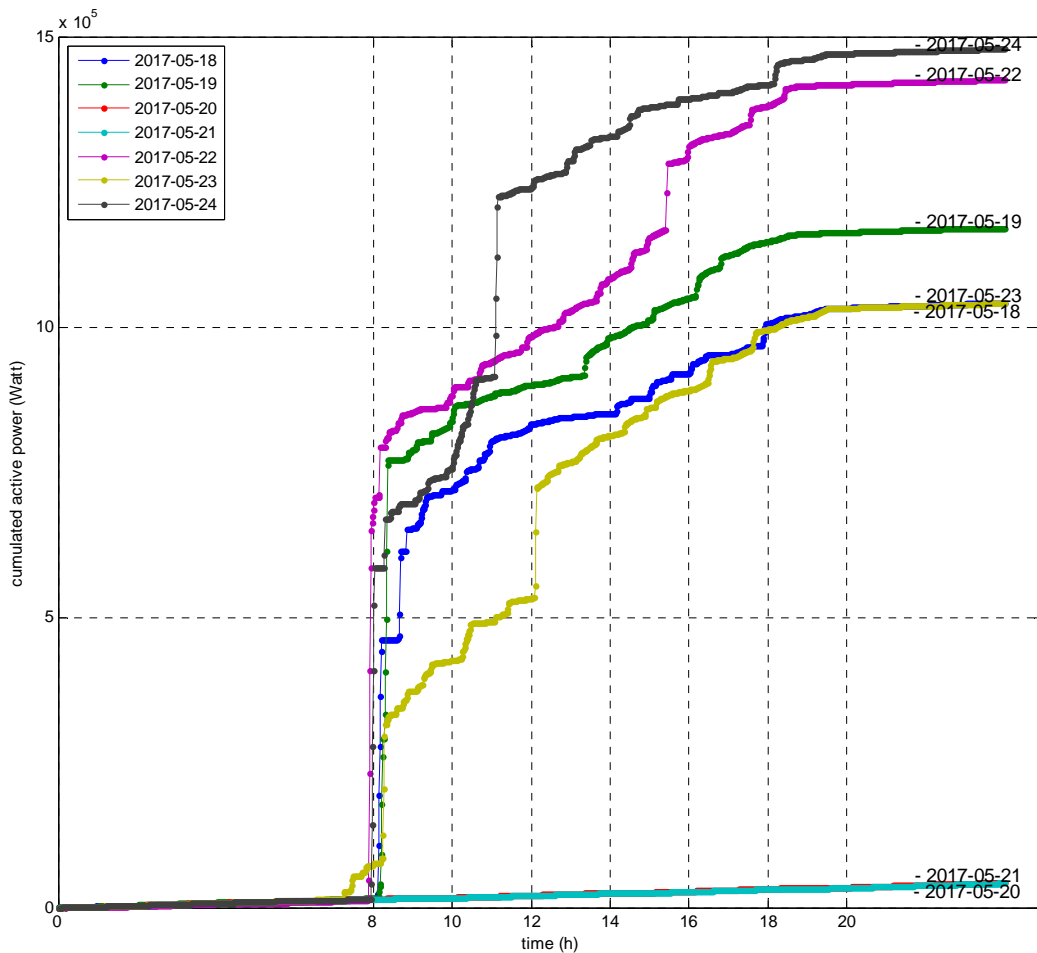


Figure 6.1 An example of power load curves.

For example, events detected and extracted from daily load curves can be used to trigger strategy changes and or parameters changes for the classifier. Some temporal indicators calculated on a sliding window can also be associated to the frequency features as the inputs of the classifier. A load curve represents the power consumed by a customer or group of customers based on time, i.e., in successive time intervals. A load curve is therefore expressed as a unit of power, and each point of the curve should generally be interpreted as a middle power for a short period of time. [Figure 6.1](#) gives an example of power load curves. Indeed, the cumulated values of the consumed power have been recorded over one week (7 days, from May 18 to 24, 2017) with a precision of 1 minute in a kitchen of a working office (here in the Université de Haute-Alsace). The kitchen contains several appliances which are a fridge, a kettle and two coffee machines. One can easily recognize and separate working-days from weekend-days, one can also clearly see different important moments appearing during working-days.

According to the advantages and limitations of the machine learning approaches proposed in this thesis, we can provide some directions for the future work as follows:

- Develop other new load signatures for NILM, Energy Disaggregation.
- Test experiments with real open well-known data sets.
- Develop and implement hidden Markov models for NILM with the low frequency sampling data sets.
- Develop original NILM approaches by using deep learning techniques.
- Implement the proposed learning methods with Python, R, and Java languages.
- Develop and implement the proposed methods on open neural network toolkits: TensorFlow, DeepLearning4j (a deep learning toolkit for Java).

Abbreviations

ADALINE	Adaptive Linear Element
ANN	Artificial Neural Network
APF	Active Power Filter
CZT	Chirp Z–Transform
DFT	Discrete Fourier Transform
ECG	Electrocardiography
ESPRIT	Estimation of Signal Parameters via Rotational Invariant Techniques
FFT	Fast Fourier Transform
GA	Genetic Algorithm
HHT	Hilbert–Huang Transform
IPT	Instantaneous Power Theory
KF	Kalman Filter
LMS	Least Mean Square
MLP	Multi-Layer Perceptron
MSE	Mean Square Error
MUSIC	MULTiple SIGNAL Classification
NILM	Nonintrusive Appliance Load Monitoring
PFC	Power Factor Correction
PLL	Phase Locked Loop
PSO	Particle Swarm Optimization
RBF	Radial Basic Function
RBFNN	Radial Basis Function Neural Network
RNN	Recurrent Neural Network
SNR	Signal-to-Noise Ratio
SOM	Self–Organizing Map
SVM	Support Vector Machine
TDAF	Transform Domain Adaptive Filter
TFD	Time–Frequency Distribution
THD	Total Harmonic Distortion (rate)
WT	Wavelet Transform

List of Figures

Figure 1.1	Detailed block diagram of an enhanced shunt APF.	1
Figure 1.2	A shunt APF.	2
Figure 1.3	The first neuron model of McCulloch and Pitts in 1943.	3
Figure 1.4	A perceptron neural network model of Rosenblatt in 1958.	3
Figure 1.5	Typical architecture of an ADALINE network.	4
Figure 1.6	Typical architecture of a multilayer perceptron network.	4
Figure 1.7	Identification of power system harmonics.	5
Figure 1.8	Appliance signatures on total load waveform in (Hart, 1992).	8
Figure 1.9	Classification of NILM techniques.	8
Figure 1.10	System diagram of nonlinear load classification.	9
Figure 1.11	Thesis research contributions.	10
Figure 2.1	ADALINE architecture with harmonic terms as inputs.	18
Figure 2.2	Block diagram of the LMS spectrum analyzer in (Widrow <i>et al.</i> , 1987).	22
Figure 2.3	Fourier linear combiner for harmonic estimation as an ADALINE.	22
Figure 2.4	An ADALINE for tracking 3-phase voltages and currents in (Dash <i>et al.</i> , 1998).	23
Figure 2.5	A two-stage ADALINE for harmonics and interharmonics measurement.	23
Figure 2.6	The architecture of S-ADALINE (Sakar and Sengupta, 2009).	24
Figure 2.7	Modified ADALINE with TVWH rule.	24
Figure 2.8	Methods based on ADALINE in (Wira <i>et al.</i> , 2010).	25
Figure 2.9	The structured NN for harmonic estimator in (Hattana and Richard, 1990).	26
Figure 2.10	A MLP for estimation of 3rd and 5th harmonics (Pecharanin <i>et al.</i> , 1995).	27
Figure 2.11	Harmonic detection process.	28
Figure 2.12	The MLP configuration for harmonic detection in (Lin, 2007).	28
Figure 2.13	MLPs for harmonic extraction in (Tümay <i>et al.</i> , 2008).	29
Figure 2.14	A MLP based structure for harmonics coefficient and phase angle detection (Temurtas and Temurtas, 2011).	29
Figure 2.15	MLP based structure for the neural-network-method for estimating A and B coefficients of harmonics (Nascimento <i>et al.</i> , 2013).	30
Figure 2.16	4 types of RNN used of harmonic prediction in (Mori and Suga, 1992).	31
Figure 2.17	Elman's RNN structures for harmonic detection in (Temurtas <i>et al.</i> , 2004).	32
Figure 2.18	Proposed scheme for estimating the true harmonic distortion of a nonlinear load in (Mazumdar and Harley, 2008).	32
Figure 2.19	A typical RBFNN in (Guangjie and Hailong, 2009).	33
Figure 3.1	Sketch of large margin classifiers metering system in (Onoda <i>et al.</i> , 2000).	39
Figure 3.2	Multilayer perceptron designed for NILM system in (Yoshimoto <i>et al.</i> , 2000).	40
Figure 4.1	The linear MLP architecture for harmonic estimation.	48
Figure 4.2	Performance of a linear MLP (with 3 hidden neurons) and an ADALINE in identifying the harmonics of the noisy sine wave $s(t)$ with harmonics of rank 3, 5 and 7, a) real constructed signals (with \mathbf{x}_{1-10}), b) normalized spectrum histograms with by \mathbf{x}_{1-10} , and c) normalized spectrum histograms with \mathbf{x}_{1-23}	57

Figure 4.3	Estimation of the harmonic terms of a current from a real nonlinear load with a linear MLP and an ADALINE. a) Real and constructed signals b) Estimated spectrum histograms	58
Figure 4.4	General principle for characterizing ECG records.	59
Figure 4.5	On–line fundamental tracking of an ECG.	61
Figure 4.6	Performances of a linear MLP with 3 hidden neurons, an ADALINE and the FFT in identifying harmonics of an ECG.	63
Figure 4.7	A linear MLP with one hidden neuron for harmonic identification.....	64
Figure 4.8	A one–neuron neural network reduced from the linear MLP with one neuron in hidden layer for harmonic identification.....	66
Figure 4.9	An ADALINE using LMS rule for harmonic identification.	67
Figure 4.10	Proposed MLP architecture for estimating harmonic distortions, a) principle for one harmonic component, and b) with several MLP in parallel for each harmonic component.	68
Figure 4.11	Training performance of the proposed neural approach in detecting harmonic of rank 23.....	71
Figure 4.12	Harmonic identification of a sine wave with harmonic of ranks 3, 5, 7. a) with the proposed approach b) with the approach of (Nascimento <i>et al.</i> , 2011)	72
Figure 4.13	Experimental results of harmonic identification of a current measured from a real nonlinear load, a) with the proposed approach, b) with the approach of (Nascimento <i>et al.</i> , 2011).	73
Figure 5.1	Electric appliances classification by harmonic features with 2 steps.....	77
Figure 5.2	Proposed Model 1 – A Binary-Output MLP for Nonlinear Load Classification.	78
Figure 5.3	Proposed Model 2 – A Multiple Binary–Output MLP for Nonlinear Load Classification.....	79
Figure 5.4	Proposed Model 3 – A Multiple SVM for Nonlinear Load Classification.....	80
Figure 5.5	A MLP implemented in MATLAB for model 1	81
Figure 5.6	A MLP implemented in MATLAB for the multiple MLP in model 2.....	82
Figure 5.7	Harmonic coefficient magnitude signatures of 8 home appliances in the system. a) Monitor, b) CPU, c) Fluorescent lamp, d) Television, e) Battery charger, f) Fan, g) Fridge, h) Light bulb from (Srinivasan <i>et al.</i> , 2006).....	88
Figure 6.1	An example of power load curves.	105

List of Tables

Table 3.1	Summary of steady–state methods from (Zoha <i>et al.</i> , 2012).....	37
Table 3.2	Summary of transient–state methods from (Zoha <i>et al.</i> , 2012).....	38
Table 4.1	Performance comparison between ADALINE and linear MLP with \mathbf{x}_{1-10}	56
Table 4.2	Performance comparison between the linear MLP, ADALINE and conventional FFT in estimating the harmonic content of an ECG.....	62
Table 4.3	Performances of MLP approaches in estimating the harmonic content of signal with only 3 rd , 5 th and 7 th harmonics.....	72
Table 4.4	Performances of MLP approaches in estimating the harmonic content of a real nonlinear load current	74
Table 5.1	List of home appliance types used in the experiment.....	84
Table 5.2	The magnitudes and fluctuations of coefficients A_n and B_n of n -th harmonics ($n = 1, 3, 5, 7, 9, 11, 13, 15$) of 8 appliances used to generate the training dataset and the validation set in the experimental tests.	90
Table 5.3	Accuracy comparison of the configurations of the binary-output MLP (Model 1) with the number of hidden neurons changes from 2 to 22.....	92
Table 5.4	Accuracy comparison of the configurations of Model 2 with the number of hidden neurons changes from 2 to 6	93
Table 5.5	Accuracy comparison of classification of 3 models	94
Table 5.6	Accuracy comparison of The Binary-Output MLP (Model 1) with the number of hidden neurons changes from 2 to 22	96
Table 5.7	Accuracy comparison of The Multiple Binary-Output MLP (Model 2) with the number of hidden neurons changes from 2 to 22.....	97
Table 5.8	Comparison of classification accuracy of 3 models	98
Table 5.9	MSE comparison between Linear MLP Harmonic Estimator and Multiple MLP harmonic estimator on noised signals with signal-to-noise ratio from 46dB to 0dB....	99
Table 5.10	Accuracy and performance time comparison of 2 harmonic estimators/identifiers and of 3 proposed classifiers with noised signals with signal-to-noise ratio from 46 dB to 0 dB.....	100
Table 5.11	Accuracy comparison of classification of 2 SVM with RBF kernel approaches	101

List of References

- (Abdel-Galil *et al.*, 2003) T. Abdel-Galil, E. El-Saadany, and M. Salama, "Power quality event detection using adaline," *Electric Power Systems Research*, vol. 64, no. 2, pp. 137-144, 2003
- (Abdollahi and Matifar, 2011) A. Abdollahi and F. Matifar, "Frequency estimation: A least-squares new approach," *IEEE Transactions on Power Delivery*, vol. 26, no. 2, pp. 790-798, 2011
- (Ai *et al.*, 2007) Q. Ai, Y. Zhoua, and W. Xu, "Adaline and its application in power quality disturbances detection and frequency tracking," *Electric Power Systems Research*, vol. 77, no. 5-6, pp. 462-469, 2007
- (Akagi, 1996) H. Akagi, "New trends in active filters for power conditioning," in *IEEE Transactions on Industry Applications*, vol. 32, no. 6, pp. 1312-1322, 1996
- (Akagi, 2005) H. Akagi, "Active harmonic filter," in *Proceedings of IEEE*, vol. 93, no. 12, pp. 12-45, 2005
- (Alhaj *et al.*, 2013) H.M.M. Alhaj, N.M. Nor, V.S. Asirvadam, and M.F. Abdullah, "Power system harmonics estimation using sliding window based LMS," in *2013 IEEE International Conference on Signal and Image Processing Applications (ICSIPA)*, pp. 327-332, 8-10 October 2013
- (Almaita and Asumadu, 2011) E. Almaita and J.A. Asumadu, , "On-line harmonic estimation in power system based on sequential training radial basis function neural network," in *2011 IEEE International Conference on Industrial Technology (ICIT)*, pp. 139-144, 14-16 March 2011
- (Anderson *et al.*, 2012) K.D. Anderson, M.E. Berges, A. Ocneanu, D. Benitez, and J.M.F. Moura, "Event detection for nonintrusive load monitoring," in *IECON 2012 - 38th Annual Conference on IEEE Industrial Electronics Society* , pp. 3312-3317, Montreal, Canada, 25-28 October 2012
- (Andria *et al.*, 1992) G. Andria, L. Salvatore, M. Savino, and A. Trotta, "Techniques for identification of harmonics in industrial power systems," in *IMTC '92 - 9th IEEE Instrumentation and Measurement Technology Conference*, pp. 114-119, 12-14 May 1992

- (Arrillaga and Watson, 2003) J. Arrillaga and N.R. Watson, *Power System Harmonic 2nd Edition*. John Wiley and Sons, 2003
- (Baranski and Voss, 2003) M. Baranski, J. Voss, “Nonintrusive appliance load monitoring based on an optical sensor,” in *Proceedings of IEEE Power Tech Conference*, pp. 8–16, Bologna, Italy, 23–26 June 2003
- (Baranski and Voss, 2004) M. Baranski and J. Voss “Genetic algorithm for pattern detection in NIALM systems,” in *Proceedings of IEEE International Conference on Systems, Man and Cybernetics*, vol. 4, pp. 3462–3468, Hague, The Netherlands, 10–13 October 2004
- (Barros and Diego, 2006) J. Barros and R.I. Diego, “On the use of the Hanning window for harmonic analysis in the standard framework,” in *IEEE Transactions on Power Delivery*, vol. 21, no. 1, pp. 538–539, January 2006
- (Bettayeb and Qidwai, 2003) M. Bettayeb and U. Qidwai, “A hybrid least squares–GA–based algorithm for harmonic estimation,” in *IEEE Transactions on Power Delivery*, vol. 18, no. 2, pp. 377–382, April 2003
- (Bishop, 1995) C.M. Bishop, *Neural Networks for Pattern Recognition*. Oxford, 1995
- (Biwas *et al.*, 2013) S. Biswas, A. Chatterjee, S.K. Goswami, “An artificial bee colony–least square algorithm for solving harmonic estimation problems,” in *Applied Soft Computing*, vol. 13, issue 5, pp. 2343–2355, May 2013
- (Bose, 2007) B.K. Bose, “Neural Network Applications in Power Electronics and Motor Drivers – An Introduction and Perspective,” in *IEEE Trans. on Industrial Electronics*, vol. 54, no. 1, pp. 14–33, 2007
- (Bracale and Carpinelli, 2009) A. Bracale and G. Carpinelli, “An ESPRIT and DFT–based new method for the waveform distortion assessment in power systems,” in *The 20th International Conference and Exhibition on Electricity Distribution – Part 2 (CIRED 2009)*, pp. 1–17, 8–11 June 2009
- (Cabal–Yepez *et al.*, 2013) E. Cabal–Yepez, H. Miranda–Vidales, A. Garcia–Perez, J.M. Lozano–Garcia, R. Alvarez–Salas, and A.L. Martinez–Herrera, “Harmonic component estimation through DFSWT for active power filter applications,” in *IECON 2013 – 39th*

Annual Conference of the IEEE Industrial Electronics Society, pp. 810–815, 10–13 November 2013

- (Chang *et al.*, 2008) H.H. Chang, H.T. Yang, C.L. Lin, “Load identification in neural networks for a non-intrusive monitoring of industrial electrical loads,” in *Computer Supported Cooperative Work in Design IV*, vol. 5236, pp. 664–674, Springer, Berlin, Germany, 2008
- (Chang *et al.*, 2009) G.W. Chang, C-I. Chen, and Q-W. Liang, “A two-stage ADALINE for harmonics and interharmonics measurement,” in *IEEE Transactions on Industrial Electronics*, vol. 56, no. 6, pp. 2220–2228, June 2009
- (Chang *et al.*, 2010) G. Chang, C-I. Chen, and Y-F. Teng, “Radial-basis-function neural network for harmonic detection,” in *IEEE Transactions on Industrial Electronics*, vol. 57, no. 6, pp. 2171–2179, 2010
- (Chang, 2012) H.H. Chang, “Non-intrusive demand monitoring and load identification for energy management systems based on transient feature analyses,” in *Energies*, vol. 5, no. 11, pp. 4569–4589, November 2012
- (Chen and Chang, 2009) C-I. Chen and G.W. Chang, “An efficient Prony's method for time-varying power system harmonic estimation,” in *2009 IEEE International Symposium on Circuits and Systems (ISCAS 2009)*, pp.1701–1704, 24–27 May 2009
- (Chen *et al.*, 2009) C. Chen, T. Xu, Z. Piao, W. Liang, and Y. Yuan, “The study on FFT harmonic detecting method of rural network based on wavelet denoising,” in *2009 International Conference on Energy and Environment Technology (ICEET '09)*, vol. 2, pp. 365–368, 16–18 October 2009
- (Chen, 2008) Y. Chen, “Harmonic Detection in Electric Power System Based on Wavelet Multi-resolution Analysis,” in *2008 International Conference on Computer Science and Software Engineering*, vol. 5, pp. 1204–1207, 12–14 December 2008
- (Cole and Albicki, 1998) A.I. Cole and A. Albicki, “Data extraction for effective non-intrusive identification of residential power loads,” in *Conference Proceedings of 1998 IEEE Instrumentation and Measurement Technology Conference (IMTC/98)*, vol. 2, pp. 812–815, 18–21 May 1998

- (Cole and Albicki, 2000) A. Cole and A. Albicki, “Nonintrusive identification of electrical loads in a three-phase environment based on harmonic content,” in *Proceedings of Instrumentation and Measurement Technology Conference*, vol. 716, pp. 24–29, Baltimore, MD, USA, 1–4 May 2000
- (Cooley and Tukey, 1965) J.W. Cooley and J.W. Tukey, “An algorithm for the machine calculation of complex Fourier series,” in *Mathematics of Computation*, vol. 19, pp. 297–301, April 1965
- (Costa and Cardoso, 2006) F.F. Costa and A.J.M. Cardoso, “Harmonic and Interharmonic Identification Based on Improved Prony's Method,” in *IECON 2006 – 32nd Annual Conference on IEEE Industrial Electronics*, pp. 1047–1052, 6–10 November 2006
- (Costa *et al.*, 2007) F.F. Costa, A.J.M. Cardoso, and D.A. Fernandes, “Harmonic Analysis Based on Kalman Filtering and Prony's Method,” in *International Conference on Power Engineering, Energy and Electrical Drives (POWERENG 2007)*, pp. 696–701, 12–14 April 2007
- (Cupertino *et al.*, 2011) F. Cupertino, E. Lavopa, P. Zanchetta, M. Sumner, and L. Salvatore, “Running DFT-based PLL algorithm for frequency, phase, and amplitude tracking in aircraft electrical systems,” in *IEEE Transactions on Industrial Electronics*, vol. 58, no. 3, pp. 1027–1035, March 2011
- (Daponte *et al.*, 1996) P. Daponte, D. Menniti, and A. Testa, “Segmented chirp Z-transform and multiple deep dip windows for electrical power system harmonic analysis,” in *Measurement*, vol. 18, issue 4, pp. 215–224, August 1996
- (Dash *et al.*, 1996) P. Dash, D. Swain, A. Liew, and S. Rahman, “An adaptive linear combiner for on-line tracking of power harmonic,” in *IEEE Transactions on Power Systems*, vol. 11, no. 4, pp. 1730–1735, 1996
- (Dash *et al.*, 1997) P. Dash, D. Swain, A. Routray, and A. Liew, “An adaptive neural network approach for estimation of power system frequency,” *Electric Power Systems Research*, vol. 41, pp. 203–210, 1997
- (Dash *et al.*, 1998) P.K. Dash, S.K. Panda, A.C. Liew, and R.K. Jena, “A new approach to monitoring electric power quality,” in *Electric Power Systems Research*, vol. 46, issue 1, pp. 11–20, July 1998

- (Dash *et al.*, 2010) P.K. Dash, S. Hasan, B.K. Panigrahi, “A hybrid unscented filtering and particle swarm optimization technique for harmonic analysis of nonstationary signals,” in *Measurement*, vol. 43, issue 10, pp. 1447–1457, December 2010
- (El Shatshat *et al.*, 2002) R. El Shatshat, M. Kazerani, and M. Salama, “Power quality improvement in 3-phase 3-wire distribution systems using modular active power filter,” *Electric Power Systems Research*, vol. 61, no. 3, pp. 185-194, 2002
- (Farinaccio and Zmeureanu, 1999) L. Farinaccio, R. Zmeureanu, “Using a pattern recognition approach to disaggregate the total electricity consumption in a house into the major end–uses,” in *Energy and Buildings*, vol. 30, Issue 3, pp. 245–259, August 1999
- (Figueiredo *et al.*, 2011) M. Figueiredo, A. de Almeida, and B. Ribeiro, “An experimental study on electrical signature identification of Non–Intrusive Load Monitoring (NILM) systems,” in *Adaptive and Natural Computing Algorithms*, vol. 6594, pp. 31–40, Springer, Berlin, Germany, 2011
- (Girgis *et al.*, 1991) A.A. Girgis, W.B. Chang, and E.B. Makram, “A digital recursive measurement scheme for online tracking of power system harmonics,” in *IEEE Transaction on Power Delivery*, vol. 6, no. 3, pp. 1153–1160, 1991
- (Gonçalves *et al.*, 2011) H. Gonçalves, A. Ocneanu, M. Bergés, and R.H. Fan, “Unsupervised disaggregation of appliances using aggregated consumption data,” in *Proceedings of KDD 2011 Workshop on Data Mining Applications for Sustainability*, San Diego, CA, USA, 21–24 August 2011
- (Grossman and Morlet, 1984) A. Grossmann and J. Morlet, “Decomposition of hardy functions into square integrable wavelets of constant shape,” in *SIAM Journal on Mathematical Analysis* 15, pp. 723–736, 1984
- (Guangjie and Hailong, 2009) F. Guangjie and Z. Hailong, “The Study of the Electric Power Harmonics Detecting Method Based on the Immune RBF Neural Network,” in *2009 Second International Conference on Intelligent Computation Technology and Automation (ICICTA '09)*, vol. 1, pp. 121–124, 10–11 October 2009
- (Gupta *et al.*, 2010) S. Gupta, M.S. Reynolds, S.N. Patel, “ElectriSense: Single–point sensing using EMI for electrical event detection and classification in the home,” in *Proceedings of the 12th ACM*

- International Conference on Ubiquitous Computing*, pp. 139–148, Copenhagen, Denmark, 26–29 September 2010
- (Hagan *et al.*, 1995) M.T. Hagan, H.B. Demuth, and M.H. Beale, *Neural Network Design*. International Thomson Publishing Inc., 1995
- (Harris, 1978) F.J. Harris, “On the use of windows for harmonic analysis with the discrete Fourier transform,” in *Proceedings of the IEEE*, vol. 66, no. 1, pp. 51–83, January 1978
- (Hart, 1992) G.W. Hart, “Nonintrusive appliance load monitoring,” in *Proceedings of the IEEE*, vol. 80, no. 12, pp. 1870–1891, 1992
- (Hartana and Richard, 1990) R.K. Hartana and G.G. Richards, “Harmonic source monitoring and identification using neural networks,” in *IEEE Transactions on Power Systems*, vol. 5, no. 4, pp. 1098–1104, November 1990
- (Haykin, 1999) S. Haykin, *Neural Networks: A Comprehensive Foundation, 2nd Edition*. Prentice Hall, 1999
- (Hazas *et al.*, 2011) M. Hazas, A. Friday, and J. Scott, “Look back before leaping forward: Four decades of domestic energy inquiry,” in *IEEE Pervasive Computing*, vol. 10, no. 1, pp. 13–19, January–March 2011
- (Huang and Attoh–Okine, 2005) N.E. Huang and N.O. Attoh–Okine, *The Hilbert–Huang Transform in Engineering*. Taylor & Francis, 2005
- (Huang *et al.*, 1998) N.E. Huang, Z. Shen, S.R. Long, M.C. Wu, H.H. Shih, Q. Zheng, N.–C Yen, C.C. Tung, and H.H. Liu, “The empirical mode decomposition and the Hilbert spectrum for nonlinear and non–stationary time series analysis,” in *Proceedings of the Royal Society of London 454*, pp. 903–995, 1998
- (Jain and Singh, 2012) S.K. Jain and S.N. Singh, “ESPRIT assisted artificial neural network for harmonics detection of time–varying signals,” in *2012 IEEE Power and Energy Society General Meeting*, pp. 1–7, 22–26 July 2012
- (Janani and Himavathi, 2013) K. Janani and S. Himavathi, “Non–intrusive harmonic source identification using neural networks,” in *2013 International Conference on Computation of Power, Energy, Information and Communication (ICCPEIC)*, pp. 59–64, 17–18 April 2013

- (Jin *et al.*, 2011) Y. Jin, E. Tebekaemi, M. Berges, and L. Soibelman, “Robust adaptive event detection in non-intrusive load monitoring for energy aware smart facilities,” in *2011 IEEE International Conference on Acoustics, Speech and Signal Processing (ICASSP)*, pp. 4340–4343, May 22–27, 2011
- (Kalman, 1960) R.E. Kalman, “A new approach to linear filtering prediction problems,” in *Transactions of ASME Journal of Basic Engineering*, vol. 82, pp. 35–45, March 1960
- (Karimi-Ghartemani and Iravani, 2003) M. Karimi-Ghartemani and M.R. Iravani, “Wide-range, fast and robust estimation of power system frequency,” in *Electric Power Systems Research*, vol. 65, issue 2, pp. 109–117, 2003
- (Kato *et al.*, 2009) T. Kato, H.S. Cho, and D. Lee, “Appliance recognition from electric current signals for information-energy integrated network in home environments,” in *Proceedings of the 7th International Conference on Smart Homes and Health Telematics*, vol. 5597, pp. 150–157, Tours, France, 1–3 July 2009
- (Keaochantranond and Boonseng, 2002) T. Keaochantranond and C. Boonseng, “Harmonics and interharmonics estimation using wavelet transform,” in *IEEE/PES Transmission and Distribution Conference and Exhibition 2002: Asia Pacific*, vol. 2, pp. 775–779, 6–10 October 2002
- (Kennedy *et al.*, 2003) K. Kennedy, G. Lightbody, and R. Yacamini, “Power system harmonic analysis using the Kalman filter,” in *2003 IEEE Power Engineering Society General Meeting*, vol. 2, pp. 757, 13–17 July 2003
- (Kim *et al.*, 2011) H. Kim, M. Marwah, M. Arlitt, G. Lyon, and J. Han, “Unsupervised Disaggregation of Low Frequency Power Measurements,” in *Proceedings of the 11th SIAM International Conference on Data Mining*, pp. 747–758, Mesa, AZ, USA, 28–30 April 2011
- (Kim *et al.*, 2011) H. Kim, M. Marwah, M. Arlitt, G. Lyon, and J. Han, “Unsupervised Disaggregation of Low Frequency Power Measurements,” in *Proceedings of the 11th SIAM International Conference on Data Mining*, Mesa, AZ, USA, 28–30 April 2011
- (Kolter and Jaakkola, 2012) J.Z. Kolter and T. Jaakkola, “Approximate inference in additive factorial HMMs with application to energy

- disaggregation,” in *Proceedings of the Fifteenth International Conference on Artificial Intelligence and Statistics (AISTATS-12)*, pp. 1472–1482, 2012
- (Kolter and Johnson, 2011) J.Z. Kolter, M.J. Johnson, “REDD: A public data set for energy disaggregation research,” in *ACM Special Interest Group on Knowledge Discovery and Data Mining, Workshop on Data Mining Applications in Sustainability*, San Diego, USA, 2011
- (Köse *et al.*, 2010) N. Köse, Ö. Salor, and K. Leblebicioglu, “Interharmonics analysis of power signals with fundamental frequency deviation using Kalman filtering,” in *Electric Power System Research*, vol. 80, pp. 1145–1153, September 2010
- (Lam *et al.*, 2007) H.Y. Lam, G.S.K. Fung, W.K. Lee, “A Novel Method to Construct Taxonomy of Electrical Appliances Based on Load Signatures,” in *IEEE Transactions on Consumer Electronics*, vol. 53, no. 2, pp. 653–660, May 2007
- (Laughman *et al.*, 2003) C. Laughman, K. Lee, R. Cox, S. Show, S.B. Leeb, L. Norford, and P. Armstrong, “Power signature analysis,” in *IEEE Power & Energy Magazine*, vol. 1, no.2, pp. 56–63, March–April 2003
- (Lavopa *et al.*, 2009) E. Lavopa, P. Zanchetta, M. Sumner, and F. Cupertino, “Real-time estimation of fundamental frequency and harmonics for active shunt power filters in aircraft electrical systems,” in *IEEE Transactions on Industrial Electronics*, vol. 56, no. 8, pp. 2875–2884, 2009
- (Lee *et al.*, 2004) W.K. Lee, G.S.K. Fung, G.S.K. Lam, F.H.Y. Chan, and M. Lucente, “Exploration on Load Signatures,” in *Proceedings of International Conference on Electrical Engineering (ICEE)*, pp. 1–5, Sapporo, Japan, 4–6 July 2004
- (Li *et al.*, 2012) J. Li, S. West, and G. Platt, “Power decomposition based on SVM regression,” in *2012 Proceedings of International Conference on Modelling, Identification & Control (ICMIC)*, pp. 1195–1199, 24–26 June 2012
- (Liang *et al.*, 2010) J. Liang, S.K.K. Ng, G. Kendall, and J.W.M. Cheng, “Load signature study—Part I: Basic concept, structure, and methodology,” in *IEEE Transactions on Power Delivery*, vol. 25, no. 2, pp. 551–560, April 2010

- (Lin, 2004) H.C. Lin, "Dynamic power system harmonic detection using neural network," in *2004 IEEE Conference on Cybernetics and Intelligent Systems*, vol. 2, pp. 757–762, Singapore, 1–3 December 2004
- (Lin, 2007) H.C. Lin, "Intelligent Neural Network–Based Fast Power System Harmonic Detection," in *IEEE Transactions on Industrial Electronics*, vol. 54, no. 1, pp. 43–52, Feb. 2007
- (Liu, 1998) S. Liu, "An adaptive Kalman filter for dynamic estimation of harmonic signals," in *Proceedings of 8th International Conference on Harmonics and Quality of Power*, vol. 2, pp. 636–640, 14–18 October 1998
- (Lobos *et al.*, 2000) T. Lobos, Z. Leonowicz, J. Rezmer, "Harmonics and interharmonics estimation using advanced signal processing methods," in *International Conference on Harmonics and Quality of Power*, pp. 335–340, Orlando, Florida, USA, 2000
- (Lu *et al.*, 2008) Z. Lu, T.Y. Ji, W.H. Tang, and Q.H. Wu, "Optimal harmonic estimation using a particle swarm optimizer," in *IEEE Transactions on Power Delivery*, vol. 23, no. 2, pp. 1166–1174, April 2008
- (Ma and Girgis, 1996) H. Ma and A.A. Girgis, "Identification and tracking of harmonic sources in a power system using a Kalman filter," in *IEEE Transactions on Power Delivery*, vol. 11, no. 3, pp. 1659–1665, July 1996
- (Mallat, 1989) S.G. Mallat, "A theory for multiresolution signal decomposition: the wavelet representation," in *IEEE Transactions on Pattern Analysis and Machine Intelligence*, vol. 11, no. 7, pp. 674–693, July 1989
- (Marceau and Zmeureanu, 2000) M.L. Marceau, R. Zmeureanu, "Nonintrusive load disaggregation computer program to estimate the energy consumption of major end uses in residential buildings," in *Energy Conversion and Management*, vol. 41, Issue 13, pp. 1389–1403, 1 September 2000
- (Mazumdar and Harley, 2008) J. Mazumdar and R.G. Harley, "Recurrent Neural Networks Trained With Backpropagation Through Time Algorithm to Estimate Nonlinear Load Harmonic Currents," in *IEEE Transactions on Industrial Electronics*, vol. 55, no. 9, pp. 3484–3491, September 2008

- (McCulloch and Pitts, 1943) W. McCulloch and W. Pitts, “A logical calculus of ideas imminent in nervous activity,” in *Bulletin of Mathematical Biophysics*, vol. 5, pp. 115–133, 1943
- (Mishra, 2005) Mishra, S., “A hybrid least square–fuzzy bacterial foraging strategy for harmonic estimation,” in *IEEE Transactions on Evolutionary Computation*, vol. 9, no. 1, pp. 61–73, February 2005
- (Missaoui Badreddine, 2012) R. Missaoui Badreddine, “Gestion énergétique optimisée pour un bâtiment intelligent multi–sources multi–charges : différents principes de validations,” Thèse de doctorat, Université de Grenoble, 2012
- (Moody and Mark, 1996) G.B. Moody and R.G. Mark, “A database to support development and evaluation of intelligent intensive care monitoring,” in *Computers in Cardiology*, pp. 657–660, 1996
- (Mori and Suga, 1991) H. Mori and S. Suga, “Power system harmonics prediction with an artificial neural network,” in *1991 IEEE International Symposium on Circuits and Systems*, vol. 2, pp. 1129–1132, 11–14 June 1991
- (Najmeddine *et al.*, 2008) H. Najmeddine, K.K. Drissi, C. Pasquier, C. Faure, K. Kerroum, A. Diop, T. Jouannet, and M. Michou, “State of art on load monitoring methods,” in *2nd IEEE International Conference on Power and Energy (PECon 08)*, Johor Baharu, Malaysia, December 2008
- (Nascimento *et al.*, 2011) C.F. do Nascimento, A.A. Oliveira Jr., A. Goedtel, and P.J.A. Serni, “Harmonic identification using parallel neural networks in single–phase systems,” in *Applied Soft Computing*, vol. 11, issue 2, pp. 2178–2185, March 2011
- (Nascimento *et al.*, 2013) C.F. Nascimento, A.A. Oliveira Jr., A. Goedtel, and A.B. Dietrich, “Harmonic distortion monitoring for nonlinear loads using neural–network–method,” in *Applied Soft Computing*, vol. 13, issue 1, pp. 475–482, January 2013
- (Nguyen and Wira, 2013a) T.M. Nguyen and P. Wira, “A new approach based on a linear Multi–Layer Perceptron for identifying on–line harmonics,” in *39th Annual Conference of the IEEE Industrial Electronics Society (IECON 2013)*, Vienna, Austria, November 10–13, 2013
- (Nguyen and Wira, 2013b) T.M. Nguyen and P. Wira, “A linear Multi–Layer Perceptron for identifying harmonic contents of biomedical signals,” in

9th International Conference on Artificial Intelligence Applications and Innovation (AIAI 2013), Paphos, Cyprus, September 30 – October 2 2013

- (Nguyen and Wira, 2015) T.M. Nguyen and P. Wira, “Power grid higher-order harmonics estimation with multilayer Perceptrons,” in *11th International Conference of Computational Methods in Sciences and Engineering (ICCMSE 2015)*, Athens, Greece, March 20–23, 2015
- (Nguyen *et al.*, 2011) N.K. Nguyen, P. Wira, D. Flieller, D. Ould Abdeslam, and J. Mercklé, “Harmonics identification with artificial neural networks: application to active power filtering,” in *International Journal of Emerging Electric Power Systems*, Walter de Gruyter, vol. 12 (5), pp. 1–27, 2011
- (Norford and Leeb, 1996) L.K. Norford, S.B. Leeb, “Non-intrusive electrical load monitoring in commercial buildings based on steady-state and transient load-detection algorithms,” in *Energy and Buildings*, vol. 24, issue 1, pp. 51–64, 1996
- (Onoda *et al.*, 2000) T. Onoda, G. Rätsch, and K.-R. Müller, “Applying support vector machine and boosting to a non-intrusive monitoring system for household electric appliances with Inverters,” 2000
- (Onoda *et al.*, 2002) T. Onoda, H. Murata, G. Rätsch, and K.-R. Müller, “Experimental analysis of support vector machines with different kernels based on non-intrusive monitoring data,” in *Proceedings of the 2002 International Joint Conference on Neural Networks (IJCNN '02)*, vol. 3, pp. 2186–2191, 2002
- (Ould Abdeslam *et al.*, 2007) D. Ould Abdeslam, P. Wira, J. Mercklé, D. Flieller, and Y.-A. Chapuis, “A unified artificial neural network architecture for active power filters,” in *IEEE Transactions on Industrial Electronics*, vol. 54, no. 1, pp. 61–76, 2007
- (Pan and Tompkins, 1985) J. Pan and W.J. Tompkins, “A real-time QRS detection algorithm,” in *IEEE Transactions on Biomedical Engineering*, vol. BME-32, no. 3, pp. 230–236, 1985
- (Parson *et al.*, 2014) O. Parson, S. Ghosh, M. Weal, A. Rogers, “An unsupervised training method for non-intrusive appliance load monitoring,” in *Artificial Intelligence*, vol. 217, pp. 1–19, December 2014
- (Patel *et al.*, 2007) S.N. Patel, T. Robertson, J.A. Kientz, M.S. Reynolds, and G.D. Abowd, “At the flick of a switch: Detecting and

classifying unique electrical events on the residential power line,” in *Proceedings of the 9th International Conference on Ubiquitous Computing*, Innsbruck, Austria, pp. 271–288, 16–19 September 2007

- (Paulraj et al., 1986) A. Paulraj, R. Roy, and T. Kailath, “A subspace rotation approach to signal parameter estimation,” in *Proceedings of the IEEE*, vol. 74, no. 7, pp. 1044–1046, July 1986
- (Pecharanin et al., 1994) N. Pecharanin, M. Sone, and H. Mitsui, “An application of neural network for harmonic detection in active filter,” in *Proceeding of IEEE International Conference on Neural Networks*, vol. 6, pp. 3756–3760, Jun. 27–Jul. 2, 1994
- (Pecharanin et al., 1995) N. Pecharanin, H. Mitsui, and M. Sone, “Harmonic detection by using neural network,” in *Proceedings of 1995 IEEE International Conference on Neural Networks*, vol. 2, pp. 923–926, November/December 1995
- (Portnoff, 1980) M.R. Portnoff, “Time–frequency representation of digital signals and systems based on short–time Fourier analysis,” in *IEEE Transactions on Acoustics, Speech and Signal Processing*, vol. 28, no. 1, pp. 55–69, February 1980
- (Rabiner et al., 1969) L. Rabiner, R.W. Schafer, and C.M. Rader, “The chirp z–transform algorithm,” in *IEEE Transactions on Audio and Electroacoustics*, vol. 17, no. 2, pp. 86–92, June 1969
- (Rangayyan, 2002) R. Rangayyan, *Biomedical Signal Analysis: A Case Study Approach*. Wiley–IEEE Press, 2002
- (Ray and Subudhi, 2015) P. K. Ray and B. Subudhi, “Neuro–evolutionary approaches to power system harmonics estimation,” in *International Journal of Electrical Power & Energy Systems*, vol. 64, pp. 212–220, January 2015
- (Ren and Wang, 2010) Z. Ren and B. Wang, “Estimation Algorithms of Harmonic Parameters Based on the FFT,” in *Power and Energy Engineering Conference (APPEEC), 2010 Asia–Pacific*, pp. 1–4, 28–31 March 2010
- (Roos et al., 1994) J.G. Roos, I.E. Lane, E.C. Botha, and G.P. Hancke, “Using neural networks for non–intrusive monitoring of industrial electrical loads,” in *1994 IEEE Instrumentation and Measurement Technology Conference (IMTC/94)*, vol. 3, pp. 1115–1118, 10–12 May 1994

- (Rosenblatt, 1958) F. Rosenblatt, "The perceptron: a probabilistic model for information storage and organization in the brain," in *Psychological Review*, vol. 65, pp. 386–408, 1958
- (Rukonuzzaman *et al.*, 1998) Md. Rukonuzzaman, A.A.M. Zin, H. Shaibon, and K.L. Lo, "An application of neural network in power system harmonic detection," in *Proceedings of the 1998 IEEE International Joint Conference on Neural Networks*, 1998 IEEE World Congress on Computational Intelligence, vol. 1, pp. 74–78, 4 – 8 May 1998
- (Ruzzelli *et al.*, 2010) A.G. Ruzzelli, C. Nicolas, A. Schoofs, and G.M.P. O'Hare, "Real-Time Recognition and Profiling of Appliances through a Single Electricity Sensor," in *2010 7th Annual IEEE Communications Society Conference on Sensor Mesh and Ad Hoc Communications and Networks (SECON)*, pp. 1–9, 21–25 June 2010
- (Sadinezhad and Joorabian, 2009) I. Sadinezhad and M. Joorabian, "A novel frequency tracking method based on complex adaptive linear neural state vector in power systems," *Electric Power Systems Research*, vol. 79, no. 8, pp. 1216-1225, 2009
- (Sahoo *et al.*, 2009) H.K. Sahoo, P.K. Dash, N.P. Rath, and B.N. Sahu, "Harmonic estimation in a power system using hybrid H_{∞} -Adaline algorithm," in *TENCON 2009 – 2009 IEEE Region 10 Conference*, pp. 1–6, 23–26 January 2009
- (Sarkar and Sengupta, 2009) A. Sarkar and S. Sengupta, "On-line tracking of single phase reactive power in non-sinusoidal conditions using S-ADALINE networks," in *Measurement*, vol. 42, issue 4, pp. 559–569, May 2009
- (Sarkar *et al.*, 2011) A. Sarkar, S.R. Choudhury, and S. Sengupta, "A self-synchronized ADALINE network for on-line tracking of power system harmonics," in *Measurement*, vol. 44, issue 4, pp. 784–790, May 2011
- (Seifossadat *et al.*, 2007) S.G. Seifossadat, M. Razzaz, M. Moghaddasian, and M. Monadi, "Harmonic estimation in power systems using adaptive perceptrons based on a genetic algorithm," in *WSEAS Transactions on Power System*, vol. 2, issue 11, pp. 239–244, November 2007
- (Shao *et al.*, 2012) H. Shao, M. Marwah, and N. Ramakrishnan, "A temporal motif mining approach to unsupervised energy disaggregation," in *Proceedings of the 1st International*

Workshop on Non-Intrusive Load Monitoring, Pittsburgh, PA, USA, 7 May 2012

- (Sharma and Mahalanabis, 1973) K.L.S. Sharma and A.K. Mahalanabis, “Harmonic analysis via Kalman filtering technique,” in *Proceedings of the IEEE*, vol. 61, no. 3, pp. 391–392, March 1973
- (Shaw *et al.*, 2008) S.R. Shaw, S.B. Leeb, L.K. Norford, and R.W. Cox, “Nonintrusive Load Monitoring and Diagnostics in Power Systems,” in *IEEE Transactions on Instrumentation and Measurement*, vol. 57, no. 7, pp. 1445–1454, July 2008
- (Singh *et al.*, 2014) S.K. Singh, A. Nath, R. Chakraborty, J. Kalita, N. Sinha, and A.K. Goswami, “Fast transverse-RLS algorithm based power system harmonic estimation,” in *2014 International Conference on Information Communication and Embedded Systems (ICICES)*, pp. 1–5, 27–28 February 2014
- (Singh *et al.*, 2015a) S. K. Singh, A. K. Goswami, N. Sinha, “Power system harmonic parameter estimation using Bilinear Recursive Least Square (BRLS) algorithm,” in *International Journal of Electrical Power & Energy Systems*, vol. 67, pp. 1–10, May 2015
- (Singh *et al.*, 2015b) S. K. Singh, N. Sinha, A. K. Goswami, N. Sinha, “Variable Constraint based Least Mean Square algorithm for power system harmonic parameter estimation,” in *International Journal of Electrical Power & Energy Systems*, vol. 73, pp. 218–228, December 2015
- (Srinivasan *et al.*, 2006) D. Srinivasan, W.S. Ng, and A.C. Liew, “Neural-network-based signature recognition for harmonic source identification,” in *IEEE Transactions on Power Delivery*, vol. 21, no. 1, pp. 398–405, January 2006
- (Subudhi and Ray, 2009) B. Subudhi and P.K. Ray, “Estimation of power system harmonics using hybrid RLS-Adaline and KF-Adaline algorithms,” in *TENCON 2009 – 2009 IEEE Region 10 Conference*, pp. 1–6, 23–26 January 2009
- (Subudhi and Ray, 2010) B. Subudhi and P.K. Ray, “A hybrid Adaline and Bacterial Foraging approach to power system harmonics estimation,” in *2010 International Conference on Industrial Electronics, Control & Robotics (IECR)*, pp. 236–242, 27–29 December 2010

- (Sultanem, 1991) F. Sultanem, "Using appliance signatures for monitoring residential loads at meter panel level," in *IEEE Transactions on Power Delivery*, vol. 6, no. 4, pp. 1380–1385, October 1991
- (Suzuki *et al.*, 2008) K. Suzuki, S. Inagaki, T. Suzuki, H. Nakamura, and K. Ito, "Nonintrusive Appliance Load Monitoring Based on Integer Programming," in *Proceedings of SICE Annual Conference*, vol. 174, pp. 2742–2747, Tokyo, Japan, 20–22 August 2008
- (Tao *et al.*, 2010) C. Tao, D. Shanxu, R. Ting, and L. Fangrui, "A robust parametric method for power harmonic estimation based on M-estimators," in *Measurement*, vol. 43, issue 1, pp. 67–77, 2010
- (Tarasiuk, 2011) T. Tarasiuk, "Estimator-analyzer of power quality: Part I – Methods and algorithms," in *Measurement*, vol. 44, issue 1, pp. 238–247, January 2011
- (Temurtas and Temurtas, 2011) Hasan Temurtas and Feyzullah Temurtas, "An application of neural networks for harmonic coefficients and relative phase shifts detection," in *Expert Systems with Applications*, vol. 38, issue 4, pp. 3446–3450, April 2011
- (Temurtas *et al.*, 2004) F. Temurtas, R. Gunturkun, N. Yumusak, and H. Temurtas, "Harmonic detection using feed forward and recurrent neural networks for active filters," in *Electric Power Systems Research*, vol. 72, no. 1, pp. 33–40, 2004
- (Testa *et al.*, 2004) A. Testa, D. Gallo, and R. Langella, "On the processing of harmonics and interharmonics: using Hanning window in standard framework," in *IEEE Transactions on Power Delivery*, vol. 19, no. 1, pp. 28–34, January 2004
- (Tey *et al.*, 2005) L. H. Tey, P. L. So, and Y. C. Chu, "Adaptive neural network control of active filters," *Electric Power Systems Research*, vol. 74, no. 1, pp. 37–56, 2005
- (Trenn, 2008) S. Trenn, "Multilayer perceptrons: approximation order and necessary number of hidden units," in *IEEE Transactions on Neural Networks*, vol. 19, no. 5, pp. 836–844, May 2008
- (Tümay *et al.*, 2008) M. Tümay, M.E. Meral, and K.C. Bayindir, "Extraction voltage harmonics using multi-layer perceptron neural network," in *Neural Computing and Applications*, vol. 17, pp. 585–593, 2008

- (Vasumathi and Moorthi, 2011) B. Vasumathi and S. Moorthi, “Harmonic estimation using Modified ADALINE algorithm with Time-Variant Widrow — Hoff (TVWH) learning rule,” in *2011 IEEE Symposium on Computers & Informatics (ISCI)*, pp. 113–118, 20–23 March 2011
- (Vasumathi and Moorthi, 2012) B. Vasumathi and S. Moorthi, “Implementation of hybrid ANN-PSO algorithm on FPGA for harmonic estimation,” in *Engineering Applications of Artificial Intelligence*, vol. 25, issue 3, pp. 476–483, April 2012
- (Vázquez *et al.*, 2001) J.R. Vázquez, P.R. Salmerón, and F. J. Alcántara, “Neural networks applications to control an active power filter,” in *9th European Conference on Power Electronics and Applications*, Graz, Austria, 2001
- (Wang and Lu, 2006) D. Wang and Y. Lu, “The signal subspace decomposition method for extracting harmonic signal,” in *2006 IEEE Information Theory Workshop (ITW '06 Punta del Este)*, pp. 714–717, October 2006
- (Wang and Zheng, 2012) Z. Wang and G. Zheng, “Residential appliances identification and monitoring by a nonintrusive method,” in *IEEE Transactions on Smart Grid*, vol. 3, no. 1, pp. 80–92, March 2012
- (Wang *et al.*, 2000) Z.-Q. Wang, M. T. Manry, and J. L. Schiano, “LMS learning algorithms: Misconceptions and new results on convergence,” *IEEE Transactions on Neural Networks*, vol. 11, no. 1, pp. 47-56, 200
- (Wang *et al.*, 2005) F.-T Wang, S.-H Chang and J.C.-Y Lee, “Hybrid wavelet-Hilbert-Huang spectrum analysis,” in *Oceans – Europe 2005*, vol. 2, pp. 902–905, 20–23 June 2005
- (Wang, 1990) T.T. Wang, “The segmented chirp Z-transform and its application in spectrum analysis,” in *IEEE Transactions on Instrumentation and Measurement*, vol. 39, no. 2, pp. 318–323, April 1990
- (Widrow and Lehr, 1990) B. Widrow, M.A. Lehr, “30 years of adaptive neural networks: perceptron, madaline, and backpropagation,” in *Proceeding*, 78 (9), pp. 1415–1442, 1990
- (Widrow and Walach, 1996) B. Widrow and E. Walach, *Adaptive Inverse Control*. Prentice-Hall Inc., 1996

- (Widrow *et al.*, 1987) B. Widrow, P. Baudrenghien, M. Vetterli, and P. Titchener, “Fundamental relations between the LMS algorithm and the DFT,” in *IEEE Transactions on Circuits and Systems*, vol. 34, no. 7, pp. 814–820, July 1987
- (Wilamowski, 2011) B. Wilamowski, *Neural Network Architectures*, 2nd edition. CRC Press, vol. 5, chapter 6, pp. 6–17, 2011
- (Winograd, 1978) S. Winograd, “On computing the discrete Fourier transform,” in *Mathematics of Computation*, vol. 32, no. 141, pp. 175–199, January 1978
- (Wira and Nguyen, 2013) P. Wira and T.M. Nguyen, “Adaptive learning for on–line harmonic identification: An overview with study cases,” in *International Joint Conference on Neural Networks (IJCNN 2013)*, Dallas, Texas, August 4–9, 2013
- (Wira and Nguyen, 2017) P. Wira and T.M. Nguyen, “Current harmonic estimation in power transmission lines using Multi–Layer Perceptron learning strategies,” *Journal of Electrical Engineering*, vol. 5, pp. 219–230, July–Aug. 2017 (DOI: 10.17265/2328-2223/2017.05.001).
- (Wira *et al.*, 2008) P. Wira, D. Ould Abdeslam, and J. Mercklé, “Learning and adaptive techniques for harmonics compensation in power supply networks,” in *14th IEEE Mediterranean Electrotechnical Conference (MELECON’ 2008)*, Ajaccio, France 2008, pp. 719–725, 2008
- (Wira *et al.*, 2010) P. Wira, D. Ould Abdeslam, and J. Mercklé, “Artificial neural networks to improve current harmonics identification and compensation,” in *Intelligent Industrial Systems: Modelling, Automation and Adaptive Behaviour*, G. Rigatos, ed., IGI global, Hershey, PA, USA, pp. 256–290, 2010
- (Wong *et al.*, 2013) Y.F. Wong, Y.A. Sekercioglu, T. Drummond, and V.S. Wong, “Recent approaches to non–intrusive load monitoring techniques in residential settings,” in *2013 IEEE Symposium on Computational Intelligence Applications In Smart Grid (CIASG)*, pp. 73–79, 16–19 April 2013
- (Yang *et al.*, 2014) C.C. Yang, C.S. Soh, and V.V. Yap, “Comparative study of event detection methods for non–intrusive appliance load monitoring,” in *The 6th International Conference on Applied Energy – ICAE2014*, pp. 1840–1843, 2014

- (Ye and Liu, 2009) X.-M Ye and X.-H Liu, "The harmonic detection based on wavelet transform and FFT for electric ARC furnaces," in *2009 International Conference on Wavelet Analysis and Pattern Recognition (ICWAPR 2009)*, pp. 408–412, 12–15 July 2009
- (Yoshimoto *et al.*, 2000) K. Yoshimoto, Y. Nakano, Y. Amano, and B. Kermanshahi, "Non-intrusive appliances load monitoring system using neural networks," in *Conference Proceedings of Information and Electronic Technologies*, vol. 7, pp. 183–194, 2000
- (Yu and Yang, 2009) J. Yu and L. Yang, "Analysis of Harmonic and Inter-Harmonic Based on Hilbert–Huang Transform," in *International Conference on Computational Intelligence and Software Engineering (CiSE 2009)*, pp. 1–4, 11–13 December 2009
- (Zadeh *et al.*, 2010) R.A. Zadeh, A. Ghosh, and G. Ledwich, "Combination of Kalman Filter and Least-Error Square Techniques in Power System," in *IEEE Transactions on Power Delivery*, vol. 25, no. 4, pp. 2868–2880, October 2010
- (Zeifman and Roth, 2011) M. Zeifman and K. Roth, "Nonintrusive appliance load monitoring: Review and outlook," in *IEEE Trans. Consumer Electronics*, vol. 57, no. 1, pp. 76–84, Feb. 2011
- (Zeifman, 2012) M. Zeifman, "Disaggregation of home energy display data using probabilistic approach," in *IEEE Transactions on Consumer Electronics*, vol. 58, no. 1, pp. 23–31, February 2012
- (Zeng *et al.*, 2006) X. Zeng, Y. Wang, and K. Zhang, "Computation of adalines' sensitivity to weight perturbation," *IEEE Transactions on Neural Networks*, vol. 17, no. 2, pp. 515–519, 2006
- (Zhan and Cheng, 2005) Y. Zhan and H. Cheng, "A robust support vector algorithm for harmonic and interharmonic analysis of electric power system," in *Electric Power Systems Research*, vol. 73, issue 3, pp. 393–400, March 2005
- (Zhang *et al.*, 2009) S. Zhang, Q. Wang, and R. Liu, "Power system harmonic analysis based on improved Hilbert–Huang transform," in *9th International Conference on Electronic Measurement & Instruments (ICEMI '09)*, pp. 4–343 – 4–347, 16–19 August 2009

(Zia *et al.*, 2010)

T. Zia, D. Bruckner, A. Zaidi, , “A hidden Markov model based procedure for identifying household electric loads,” in *IECON 2011 – 37th Annual Conference on IEEE Industrial Electronics Society*, pp. 3218–3223, 7–10 Nov. 2011

(Zoha *et al.*, 2012)

A. Zoha, A. Gluhak, M.A. Imran, and S. Rajasegarar, “Non-intrusive load monitoring approaches for disaggregated energy sensing: A survey,” in *Sensors 12/2012*, pp. 16838–16866, December 2012